UNIVERSITÀ
DEGLI STUDI
FIRENZE

DOTTORATO DI RICERCA IN SCIENZE BIOMEDICHE

INDIRIZZO IN BIOCHIMICA E BIOLOGIA APPLICATA

CICLO XXVII

Coordinatore Prof. Persio Dello Sbarba

Molecular insights into amyloid aggregation and cytotoxicity

Settore Scientifico Disciplinare BIO/10

Dottorando
Dott. Manuela Leri

Tutor
Prof. Massimo Stefani

Coordinatore
Prof. Persio Dello Sbarba

Anni 2012/2014

“Il processo di una scoperta scientifica è,
in effetti, un continuo conflitto di meraviglie.”
Albert Einstein

Indice

Abstract

Introduction

Aim of the study

Materials and Methods

Results

Abstract

1. Oleuropein Aglycone: a natural polyphenol which protects against the cytotoxicity associated with Transthyretin fibrillogenesis

Transthyretin (TTR) is a plasma protein secreted by hepatocytes into the blood and cerebrospinal fluid, where it transports thyroid hormones, thyroxine (T4) and triiodothyronine (T3) and cotransport of vitamin A through Retinol Binding Protein (RBP). TTR is an amyloidogenic protein implicated in diseases such as senile systemic amyloidosis (SSA) and familial amyloid polyneuropathy (FAP), both characterized by extracellular deposition of insoluble amyloid fibrils in heart, peripheral nerves and other organs. In particular, fibrils in FAP patients are composed of single-site mutant TTR and among the numerous pathogenic variants Leu55 → Pro55 (L55P) is highly amyloidogenic and forms amyloid fibrils *in vitro*. It is suspected that the single-point mutations accelerate amyloidogenesis by destabilizing the monomeric partially unfolded amyloidogenic intermediate state rather than by altering the tetrameric native state. TTR fibrils have been considered direct responsible of tissue impairment in FAP and SSA, but the unstable fibril precursors are increasingly considered the main responsible of cell sufferance and tissue impairment in amyloid diseases. In particular, the early unstable oligomeric intermediates are highly toxic due to their ability to interact with, disassemble and permeabilize cell membranes. Moreover, increasing information on polymorphism of pre-fibrillar and fibrillar assemblies has led to propose that apparently similar fibrils can display different stability and efficiency in generating toxic species. These data suggest the opportunity to search natural or synthetic molecules interfering with amyloid aggregation by stabilizing the TTR native state by hindering the appearance of toxic species, or by favouring the growth of less toxic assemblies. We have recently described a natural compound (oleuropein aglycone) which is protective in Tg animal models of Abeta deposition and cultured cells by stimulating cell autophagy and the endolysosomal path and by modifying the pattern of aggregation of amylin and Abeta peptides skipping the appearance of toxic oligomers and reducing plaque load. Our study is focused on the ability of oleuropein aglycone (the main phenolic component of the extra virgin olive oil) to inhibit the toxic effects to HL-1 cells of amyloid aggregates of both wild-type TTR and its highly amyloidogenic L55P variant. Our data offer the possibility to validate and optimize the use of

oleuropein as itself or as a starting point to rationally designe promising drugs that could enter in a clinical experimental phase.

2. Wild-type and Leu55Pro Transthyretin Homocysteynilation, worsening of cardiomiopathy onset

Homocysteine (Hcy) is a homologue of the amino acid cysteine, differing by an additional methylene bridge (-CH_2-), and it is biosynthesized from methionine. Some diseases are associated with higher homocysteine levels.

One of proposed mechanisms of homocysteine toxicity includes endoplasmatic reticulum stress and the unfolded protein response. In particular, protein homocysteinylation is a novel example of protein damage that may explain the involvement of Hcy in the pathology of human vascular diseases. Post-translational modifications in addition to amino acid substitution can affect the structure of TTR affecting its ability to bind these receptors. Recent data show that L-homocysteine reacts with transthyretin in the human plasma to form a stable covalent adduct. TTR undergoes homocysteinylation at its single cysteine residue (Cys10). The ratio TTR-Cys10-S-S-homocysteine/unmodified TTR increased with increasing homocysteine plasma concentrations. In our study we decided to perform some *in vitro* and *in vivo* experiments to study the effect of Hcy on wt- and L55P-TTR in physiological conditions by using HL-1 cells, a cardiomyocyte cell line.

Our results showed that Hcy in physiological conditions have a double effect, it is able to stabilize the tetrameric form of wt-TTR and to destabilize the mutant L55P enriching the solution with monomeric species and faciliting the formation of fibrils. The kinetics of aggregation of both wt- and L55P-TTR were analyzed by biophysical analysis such as: dynamic light scattering, circular dichroism, resveratrol binding assay and turbidimetry. The toxicity on the HL-1 cardiomyocyte cell line was analyzed by the MTT assay. Our data confirm the binding of Hcy to TTR and this modification may contribute to worsening the cardiomiopathy onset.

3. Molecular insights into membrane interaction of a new amyloidogenic variant of β2-microglobulin

Systemic amyloidosis is a fatal disease caused by misfolding of β2-microglobulin, a normally soluble protein, which then aggregate into insoluble fibrils. β2-microglobulin (β2-m) is present at the surface of all nucleated cells, where it participates to the formation of the major histocompatibility complex. In patients with end stage renal failure subjected to haemodialysis, blood levels of β2-m increase remarkably causing protein precipitation into fibrils deposited in bones, skeletal muscle and joints, causing arthropathy, an event which ultimately leads to a pathological condition known as dialysis-related amyloidosis (DRA), a pathology for which were not described familial forms. However, recently, kindreds were found with slowly progressive gastrointestinal symptoms caused by the autosomal dominant D76N mutation in the β2-m gene; unlike patients with dialysis-related amyloidosis, this family displayed normal renal function. Extensive amyloid deposits were found in the spleen, liver, heart, salivary glands and nerves. The D76N variant was thermodynamically unstable and remarkably fibrillogenic *in vitro* under physiological conditions. The aim of this study was to examine the correlation between the structural features of amyloid aggregates of D76N and their toxic effects on human neuroblastoma cell line SH-SY5Y. The results showed that the D76N fibrillar species interacted with the ganglioside GM1, a key component of raft domains at the SH-SY5Y membrane. The resulting toxic effects resulted from increases of both ROS levels and calcium permeability whichtriggered necrotic cell death. In summary, our data provide a mechanistic insight into the mechanisms of cytotoxicity of aggregated β2-m D76N and support the idea that GM1 is a key site of interaction of amyloid species with the cell membrane, stressing the role of lipid rafts as fundamental mediators of amyloid toxicity.

Introduction

1 Protein Folding and Misfolding

1.1 Protein Folding

The folding of proteins into their compact three-dimensional structures is the most fundamental and universal example of biological self-assembly; understanding this complex process will therefore provide a unique insight into the way evolutionary selection has influenced the properties of a molecular system for functional advantage (Dobson 2003). The process of protein folding has been widely studied, and for better understanding its characteristics the theory of "energy landscape" has been developed that considers the native state of a protein as the absolute minimum in the folding energy landscape that depends on a large number of degrees of freedom. The folding process allows proteins to assume their native structure correctly and achieve their physiological function. Secondary structure, including strands, helices and sheets that are found in nearly all native protein structures, is stabilized primarily by hydrogen bonding between the amide and carbonyl groups of the main chain (the so-called backbone). The formation of such structure is an important element in the overall folding process, although it might not have a role as fundamental as the establishment of the overall chain topology (Makarov *et al*. 2003). The folding mechanism is very fast, ranging from milliseconds to fractions of a second, so it is difficult to describe, given the multiple conformations that unfolded polypeptide chains can take. Levinthal, in 1969, indicated the infinity of degrees of freedom that a nascent polypeptide could display. If the protein would pass through all of these possible conformations, it would need a time enormously greater than that measured *in vivo* (*E.coli* produces a protein of 100 amino acids in 5 seconds at 37 C). The difference that exists between the theoretical time for the correct folding to be achieved and the observed one it is known as the "Levinthal's paradox" (Levinthal 1968).

Currently, the "core folding" of a polypeptide chain is considered to be entirely contained within its amino acid sequence; the protein folding exploits molecular dynamics that allow specific residues, although very distant in the amino acid sequence, to quickly enter in close contact. The formation of these contacts is a cooperative process, and conformational restrictions provided by an interaction will favour other interactions in a self-reinforcing process (Stefani 2008). The inherent fluctuations in the conformation of an unfolded or incompletely folded polypeptide chain enable residues that are far in the amino-acid sequence to come into contact with other residues. Since,

on average, native-like interactions between residues are more stable than non-native ones, they are more persistent and the polypeptide chain is able to find its lowest-energy structure by a trial-and-error process. Moreover, if the energy surface or 'landscape' has the right shape (Fig.1) only a small number among all possible conformations needs to be sampled by any given protein molecule during its transition from a random coil to a native structure (Dobson *et al*.1998).

The energy landscape contains all conformational stages accessible to the polypeptide chain, with their entropy, free energy and fraction of native contacts. These species are heterogeneous and include highly dynamic and complex disordered conformations, whose structures are far from the native ones. Initially they form most of the secondary structure: alpha helices and β sheets. Subsequently, the increasing interactions of non-polar hydrophobic residues near the central core of the protein lead to a collapse of the polypeptide chain in a state called "Molten Globule". Molten Globules are deprived of many bonds between side chains that the protein shows in its final tertiary structure. The final steps to reach the native state include bond formation between side chains and the formation of covalent disulfide bridges. Although it is still not well clear how a protein may contain information for training of its structure, it has been hypothesized that this is due to the presence of hydrophobic and polar residues, which favour the formation of specific interactions between residues ensuring the compactness of the structure. Within the cell are present both natively folded and natively unfolded proteins (NUPS). Many of these proteins are involved in cell cycle control, DNA transcription and in ribosome structure; they are characterized by low hydrophobicity and high net charge; these features make them incapable of folding in the intracellular environment and simultaneously prevent their possible aggregation (Uversky *et al.* 2002). In addition, their lack of structure favours the binding of chaperones with these proteins favouring their clearance and preventing their aggregation (Uversky *et al*. 2002). These proteins are an example of how the presence of surfaces can play an important role in facilitating the folding process. In fact, many NUPS reach their correct three-dimensional structure upon binding to their target proteins, which have a surface adequate for NUP folding, (Dedmon *et al.* 2002).

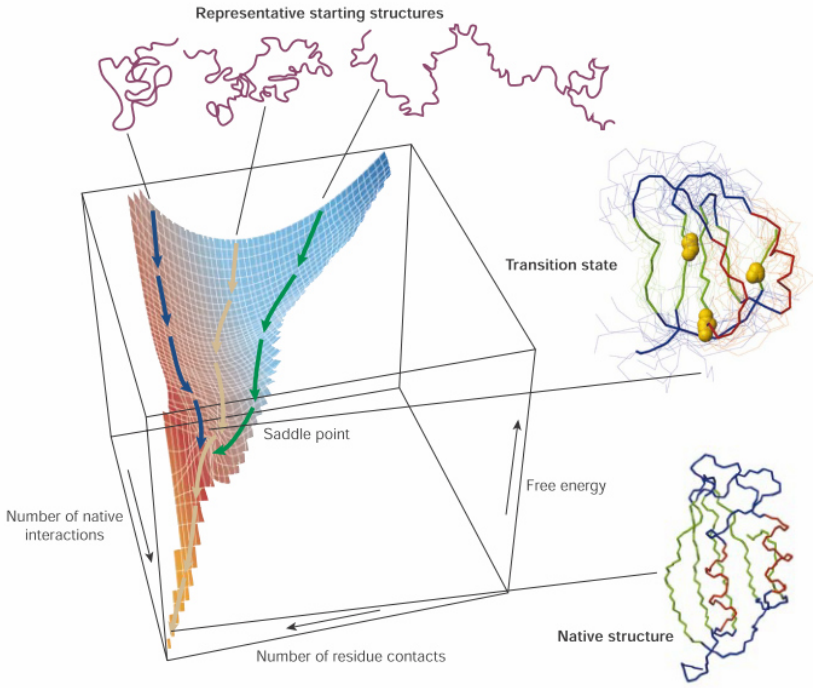

Figure 1. A schematic energy landscape for protein folding. The surface 'funnels' the multitude of denatured conformations to the unique native structure. The critical region on a simple surface such as this one is the saddle point corresponding to the transition state, the barrier that all molecules must cross if they are to fold to the native state. Superimposed on this schematic surface are ensembles of structures corresponding to different stages of the folding process. The structure of the native state is shown at the bottom of the surface; at the top are indicated schematically some contributors to the distribution of unfolded species that represent the starting point for folding.

Probably, targets contain structural information, as charged and hydrophobic residues, required for NUP folding. Alternatively, naturally unfolded proteins undergo rapid intracellular turnover such that their unfolded state represents a mechanism of cellular control (Wright *et al*. 1999).

Experiments carried out *in vitro* led to understand the bases of the folding process in a simple environment consisting of a buffered pH and a known ionic strength, sometimes containing a co-solvent or a denaturing agent. These conditions are very different from those present in the intracellular environment where other factors can potentially affect protein folding, misfolding or aggregation (Stefani 2008). The intracellular protein concentration is about 300 - 400 mg / mL. This feature, known as "macromolecular crowding", is very important in thermodynamics terms as it can affect the conformational states of proteins (Ellis *et al*. 2001). The cell membrane can promote the crowding and a reversible unfolding / refolding of specific proteins when they

physiologically translocate through the membrane (Bychkova *et al*. 1988). Intracellular macromolecules can facilitate the folding of specific proteins. Some of these are a heterogeneous family of proteins termed "chaperones", including prokaryotic GroES / GroEL and DnaK / DnaJ, also known in eukaryotes as Hsp70 / Hsp40. The role of chaperones is to facilitate the correct folding of other proteins, ensuring the presence of an appropriate environment, contacts with surfaces with which a protein can fold quickly and effectively and avoiding the formation of inappropriate interactions (Hartl *et al*. 2002). In the absence of chaperones, proteins will fail to achieve their native state (a process known as misfolding) and instead may associate with other unfolded polypeptide chains to form large aggregated structures (*in vivo*, this may result in deposition of extracellular aggregates or inclusion body formation). A similar scenario can occur when proteins acquire mutations or when they are exposed to unfavourable conditions, such as extreme heat or pH. Indeed, the presence of unfolded peptides, that expose to the aqueous environment their hydrophobic amino acid residues, induces a tendency to aggregation of hydrophobic side chains belonging to the same protein or different proteins, in the logic of decreasing the surface contact area with the solvent. In this case the polar solvent drives the formation of oligomeric protein aggregates, characterized by a high content of β-structures (Dobson 2001). Protein folding and misfolding are associated with the regulation a wide range of cellular processes, leading to the conclusion that uncorrect folding may alter protein functionality with the consequent onset of pathologies (Stefani and Dobson 2003). Misfolded proteins are devoid of their biological and functional activity and they are prone to aggregate and/or interact inappropriately with other cell components, eventually leading to cell death. Some diseases often known as conformational diseases are due to misfolding and, as a consequence, the proteins acquire some normally absenttoxicity (gain of function) or lose their functional activity (loss of function) (Thomas *et al*. 1995). Misfolding and growth of molecular aggregates with amyloid characteristics are two closely related phenomena. Indeed, it is not a coincidence that many amyloidoses are associated with mutations of specific chaperones or of proteins involved in the ubiquitin-proteasome system, that drive the polypeptide chain to a correct folding or degrade proteins that lose thair correct tertiary structure, respectively (Macario *et al*. 2002 - Layfield *et al*. 2001). Amyloidogenic proteins are diverse in sequence and share few characteristics – they can be large or small, have a catalytic or a structural role, be abundant or sparse. The lack of sequence or structural similarity amongst amyloidogenic proteins reinforces the notion

that amyloid is a primitive structure that can be generated by many polypeptide sequences at proper conditions. Thus, it has been hypothesized that amyloid has existed as long as proteins exists, and it was probably a prominent fold in the early evolution of life (Chernoff 2004). Recent studies have identified amyloid fibers in bacteria, fungi, insects, invertebrates and humans that have a functional role. As an example, human Pmel17 has important roles in the biosynthesis of the pigment melanin, and the factor XII protein of the homeostatic system is activated by amyloid (referenze). The functional amyloid hypothesis states that organisms have evolved to take advantage of the fact that many polypeptides can form amyloid, despite the fact that amyloid can be toxic (Mackay *et al*. 2001; Fowler *et al*. 2006). However, the discovery of functional amyloid was surprising because amyloid has been associated solely with human diseases for over a century before its physiological role was discovered. Functional amyloid was identified initially within the past decade in several lower organisms, including bacteria (Chapman *et al*. 2002; Claessen *et al*. 2003), fungi (Mackay *et al*. 2001), and insects (Iconomidou *et al*. 2006) and subsequently in humans (Fowler *et al*. 2006).

1.2 Amyloid diseases

Many human degenerative diseases, such as Alzheimer's disease (AD), Parkinson's disease (PD), transmissible spongiform encephalopathies (TSEs) and non-insulin-dependent type II diabetes (NIMMD), are associated with an abnormal deposition of proteinaceous fibrillar aggregates (amyloid fibrils) in various tissues and organs (Stefani and Dobson, 2003; Stefani 2004). In medicine, these pathologies are called "Amyloidoses". Approximately 25 different proteins and peptides are known to be able to form amyloid fibrils in various diseases. The polypeptides involved include full-length proteins (e.g. lysozyme, transthyretin), biological peptides (e.g. insulin, human amylin) and fragments of larger proteins produced by specific processing or by more general degradation (e.g the Alzheimer β-peptide). The peptides and proteins associated with the main amyloid diseases are listed in Table 1.2. These diseases can be grouped into three different categories (Chiti and Dobson 2006):

- neurodegenerative diseases, in which aggregation occurs in the brain (such as AD, PD, TSEs and Huntington's disease).
- non-neuropathic localized amyloidoses, in which aggregation occurs in a single type of tissue other than the brain (such as NIMMD and medullary carcinoma of the thyroid).
- non-neuropathic systemic amyloidosis, in which aggregation occurs in multiple tissues (such as lysozyme amyloidosis and fibrinogen amyloidosis).

Spinocerebellar ataxia 17	TATA box-binding protein [whole or poly(Q) fragments]
Alzheimer's disease	Aβ peptides (plaques); tau protein (tangles)
Spongiform encephalopathies	Prion (whole or fragments)
Parkinson's disease	α-synuclein (wt or mutant)
Primary systemic amyloidosis	Ig light chains (whole or fragments)
Secondary systemic amyloidosis	Serum amyloid A (whole or 76-residue fragment)
Fronto-temporal dementias	Tau (wt or mutant)
Senile systemic amyloidosis	Transthyretin (whole or fragments)
Familial amyloid polyneuropathy I	Transthyretin (over 45 mutants)
Hereditary cerebral amyloid angiopathy	Cystatin C (minus a 10-residue fragment)
Haemodialysis-related amyloidosis	β_2-microglobulin
Familial amyloid polyneuropathy III	Apolipoprotein AI (fragments)
Finnish hereditary systemic amyloidosis	Gelsolin (71 amino acid fragment)
Type II diabetes	Amylin (fragment)
Medullary carcinoma of the thyroid	Calcitonin (fragment)
Atrial amyloidosis	Atrial natriuretic factor
Hereditary non-neuropathic systemic amyloidosis	Lysozyme (whole or fragments)
Injection-localised amyloidosis	Insulin
Hereditary renal amyloidosis	Fibrinogen α-A chain, transthyretin, apolipoprotein AI, apolipoprotein AII, lysozyme, gelsolin, cystatin C
Amyotrophic lateral sclerosis	Superoxide dismutase 1 (wt or mutant)
Huntington's disease	Huntingtin
Spinal and bulbar muscular atrophy	Androgen receptor [whole or poly(Q) fragments]
Spinocerebellar ataxias	Ataxins [whole or poly(Q) fragments]

Table 1. A summary of the main amyloidoses and proteins or peptides involved.

It has also been demonstrated that many non-pathological peptides and proteins can aggregate *in vitro*, under appropriate conditions, into fibrils which are indistinguishable from those associated with amyloid diseases (Guijarro *et al.* 1998; Litvinovitch *et al.* 1998; Chiti *et al.* 2001; Uversky and Fink 2004). The amyloidogenic proteins, either related or unrelated to a disease, are very different in their sequence, function, size and tertiary structure, but all of them are able to form fibrils that share very similar morphological, structural and tinctorial features with amyloid. All these evidences led to the idea that the propensity to form amyloid fibrils is not an unusual feature of the small number of proteins associated with diseases, but is instead a generic property of polypeptide chains. A modification in the three-dimensional structure can be therefore sufficient to enable the production of aggregation-prone species by many, if not all, proteins or peptides.

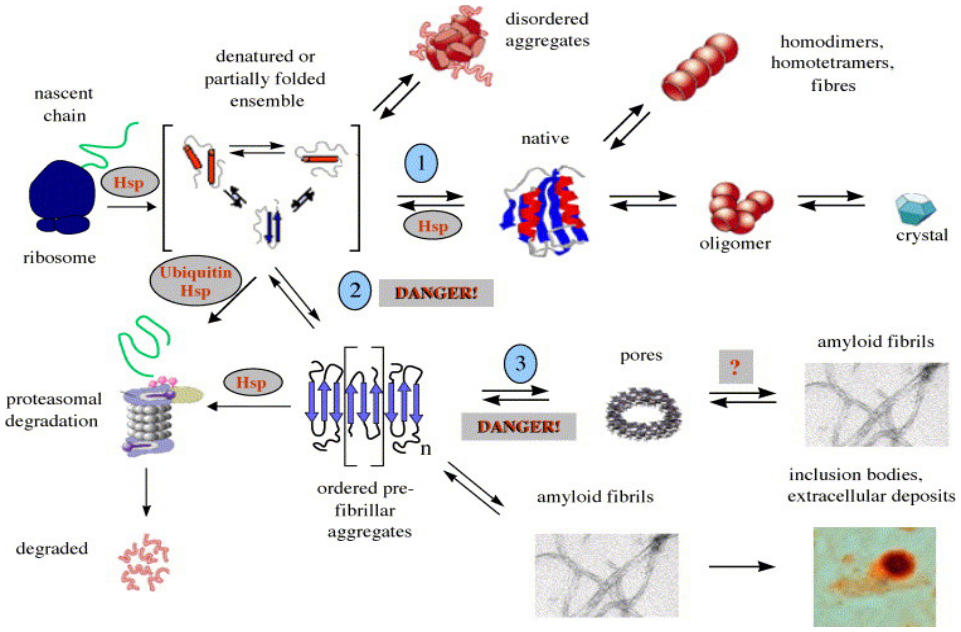

Figure 2. The possible fates of newly synthesized polypeptide chains. The equilibrium 1 between partially folded and native molecules is usually strongly in favour of the latter, except as results of mutations, chemical modifications or destabilizing solution conditions. Under normal conditions, the increased partially or completely unfolded populations are refolded by molecular chaperones (Hsp) or cleared by the ubiquitin–proteasome machinery. When these clearance machineries are impaired, disordered aggregates arise or the aggregation path (equilibrium 2) is undertaken, towards the nucleation of prefibrillar assemblies that eventually grow into mature amyloid fibrils (equilibrium 3). The formation of prefibrillar assemblies as amyloid pores could be directly related to the cytotoxic effects of amyloids. The question mark indicates that it is not known whether amyloid pores are on path or dead end intermediates of fibril formation. DANGER! indicates the processes generating prefibrillar assemblies, presently considered mostly associated with cell impairment. Molecular chaperones may suppress the appearance of prefibrillar aggregates by reducing the population of misfolded protein molecules assisting their correct folding or favouring their complete misfolding for proteasome degradation (Stefani 2004).

Amyloidoses belong to the larger group of misfolding or conformational diseases, because protein aggregation into amyloid fibrils results from the presence of "misfolded" forms of a specific protein/peptide that lose their functional, native conformation and are often devoid of their normal biological activity. Such proteins, fail to reach or to maintain their correct native three-dimensional structure and may aggregate and/or interact inappropriately with other cellular components, leading to impairment of cell viability. These events can be due to mutations, changes in the environmental conditions, such as pH or temperature, misprocessing or proteolysis. The possible fates of a newly synthesized polypeptide chain are described in Figure 2. Perturbations of the conformational properties of the polypeptide may affect equilibrium 1, increasing the population of partially unfolded or misfolded species which are more prone to aggregation than the native state.

1.3 Structure and formation of amyloid fibrils

In general a protein or a peptide is termed as amyloid if, due to an alteration of its native functional state, it converts from its soluble functional state to a particular insoluble form, called the β-pleated-sheet, whose polymerization originates highly organized fibrillar aggregates. These structures are defined "amyloid fibrils" or "plaques" when they accumulate extracellularly or as "intracellular inclusions" when they are formed inside the cell (Chiti and Dobson 2006). The presence of amyloid fibrils (either ex vivo or *in vitro*) is defined by the following three criteria (Nilsson 2004):

1) All amyloid fibrils are able to bind the dye Congo red, giving rise to an apple-green birefringence when observed under cross-polarized light.
2) All amyloid fibrils have a fibrillar morphology and appear as long, straight, unbranched fibers, with a diameter of 70-120 Å and a variable length (Serpell 2000), when they are investigated by electron or atomic force microscopy.
3) All amyloid fibrils are enriched in β-sheet secondary structure.

The fibrils are also stained with Thioflavin T (ThT), giving a shift in the fluorescence of the dye (Levine, 1993; Munishkina and Fink 2007). Both circular dichroism (CD) and

Fourier transform infra red spectroscopy (FT-IR) detect a high β-sheet content in amyloid fibrils, even when the precursor monomeric peptide or protein is substantially disordered or rich in α-helical structure. Finally, amyloid fibrils reveal a typical X-ray diffraction pattern indicating the presence of the characteristic cross-β structure in the fiber (Sunde *et al.* 1997).

The cross-β structure and texture is a robust, stable structure in which the protein chains are securely held together by repetitive hydrogen-bonding that extends for the whole length of the fibrils. An amyloid fibril usually appears as composed by two to six 20-35 Å wide "protofilaments", which are often twisted around each other to form supercoiled rope-like structures arranged around a hollow centre (Serpell *et al.* 2000). Each protofilament in such structures appears to have a highly ordered inner core that consists of polypeptide chains arranged in the characteristic cross-β structure. In this organization, the β-strands run perpendicularly to the protofilament axis, resulting in a series of β-sheets that propagate along the fibril axis (Fig.3). So the cross-β structure of the core of the amyloid aggregates is the main structural peculiarity of these assemblies.

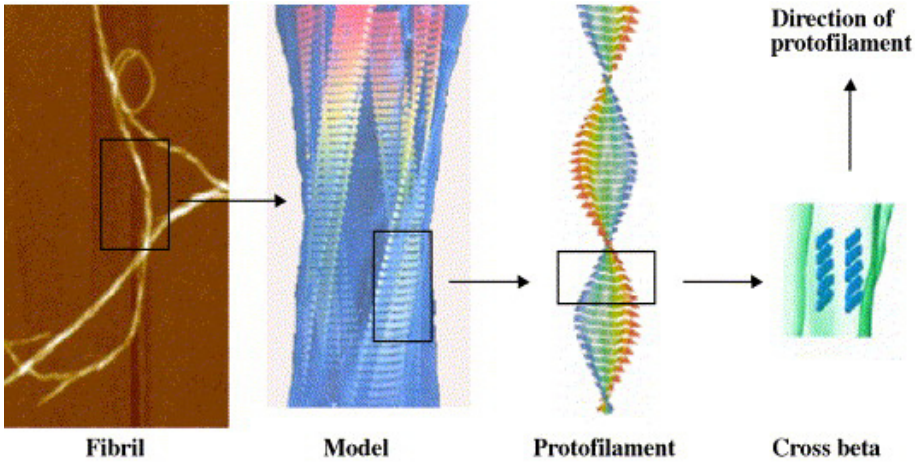

Figure 3. Close-up view of the structural organization of an amyloid fibril. Four protofilaments are wound around each other and their core structure is a row of β-sheets where each strand runs perpendicular to the fibril axis (Stefani, 2004).

The X-ray diffraction pattern characteristic of the cross-β structure consists of a sharp 4.7 Å meridional reflection arising from the spacing between hydrogen-bonded β-strands within a β-sheet. A broad reflection centred at 10 Å on the equator is also observed, which arises from the inter-sheet spacing (Fig.4). The spacing between the β-sheets depends on the size of the side-chain groups (Makin and Serpell 2005).

So far, little is known about the detailed arrangement of the polypeptide chains into the amyloid fibrils, either those parts which form the core β-strands or the regions that connect the β-strands. Recent studies indicate that the sheets are relatively untwisted and they may exist, at least in some cases, in specific super secondary structure such as β-helices (Wetzel, 2002) or the α-helix (Kourie *et al.* 2001). There may be important differences in the way the strands are assembled depending on characteristics of the involved polypeptide chain, including length, sequence (Wetzel 2002; Chamberlain *et al.* 2000) and presence of intramolecular disulfide bonds that stabilize the proteins (Fink 2007).

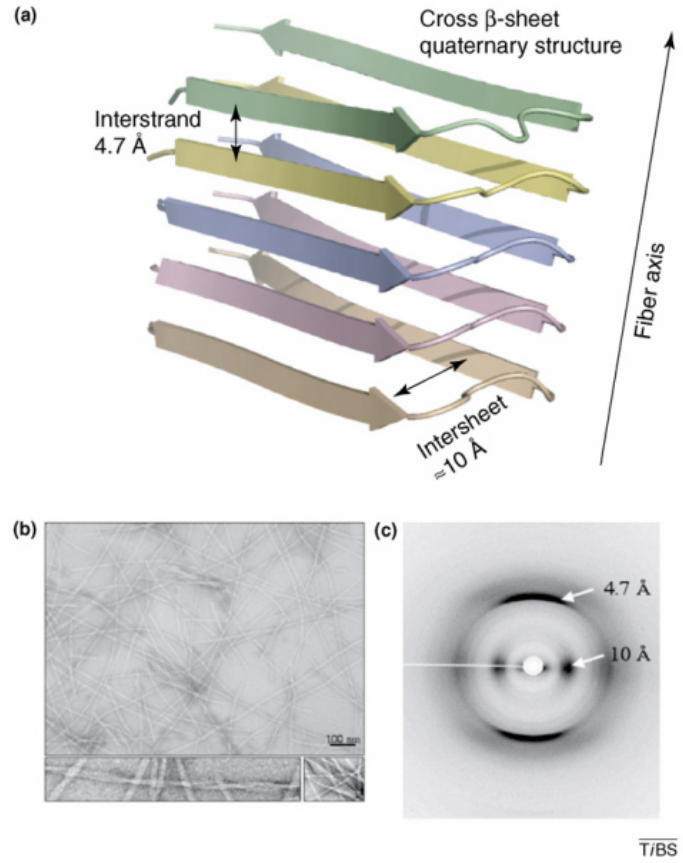

Figure 4. Amyloid is a fibrous protein quaternary structure that has a cross b-sheet fold. (a) The Aβ (1–42) fiber structure obtained from NMR and complementation mutagenesis methodology reveals the characteristic cross b-sheet amyloid structure (PDB code: 2BEG) (Luhrs *et al*. 2005). (b) A transmission electron micrograph of negatively stained amyloid fibers formed from full-length islet amyloid polypeptide (IAPP). Higher magnifications (lower panels) reveal twisted-rope and sheet-like arrangements of individual protofilaments. (c) An X-ray fiber-diffraction pattern from partially aligned Aβ (1–42) amyloid fibers associated with Alzheimer's disease exhibiting the characteristic reflections at 4.7 Å and ~10 Å The meridional reflection at 4.7 Å results from the interstrand repeats, and the ~10 Å equatorial reflection arises from intersheet packing. Molecular graphics were produced with Pymol (http://www.pymol.org) (Fowler *et al.* 2006).

At present, the physico-chemical basis of amyloid formation remains poorly understood. It is largely believed that most amyloidogenic proteins aggregate via a nucleation dependent pathway from an ensemble of partially unfolded conformations. This may occur under solution conditions (such as low pH, lack of specific ligands, high temperature, moderate concentrations of salts or co-solvents), such that the native structure is partially or completely disrupted but under which interactions such as hydrogen-bonds are not completely inhibited. However, native-like mechanisms of aggregation have also been described. For example, "lithostathine" maintains its native content of secondary structure upon aggregation into fibrils (Laurine *et al.* 2003). Association of protein molecules in their native-like states can therefore be the first event in the aggregation process, with the structural conversion into an amyloid conformation occurring subsequently. The time course to convert a peptide or a protein into amyloid fibrils typically includes a lag phase which is followed by a rapid exponential growth phase. The lag phase is assumed to be the time required for "nuclei" to form, where a nucleus is an ordered oligomeric amyloid species that can serve as a template for amyloid growth. When a nucleus is formed, fibril growth proceeds rapidly by further association with the nucleus of either monomers or oligomers. This protein aggregation eventually gives rise to short fibrillar structures referred to as protofibrils, which appear to be precursors of the mature fibrils and are generally shorter than the latter. Moreover, to form amyloid fibrils, proteins adopt at least in most cases, β-sheet-rich conformations. For example, in the case of the Aβ peptides, the main constituents of amyloid plaques in AD, small ordered, β-sheet-rich aggregates or "protofibrils" formed at early stages of amyloid growth have been described (Harper *et al*. 1997). Protofibrils have been observed in heterogeneous populations of small, roughly spherical or tubular assemblies, 2.5-5.0 nm in diameter (Lashuel *et al*. 2002; Poirier *et al.* 2002; Quintas *et al.* 2001). These species are often associated into bead-like chains or annular "doughnut"-shaped rings and appear, in most cases, to be precursors of longer protofilaments and mature fibrils that appear only at later stages of the assembly process. These "early aggregates" formed from different peptides and proteins may be very important to understand the nature and origins of the pathological properties of amyloid structures associated with neurodegenerative diseases. The soluble prefibrillar aggregates of different peptides and proteins have been shown to be equally recognised by polyclonal antibodies raised against prefibrillar assemblies grown from Aβ peptides (Kayed *et al.* 2003). The same antibodies, however, are unable to recognise the

corresponding monomers and fibrillar aggregates, thus confirming that prefibrillar assemblies from very different peptides and proteins share common structural features which are different form those exhibited by the monomers or the mature fibrils.

1.4 Cytotoxicity of amyloid aggregates

The presence of amyloid fibrils in post-mortem brains of demented patients led to the first description of AD and resulted in the hypothesis that mature fibrils themselves could be the primary pathogenic species. However, the absence of any correlation between the amount of fibrillar Aβ deposits at autopsy and the clinical severity of AD during life, the appearance of clinical symptoms of the disease before amyloid plaques can be detected, and several other evidences led to the failure of this initial hypothesis. At present, it is widely believed that early soluble, oligomeric precursors, rather than mature fibrils, are the main pathogenic species of amyloidosis (Hardy and Selkoe 2002). Indeed, many studies carried out on Aβ peptides and other amyloidogenic proteins showed that spherical and/or chain-like oligomers are highly neurotoxic (Lashuel and Lansbury 2006). Moreover, the soluble Aβ levels in human brain are better correlated with the severity of AD than plaques are (Lue *et al.* 1999).

Therefore, the mature fibrils could be seen as inert material substantially harmless to cells, although great controversy still exists on the biological role of fibrils.Indeed, it has been suggested that the large insoluble amyloid deposits may serve as reservoirs that release toxic soluble oligomers (Haass and Selkoe 2007) and recent findings support the existence of a dynamic equilibrium between fibrils and their constituent monomers (Carulla *et al.* 2005). Recently, mature amyloid fibrils produced from full-length recombinant mammalian prion protein (PrP) have been shown to be highly toxic to cultured cells and primary hippocampal and cerebellar neurons, in a manner comparable to that of soluble small β-oligomers generated from the same protein (Novitskaya *et al.* 2006).

Similarly, both oligomers and amyloid fibrils grown from hen lysozyme are toxic to cultured cells, though with different mechanisms and time-scales (Gharibyan *et al.* 2006). Finally, mature fibrils from Aβ1-40 exhibit different morphologies with differing cytotoxicity when they are produced under different conditions.(Petkova *et al.* 2005).

In conclusion, it remains to be established which aggregation state is the main responsible of neurotoxicity, and difficulties in preparing highly homogeneous and stable populations of monomers, oligomeric intermediates and fibrils may account for the reported highly variable experimental results (Kawahara *et al.* 2000). Many amyloid proteins have been shown to induce cellular toxicity by common mechanisms; such a toxicity is likely to arise from the "misfolded' nature of the aggregated species and their precursors and from the exposure, in such species, of hydrophobic residues or regions that are normally buried in the native state. As many of these regions are likely to be aggregation-prone (or "sticky"), they may be able to interact with, and damage, membranes and other cellular components (Bucciantini *et al*. 2002). Indeed, by itself, the intrinsic instability of prefibrillar species that enables them to assemble further and to organize into more ordered structures reflects the presence of accessible regions. In agreement with these conclusions, prefibrillar assemblies have been shown to interact with synthetic phospholipid bilayers (Lin *et al.* 2001; Hirakura and Kagan 2001; Volles and Lansbury 2001) and cell membranes, possibly destabilizing them and impairing the function of specific membrane-bound proteins (Zhu *et al.* 2000; Kourie and Shorthouse 2000). Pre-fibrillar amyloid aggregates may interact with cell membranes in a way similar to the action of many prokaryotic or eukaryotic peptides or proteins (e.g. some bacterial toxins) that oligomerize onto the membranes of the target cells forming pore-like assemblies that destabilize cell membranes and impair ion balance across these structures (referenza). So membrane damage may be a common molecular basis for viability impairment in cells exposed to misfolded proteins or amyloid aggregates. Because of the initial membrane perturbation, changes in the intracellular redox status and free Ca^{2+} levels in cells exposed to toxic aggregates have been described as crucial events in the cell function impairment by the aggregates (Kourie 2001; Milhavet and Lehmann 2002; Wyttenbach *et al.* 2002).

A modification of the intracellular redox state in cells exposed to amyloid aggregates is associated with a sharp increase in the quantity of reactive oxygen species (ROS), resulting in a high oxidizing activity towards several molecular substrates. In addition, changes have been observed in reactive nitrogen species, lipid peroxidation, deregulation of NO metabolism, protein nitrosylation and upregulation of heme oxygenase-1, a specific marker of oxidative stress. Moreover, it has been shown that cells can be protected against amyloid toxicity by treatment with antioxidants.

Although it is not clear why protein aggregation induces production of ROS, in general terms oxidative stress could be related to some form of destabilization of cell membranes by toxic species, leading to an upregulation of the activity of hydrogen peroxidase-producing membrane enzymes, such as NADPH-oxidase and a failure in regulation of other plasma membrane proteins, such as receptors and ion pumps (Mattson 1999) and/or to impairment of mitochondrial function. Mitochondria play an important role in oxidative stress and apoptosis; in this regard, a key factor in Aβ peptide neurotoxicity could be the opening of mitochondrial permeability transition pores by Ca^{2+} entry in neuronal mitochondria followed by release of cytochrome c, a strong inducer of apoptosis. It has been suggested that intracellular ROS increase following exposure to amyloid aggregates is a consequence of Ca^{2+} entry into cells followed by stimulation of oxidative metabolism aimed at providing the ATP needed to support the activity of membrane ion pumps involved in clearing excess Ca^{2+}. ROS increase would in turn oxidize not only the proteins involved in ion transfer but also proteins such as calmodulin that, when oxidized, is unable to activate the Ca^{2+}-ATPase. The down-regulation of the Ca^{2+}-ATPase activity would then reduce the need for ATP, and hence ROS production by oxidative metabolism, leading to a further increase in intracellular Ca^{2+} concentration (Squier 2001). This hypothesis can explain the relationship between ROS, apoptosis, mitochondrial damage and intracellular free Ca^{2+} increase shown by cells exposed to toxic amyloid aggregates. Calcium dysregulation and oxidative stress have been observed in AD, PD, NIMMD and prion diseases, as well as in cultured cells exposed to prefibrillar aggregates of disease-unrelated proteins. The increase in intracellular free Ca^{2+} levels is probably a consequence of the impairment of membrane permeability and may be a consequence of the presence into the membrane of unspecific amyloid pores or may follow oxidative stress, membrane lipid peroxidation producing reactive alkenes such as 4-hydroxynonenal, and the chemical modification of membrane proteins acting as ion pumps (Varadarajan *et al.* 2000).

1.5 Protein-membrane interaction and cytotoxicity

It is largely accepted that the toxicity of protein amyloid aggregates is mainly induced by their interaction with the cell membranes. The toxic aggregates are known to interact with cellular membranes and to compromise their integrity, by forming a range of ion channels through which they lead to imbalance of ion homeostasis and oxidative stress, eventually leading to cell death. Such a mechanism is reminiscent of the action of pore-forming proteins such as peptides found in venoms and antimicrobial secretions, bacterial toxins, perforin (Stefani and Dobson, 2003). The protein-membrane interaction is enabled by the presence, at the surface of the misfolded protein/peptide, of exposed hydrophobic residues and clusters, which prefer the hydrophobic environment of the lipid membranes (Kourie and Henry, 2002).In addition to the hydrophobic interactions, electrostatic interactions can also play an important role: amyloidogenic peptides often possess distinct positively charged regions allowing them to interact with negatively charged membranes.

The extent and the mechanism of membrane destabilization depends upon the balance of the electrostatic and hydrophobic properties and the amphipatic character of the protein. Membrane alterations induced by proteins can vary depending on the nature of the protein and lipids. Some peptides disrupt the membrane by binding through electrostatic interaction to the charged residues or regions to the charged headgroups of the phospholipids (Fujii 1999). This disturbance, likely to be reversible by itself, may be followed by insertion of hydrophobic regions of the protein into the bilayer. Following protein insertion, the cell membrane can be affected in several ways (general electrostatic disturbance, fusion of vesicles, loss of membrane integrity, alteration in membrane thickness around the protein and/or pore formation).

The similarity between the mechanism of toxicity of pore-forming toxins (Kourie and Shorthouse, 2000; Kourie and Henry, 2002) and the cytotoxicity of amyloid aggregates led to propose, since 1993, the “channel hypothesis” (Arispe *et al.* 1993); a number of experimental data, coming from both artificial lipid bilayers and cell membranes, indicate that the ability of misfolded proteins and amyloid aggregates to interact with lipid membranes is of crucial importance.

Protein aggregates can exert their toxic effect in several ways:
1) by insertion into the membrane lipid bilayer to form ion channels (Kourie and Henry, 2002 ; Kourie, 2001);
2) by modifying the membrane viscosity and lipid packing (Salmona *et al.* 1997; Tagliavini *et al*. 2001) thus interfering with membrane proteins;
3) by penetrating into the cell with subsequent interaction with intracellular components (reviewed in Kourie and Henry, 2002).

Many proteins have been shown to undergo changes in secondary structure upon their toxic interaction with membranes. Both α-helix to β-sheet and β-sheet to α-helix transformations, as well as secondary structure increase from a random coil conformation, have been described. For example, for some natively unfolded polypeptides like Aβ peptides, calcitonin and human amylin, the literature strongly suggests that these peptides populate an early oligomeric helical intermediate during amyloid aggregation *in vitro*. So, unfolding of the α-helix of a protein followed by refolding to β-sheet may be an important step in inducing a membrane-active structure for cytotoxic peptides, such as prion and Aβ peptides or human amylin. However, it is important to note that both β-sheet and α-helix-based protein structural changes could confer cytotoxicity to refolded proteins.
While it appears that no particular secondary structure confers an inherent advantage for membrane interaction, it may be that, for any particular peptide, some specific structure may allow better access of the hydrophobic residues to the membrane. This means that a change in secondary structure mayundergo the ability to interact with the membrane. Anyway it is important to underline that the changes in secondary structure often arise as a consequence of the contact with the lipid environment: the hydrophobic lipids allow for lower energy exposure of hydrophobic residues, which leads to a rearrangement of the whole protein. The importance of secondary structure in hydrophobic residues exposure was shown by Gasset *et al*., who analyzed the structural requirements of α-sarcin to destabilize lipid bilayers. It was hard to explain the hydrophobic interactions of α-sarcin with a membrane, because this protein is highly polar in its native conformation. They demonstrated that, upon interaction with lipid vesicles, α-sarcin undergoes a structural change, with an increase in α-helix and decrease in β-sheet content from the most unfolded variant (Gasset *et al*. 1995).

The 106-126 fragment of PrP, which is the main part of the small amount of β-sheet in the normal cellular prion (PrP^c), contains a hydrophobic core sequence (residues 113-120), which is hypothesized to be involved in prion toxic properties via membrane interaction and destabilization, thus playing a key role in the pathological effect of the protein. It has been reported that β-sheet content of PrP[106-126] increases in the presence of lipids, and this structural change contributes to membrane destabilization and PrP[106-126] toxicity. The cytotoxic effect of amyloid β protein has been shown to involve the formation of ion channels within cell membranes, thus altering cell function and regulation. The Aβ peptide fragments, which are between 39 and 42 residues in length, are involved in forming these channels through a hydrophobic region at the C-terminus. The incorporation of Aβ peptides into membranes to form ion channels is thought to be determined preferentially by the presence of negatively charged, rather than by neutral, phospholipids (Alarcon *et al.* 2006). α-synuclein protofibrils, that are thought to be the main responsible of cell death in parkinson's disease (PD) and form annular structures which are reminiscent of the known structures of toxin pores (Ding *et al.* 2002), have also been found to tightly bind and to permeabilize acidic phospholipid vesicles in a pore-like fashion, with a strong size selectivity in allowing molecules to cross the cell membrane (Volles *et al.* 2001). Calcitonin, an amyloid-forming peptide consisting of 32 residues, is known to be able to interact with membranes either directly and/or at receptor sites. Recent data showed that annular oligomers from salmon calcitonin are able to form Ca^{2+}-permeable pores when inserted into liposomes, and that such an interaction is accompanied by an increase in the β-sheet content of the protein (Diociaiuti *et al.* 2006).

Mechanisms of membrane disruption other than pore formation have also been described: for example, according to some studies, human islet amyloid polypeptide (hIAPP), which is associated with death of insulin-producing pancreatic β-cells in type 2 diabetes mellitus and permeabilizes a variety of model membranes, could destroy the barrier properties of the cell membrane by extracting lipids from the latter and taking them up in the forming amyloid fibrils. It is important to note that the exact mechanism of membrane disruption by hIAPP aggregates is not known. However, lipid extraction has been shown to occur for a variety of proteins and has been proposed as a generic mechanism underlying amyloid toxicity (Sparr *et al*. 2004).

1.6 Membrane lipid composition influences protein aggregation

The fibrillogenic properties of membrane-bound proteins are determined by the chemical nature of membrane lipids and the mode of protein-lipid interactions. A lot of studies on membrane-mediated fibrillogenesis have been undertaken with model systems such as amyloidogenic peptides or proteins and lipid vesicles of varying composition (Bokvist *et al*. 2004; Sparr *et al*. 2004). Membranes may be implicated not only as targets of aggregate toxicity, via disruption of membrane integrity, but also as catalyst that facilitate protein conformational changes and oligomer formation. Indeed, it is well established that lipid membranes can promote the aggregation of many different proteins/peptides. In particular, lipid composition, especially the presence of negatively charged lipids in the membrane, appears as one of the primary factors that determine the extent of membrane-mediated aggregation.

Many studies have been carried out to investigate the potential of acidic phospholipid-containing membranes in providing an environment able to enhance amyloid formation. For example, the formation of fibrous aggregates by a number of proteins in the presence of acidic, negatively-charged phospholipids, such as phosphatidylglycerol (PG), cardiolipin, or phosphatidiylserine (PS), has been described in recent studies. Membranes containing PS, an acidic phospholipid which is normally expressed in the outer surface of the plasma membrane of cancer cells and vascular endothelial cells in tumours, have been suggested to create surfaces with a high local concentration of protons, required for aggregation (Zhao *et al*. 2004). All these proteins share the presence of cationic residues or cationic amino acid clusters able to interact with negatively charged lipids, with subsequent fusion. Binding to acidic phospholipids neutralizes the positive charges in these proteins; accordingly, protein-protein interactions would not be counteracted by repulsion due to cationic residues, thus facilitating protein aggregation. The fibrils formed under these conditions have also been shown to incorporate lipid molecules, thus suggesting a lipid extraction by the protein on the membrane (Sparr *et al*. 2004; Zhao *et al*. 2004). The liposome-induced fiber formation has been described as very rapid, with macroscopic structures becoming clearly visible almost instantaneously after the addition of the protein to a solution of PS-containing liposomes. Enhanced fiber formation has been seen to occur also on

negatively charged mica, thus underlining the important role of these surfaces for all amyloidogenic proteins (Zhu *et al*. 2002).

Increasing evidence has indicated that gangliosides, particularly GM1 in lipid rafts play a pivotal role in amyloid deposition of Aβ and the related cytotoxicity in AD. Despite recent efforts to characterize Aβ-lipid interactions, the effect of Aβ aggregation on dynamic properties and organization of lipid membranes is poorly understood.

1.7 The importance of GM1

Growing evidence shows that GM1 ganglioside is involved in amyloid deposition and toxicity. Glycosphingolipids possess highly heterogeneous and diverse molecular structures in their carbohydrate chains and the lipid moieties. Based on their basic carbohydrate structures, glycosphingolipids are classified into numerous series, namely ganglio-, isoganglio-, lacto-, neolacto-, lactoganglio-, globo-, isoglobo-, muco-, gala-, neogala-, mollu-, arthro-, schisto- and spirometo-series (Table 2). Acidic glycosphingolipids containing one or more sialic acid (N-acetylneuraminic acid or N-glycolylneuraminic acid) residue(s) in their carbohydrate moiety are especially referred to as gangliosides. Gangliosides are ubiquitously found in tissues and body fluids, and are more abundantly expressed in the nervous system (Yu *et al*. 2009). In cells, gangliosides are primarily, but not exclusively, localized in the outer leaflet of plasma membrane.

On the cell surface, together with other membrane components such as sphingomyelin and cholesterol, gangliosides are involved in cell-cell recognition and adhesion and signal transduction within specific cell surface microdomains, termed caveolae (Anderson RG. 1998), lipid rafts (Simons K 2000) or glycosphingolipid-enriched microdomains (Hakomori S. 1998).. In addition to the cell plasma membrane, gangliosides have been shown to be present in the nuclear membrane, and they have recently been proposed to play important roles in modulating intracellular and intranuclear calcium homeostasis and the ensuing cellular functions (Ledeen *et al*. 2008).

Series	Basic structure	Abbreviation
Globo	GalNAcβ1 −3 Galα1 −4Galβ1 −4Glcβ1 −1 'Cer	Gb
Isoglobo	GalNAcβ1 −3 Galα1 −3 Galβ1 −4Glcβ1 −1 'Cer	iGb
Ganglio	Galβ1 −3 GalNAcβ1 −4Galβ1 −4Glcβ1 −1 'Cer	Gg
Isoganglio	Galβ1–3 GalNAcβ1–3 Galβ1–4Glcβ1–1'Cer	iGg
Lacto	Galβ1 −3 GlcNAcβ1 −3 Galβ1 −4Glcβ1 −1 'Cer	Lc
Neolacto	Galβ1 −4GlcNAcβ1 −3 Galβ1 −4Glcβ1 −1 'Cer	nLc
Lactoganglio	GalNAcβ1–4(GlcNAcβ1–3)Galβ1–4Glcβ1–1'Cer	LcGg
Muco	Galβ1–4Galβ1–4Glcβ1–1'Cer	Mc
Gala	Galα1–4Galβ1–1'Cer	Ga
Neogala	Galβ1–6Galβ1–6Galβ1–1'Cer	
Mollu	GlcNAcβ1–2Manα1–3Manβ1–4Glcβ1 −1'Cer	Mu
Arthro	GalNAcβ1–4GlcNAcβ1–3Manβ1–4Glcβ1–1'Cer	At
Schisto	GalNAcβ1–4Glcβ1–1'Cer	
Spirometo	Galβ1–4Glcβ1–3Galβ1–1'Cer	

Table 2. Carbohydrate structures of glycosphingolipids (J Oleo Sci. 2011)

Gangliosides are involved in the pathology of many diseases. For example, Guillain-Barré syndrome, an acute polyradiculoneuropathy that leads to acute quadriplegia, is caused by an autoimmune response to cell surface gangliosides (Kaida *et al* 2009). In influenza, a well known viral infectious disease, influenza A viruses recognize sialic acid residues of gangliosides and glycoproteins on cell surfaces as receptor molecules for cell invasion (Suzuki Y 2005). During aging and neurodegeneration, the physicochemical properties of membranes are altered. This can result in unbalanced proportion of lipids in the membrane and/or in changed ratios of membrane lipids, which may contribute to Alzheimer's disease (AD) pathogenesis (Kalanj-Bognar, S. 2006). In brain cells, ganglioside and lipid abnormalities, in addition to pathogenic Aβ production, may contribute to the pathological conditions found in AD (Mutoh *et al*. 2006).

Altered distribution of GM1 and GM2 gangliosides has recently been found in AD brains (Pernber *et al*. 2012). The interaction with GM1 has been reported to be a crucial factor also in mediating the aggregation and toxicity of other amyloidogenic proteins and peptides (Gellermann *et al*. 2005; Wakabayashi and Matsuzaki 2009), such ashIAPP, whose aggregation and binding to the plasma membrane is thought to be the main factor determining the death of pancreatic β-cells in type II diabetes (Engel MF 2009). While plasma membrane permeation and deformation have been the subject of

many studies, the impairment and dysfunction caused by changes in mobility and lateral trafficking of membrane molecules induced by amyloid aggregates have been poorly investigated. Considering that amyloids can bind to a large number of biological molecules that range from glycosaminoglycans and nucleic acids to a variety of proteins and lipids, the change in membrane dynamics observed for GM1 may imply that amyloids can potentially harm all those cellular mechanisms that base their efficiency on molecules mobility (Calamai and Pavone 2013). Actually, growing evidence shows that amyloid aggregates can alter membrane mobility of a number of proteins and other plasma membrane components, leading either to a gain or to a loss of function. For example, the binding of Sup35 amyloid fibrils to the plasma membrane can cause an accumulation of Fas receptors associated with GM1 with subsequent activation of the extrinsic apoptotic pathway (Bucciantini *et al*. 2012). On the other hand, sequestration of neurotransmitter receptors, such as the metabotropic glutamate mGluR5, by Aβ 1-42 oligomers has been shown to impair intracellular calcium levels and synaptic network activity (Renner *et al*. 2010). Within this context, an alteration of GM1 mobility may compromise its regulatory role in neurodevelopment and neuroprotection (Furukawa *et al*. 2011; Yu *et al*. 2012), or influence cellular pathways linked to raft dynamics.

2 Proteins involved in this study

2.1 Transthyretin structure

Transthyretin (TTR) was first discovered in the cerebrospinal fluid (CSF) in 1942 (Hamilton *et al*. 2001; Kabat *et al*. 1942) and then sequenced in 1984 (Mita *et al*. 1984), and named prealbumin because of its electrophoretic migration pattern compared to albumin. Afterwards, aiming to better describe its functionality, the name was changed to transthyretin- the transporter of thyroxine (T4) and retinol binding protein (Hamilton *et al*. 2001). Transthyretin transports only 25% of all thyroxine in the blood plasma, the other 75% resulting from thyroxine-binding globulinHowever, TTR is the main thyroxine transporter in cerebrospinal fluid, implying a main role in the central nervous system. TTR has been known to "promiscuously" bind to many small molecules, particularly aromatic compounds such as resveratrol, diflunisol (a drug), and PCB (a toxin). Therefore, it is believed that transthyretin's real function is to clean the bloodstream by removing toxins and drugs.

TTR is a 55 kDa tetramer composed by four identical 127 residue monomeric subunits. Each monomer is composed of two four-stranded beta-sheets together with a small helical region. The two four-stranded beta-sheets run antiparallel, one forming the external surface and the other the binding channel surface. Two associated monomers form an extended beta-sandwich stable dimer by hydrogen bonding between beta sheets of each monomer. Further association of two dimers originates a tetrameric structure known as transthyretin. TTR has two thyroxine binding sites that sit in a central channel at the interface between the two dimers. The channel is created by contact through symmetry related loops by the two dimers. The binding sites are funnel-shaped and mainly hydrophobic, with some hydrophilic residues near the entrance of the binding site (Monaco *et al*. 1995).

The crystallographic structure of human TTR, solved in 1971 (Blake *et al*. 1971), revealed that each TTR monomer is composed of 127 amino acid residues, forming 8 β-strands named from A-H, which are arranged in a β-sandwich of two four-stranded β-sheets and one small α-helix found between β-strands E and F (Blake *et al*. 1971; Foss *et al*. 2005;). TTR monomers interact via hydrogen bonds between the antiparallel, adjacent β-strands H-H' and F-F' to form a dimeric species. The two dimers (A-B and C-D) predominantly form the tetramer through hydrophobic contacts between the

residues of the A-B and G-H loops. The tetramer forms a central hydrophobic pocket (T4 channel) with two binding sites for hormones (Blake *et al*. 1971; Foss *et al*. 2005). Each TTR monomer contains one cysteine residue at position 10 and two tryptophan residues at positions 41 and 79, which can be used as a tool to monitor protein unfolding (Silva *et al*. 2006). Many groups have studied the structure of TTR and its aggregation process to understand the factors that favour TTR aggregation, which occurs in a non-nucleated manner known as a downhill polymerisation reaction because tetramer dissociation into monomers is the rate-liming step of the aggregation reaction (Hurshman *et al*. 2004). Based on this model, many studies have focused to develop effective and selective TTR ligands that can prevent TTR dissociation and aggregation (Johnson *et al* 2012).

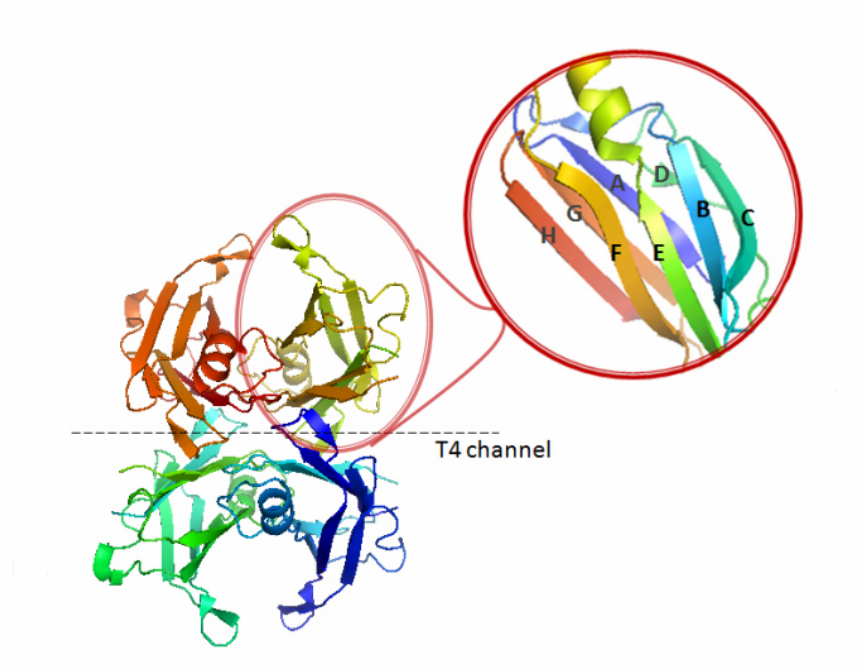

Figure 1. X-ray structure of Transthyretin. TTR is a homotetrameric protein composed of four monomers of 127 aminoacids. Structurally, in its native state, TTR contains eight stands (A-H) and a small α-helix. The contacts between the dimers form two hydrophobic pockets where T4 binds (T4 channel). As shown in red, each monomer contains one small α-helix and eight β-strands (CBEF and DAGH). Adapted from a model; PDB code 1DVQ (Azevedo *et al*. 2013).

The primary ligand of TTR, thyroxine, binds deeply in the cleft of the channel surface between the side chains of L17, A18, and L110. Thyroxine has a phenolic substituent which is important for TTR ligands. This phenolic ring interacts with S117 and T119 at the tetramer center, and also interacts with E54 and K15 near the binding channel entrance. Thyroxine makes hydrogen bond contacts well with K15 and E54 which contribute to hold thyroxine in the binding channel (Wojtczak *et al*.1996).

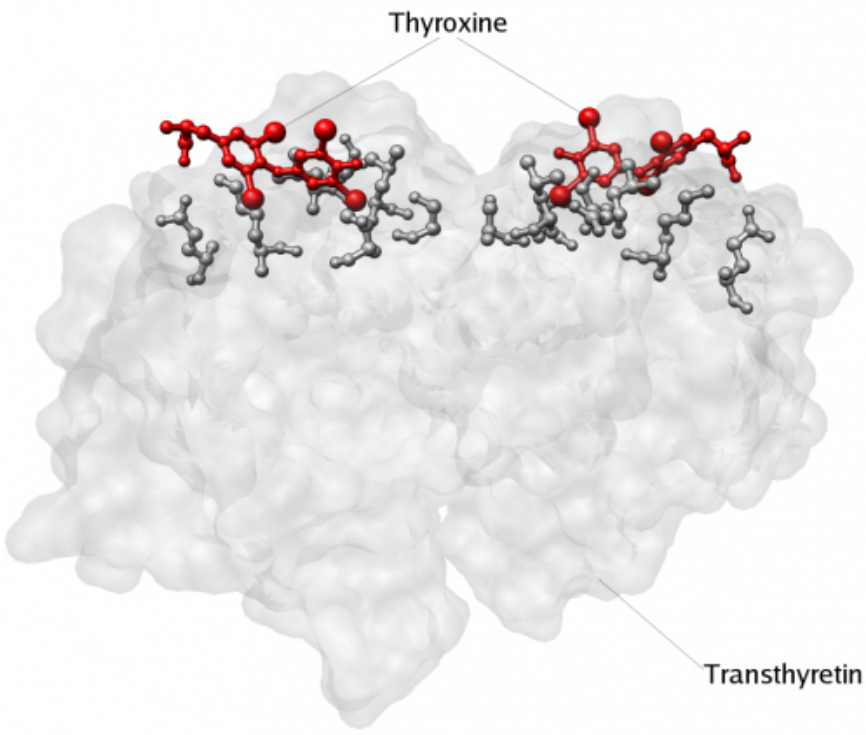

Figure 2. A surface representation of one dimer of the transthyretin tetramer along with a ball and stick representation of thyroxine showing how thyroxine sits within the cleft of the TTR binding channel. The gray ball and stick residues are those that make contact with thyroxine, colored in red. (PDB ID: 2rox, Wojtczak *et al*. 1996).

Within the binding site of TTR, there are small depressions named halogen binding pockets (HBPs) that bind the four iodine substituents of thyroxine and other ligands. Each monomer has three halogen-binding pockets, and since there are two binding sites, there are six HBPs per binding site and twelve HBPs overall. As mentioned earlier, thyroxine contains 4 iodine atoms bound in two different conformations; either a "forward" conformation or a "backward conformation". When thyroxine is bound to TTR, four of the six HBPs are occupied. Halogens are negatively charged ions, so they prefer the positively charged side chains of certain residues. HBPs occupation is of primary importance because they contribute strongly to the overall binding affinity between TTR and thyroxine. All three HBPs provide a depressed, hydrophobic surface. A conformational change in TTR provides additional residues for hydrogen binding. Halogen-binding pocket 1 (HBP1) is formed between the side chains of Methionine13, Lysine 15, Threonine106, and Alanine108. It is the outermost pocket and is positioned between strands A and G of the monomer. Lys15 and Glu54 make a significant

contribution to ligand binding near where the HBP1 pocket is formed. Halogen-binding site 2 (HBP2) is formed between the side chains of Lys15, Leu17, Ala109 and Leu110. The pocket is primarily hydrophobic and has nucleophilic contributions from the carbonyl groups of Lys15, Ala108 and Ala109. The innermost pocket in the tetramer center, the halogen-binding site 3 (HBP3), is located between the side chains of Ala108, Ala109 and Leu110 of strand G and Ser117 and Thr119 of strand H (Wojtczak *et al*. 1996).

Transthyretin binds retinol (vitamin A) through the retinol-binding protein. and favour its circulation through the body. Each TTR tetramer can bind a maximum of two retinol molecules and two RBPs may be complexed. The overall structure of the 1:2 TTR-RBP complex can be seen below in figure 4A. RBP binds to the alpha helix at the surface of the TTR molecule while the thyroxine-binding site is positioned in the hydrophobic channels at the TTR dimer-dimer interface. Retinol binds deep within RBP. Retinol must be bound to RBP for a stable complex can be made with TTR. Once retinol is removed from the complex, the complex loses stability and dissociates. A few specific residues are important for TTR-RBP complex formation. Leu35, Trp67, Lys89, Trp91, Ser95, Phe96, Leu97, and Lys99 are significant contact residues of the RBP. TTR has contributions from 3 different monomer chains at the TTR-RBP interface: Asp99 and Ser100 from the A chain, Gly83, Ile84, Ser85, and Tyr114 from the B chain, and Val20, Arg21, and Ile84 from the C chain all make contact with RBP residues (Monaco *et al*. 1995).

2.2 TTR-related amyloidosis

Transthyretin is one of the 25 known proteins that are capable of forming amyloid fibrils *in vivo*. Transthyretin amyloidosis is a systemic disorder characterized by the extracellular deposition of amyloid fibrils composed of TTR. The TTR amyloidoses include senile systemic amyloidosis (SSA), familial amyloid cardiomyopathy (FAC), familial amyloid polyneuropathy (FAP), and central nervous system selective amyloidoses (CNSA). SSA is a common age-related amyloidosis that involves the accumulation of wt TTR predominantly in the heart as well as in other organs, e.g., the lungs, kidneys and gastrointestinal tract. 10-15 % of individuals older than 65 years and one-quarter of people aged over 85 years are affected (Ueda *et al*. 2011). Pathologically, the TTR amyloid deposits exhibit a patchy plaque-like shape and develop mainly inside the ventricular wall in SSA, whereas in FAP they develop mainly in the pericardium and the surrounding muscle fascicles (Ueda *et al*. 2011). In SSA, TTR appears fragmented more than 90 % whereas in most hereditary amyloidosis cases with variant TTR it maintains full length. A series of C-terminal TTR fragments with N-terminals ranging from 46 to 55 amino acids in length have been identified in tissues from SSA patients, (Ando and Ueda 2008). A report suggested that myocardial infarction, and variations in the genes for alpha2M and tau may be associated with SSA (Tanskanen *et al*. 2008). The pre-mortem diagnosis of SSA is rare in spite of disease frequency, so it is important to develop several diagnostic methods.

FAC, which is characterized by prominent cardiomyopathy and the absence of polyneuropathy, is associated with the apparently preferential amyloid deposition in the heart of some TTR mutants causing congestive heart failure. The diagnosis of FAC can be made by means of endomyocardial biopsy (Jacobson *et al*. 2011). Three TTR mutations, A45T, L111M and V122I, are associated predominantly with FAC. V122I FAC, which is found in approximately 3–4 % of AfroAmericans and causes late-onset restrictive cardiomyopathy, originated on the west coast of Africa, and its clinical penetrance is thought to be high (Afolabi *et al*. 2000; Jacobson *et al*. 1997). Amyloidotic cardiomyopathy without leptomeningeal involvement is also associated with vitreous opacity.

CNSA, leptomeningeal amyloidosis or meningocerebrovascular amyloidosis is a form of hereditary TTR amyloidosis characterized by primary involvement of the central

nervous system. The clinical features include seizures, stroke-like episodes, dementia, psychomotor deterioration, hydrocephalus, spinal cord infarction, and variable amyloid deposition in the vitreous humor. Pathologically, amyloid is detected in the walls of leptomeningeal vessels and around connective tissue structures, and in the pio-arachnoid and subpial region, which leads to cerebral infarction and, in later stages, cerebral hemorrhage (Blevins *et al*. 2003). Several mutations of the TTR sequence (e.g., L12P, D18G, A25T, V30G, A36P, G53E, G53A, F64S, Y69H, or Y114C) have been reported to be associated with this phenotype (Blevins *et al*. 2003; Connors *et al*. 2003). Mild systemic amyloidosis may also be a complication. Familial oculoleptomeningeal amyloidosis (FOLMA) is a leptomeningeal amyloidosis in association with vitreous amyloid deposits.

FAP is an autosomal dominant inherited disease characterized by amyloid deposition in various organs. FAP, Portuguese type variant I (FAP type I), was first described in 1952 (Andrade 1952). The genetic defect in the kindreds from northern Portugal, i.e. heterozygosity for a Val-to-Met single amino acid substitution at residue 30 (Val30Met), has been reported (Saraiva *et al*. 1984).

Treatment of familial TTR amyloidosis has historically relied on liver transplantation as a crude form of gene therapy (Holmgren G *et al*. 1993). Because TTR is primarily produced in the liver, replacement of the liver gene carrying the mutation with the normal form is able to reduce the mutant TTR levels in the body to < 5% of pretransplant levels. Certain mutations, however, cause CNS amyloidosis, and due to the their production by the choroid plexus, these forms do not respond to liver transplantation.

In 2011, the European Medicines Agency approved Tafamidis or Vyndaqe (Razavi *et al*. 2003) for FAP treatment. Vyndaqel kinetically stabilizes the TTR tetramer, preventing its dissociation required for TTR amyloidogenesis and degradation of the autonomic nervous system (Ando Y and Suhr OB December 1998) and/or the peripheral nervous system and/or the heart (Hammarström *et al* 2003).

2.3 Familial Amyloidotic Polyneuropathy and Transthyretin

Classically, FAP has been classified into four types according to ethnic origin, differing amyloid proteins and patterns of neuropathy; FAP type I (Portuguese, Japanese, and Swedish type) and FAP type II (Indiana/Swiss and Maryland/German type) are associated with TTR. Several TTR mutations associated with FAP type II with the Leu58His variant, in the Maryland/German kindred, Ile84Ser, in the Indiana/Swiss kindred (Wallace *et al*. 1988), and Lys70Asn in a FAP pedigree of German ancestry residing in New Jersey (Izumoto *et al*. 1992), have been reported. Clinically, FAP type II is a systemic disease characterized by carpal tunnel syndrome (CTS), followed by a generalized polyneuropathy developing with vitreous opacity, and death due to myocardial impairment. However, it is inappropriate to classify FAP into type I or II because of the diversity of its symptoms with various TTR mutations, and it has been designated as a TTR-related amyloidosis recently. FAP type III (Iowa type) and IV (Finnish type) involve apolipoprotein A1 and gelsolin, respectively.

The hallmarks of the disease are is inherited, with onset in the second or third decade, an unremitting course to death due to cachexia and infection 7–10 years later, on average, and a characteristic pattern of symptoms; paresis, early impairment of thermal and pain sensibilities, and an- hidrosis in the lower limbs. Concomitant symptoms are nausea, vomiting, abdominal pain, and sexual and sphincter disorders. A unique feature is the dissociated sensory loss. Andrade found that the various sensation modalities were lost in the following order: temperature, pain, touch, and, finally, joint position. On postmortem examination, large amounts of amyloid deposits are found in the kidneys and peripheral nerves and, to a lesser extent, in other organs.

FAP usually presents as a peripheral neuropathy including autonomic failure. The neuropathy usually starts with small-fiber dysfunction in the lower extremities, a lack of thermal sensation being an early feature.. Walking difficulty, weakness, and cardiac or gastrointestinal manifestations are less common at onset. Dysesthesia in the distal parts of the four extremites may be prominent with or without varying degrees of pain. The level of sensory symptoms slowly progresses from the distal to the proximal parts of the four extremities bilaterally. Motor function tends to be relatively preserved until the sensory manifestations become severe. Muscular atrophy is remarkable compared with motor weakness (Benson and Cohen 1977).

Jacobson *et al*. (1992) reported a, early-onset, and rapidly progressive type of FAP with Leu55Pro and severe cardiac involvement. In that study, four of seven cases showed heavy amyloid deposition limited to the blood vessels and nerves in the heart, the thyroid, blood vessels, peripheral nerves, and the gastrointestinal tract. Biochemically, several lines of evidence of severe amyloidogenicity of TTR L55P have been reported (Sebastião *et al*. 1998). The Glu54Lys variant was reported to be an aggressive form of FAP. The Arg104His variant was found to induce structural alterations leading to an increase of tetramer stability heterozygotes for TTR Val30Met in a study of mild-type FAP with TTR Val30Met/Arg104His (Almeida *et al*. 2000). These characteristics are very similar to those found in heterozygotic carriers of TTR Val30Met/Thr119Met. TTR Asp99Asn in a Danish kindred has been reported to be a non-pathogenic benign mutation with properties similar to those of the wt TTR (Groenning *et al*. 2011). These findings suggest that a specific mutation is important for the severity of FAP. The heart and kidneys are the main sites of amyloid deposition other than peripheral nerves in FAP.

At present, no specific treatment for TTR amyloidosis has been proven to prevent or cure the disease. There are various symptoms in FAP, so several conservative therapies for orthostatic hypotension, gastro-intestinal symptoms, anemia, heart failure, neuropathic pain, hypothyroidism, hypoglycemia, decubitus ulcers, and vitreous opacity are needed.

2.4 Mechanisms of wild-type and L55P mutant TTR Aggregation

Over the last decade various groups have elucidated the crystal structure of over 20 mutant TTR variants. While these studies have shown structural differences that could be explained in terms of fibrillar structures, there is no apparent mechanism or conformational change that describes fibril formation by all mutant forms of TTR. More recently, several studies have suggested that mutations of wild-type TTR result in TTR tetramer destabilisation and dissociation into unfolded monomers and dimers which undergo further partial refolding, forming amyloidogenic intermediates (Cardoso *et al*. 2007; Lai *et al*. 1996; Lashuel *et al*. 1998, 1999). Significantly, there is a strong

correlation between the thermodynamic stability of TTR variants and their propensity to form unfolded, soluble aggregates (Quintas *et al*. 2001).

On X-ray analysis, a slight conformational change of the crystal structure of variant TTR was shown (Terry *et al*. 1993), including distortion of the T4-binding cavity, resulting in a decreased affinity for T4. As far as the mechanism underlying the onset of aggregation of wt TTR and several variants is concerned, amyloid fibril formation might be triggered by tetramer dissociation into a compact non-native monomer with low conformational stability, which results in non-fibrillar TTR aggregates or partially unfolded monomeric species that can subsequently self-assemble into profibrils and mature amyloid fibrils (Colon and Kelly 1992; Lai *et al*. 1996; Hammarström *et al*. 2003; Quintas *et al*. 2001). The folded monomer that results from dissociation must subsequently undergo partial denaturation to misassemble into aggregated structures including amyloid fibrils. The monomeric amyloidogenic intermediate undergoes self-assembly into a ladder of quaternary structural intermediates for the formation of wt, Val30Met, and Leu55Pro TTR amyloid fibrils (Lashuel *et al*. 1998).

The V30M mutation is the most frequently occurring variant and an examination of its crystal structure suggests that the substitution drives a conformational change in strand A, exposing Cys10, and increasing thiol group exposure (Terry *et al*. 1993). The growth of fibrils resulting from the association of TTR through disulphide bridges has also been suggested, however the existence of an amyloidogenic *Cys10Arg* (C10A) variant would suggest that such a mechanism is not of significance in V30M fibrillogenesis.

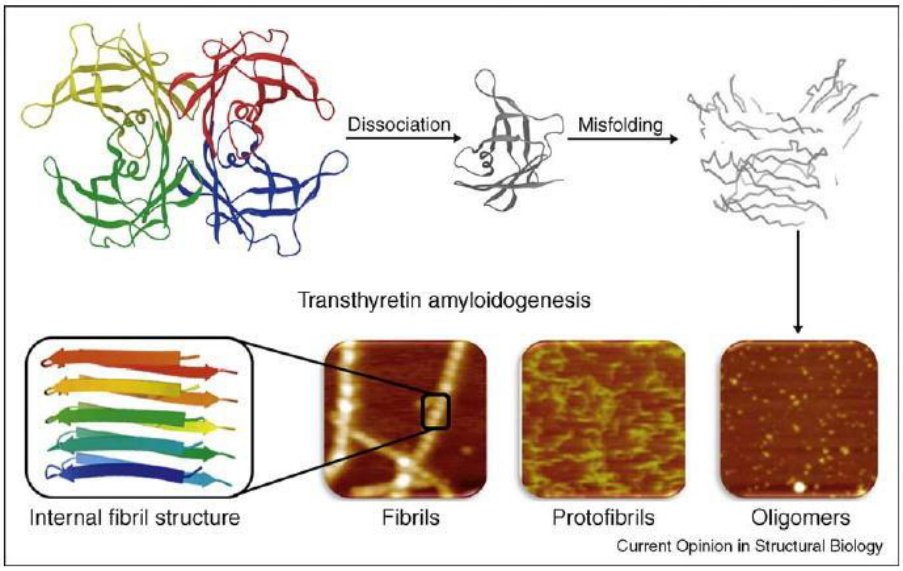

Figure 3. Transthyretin (TTR) amyloid cascade. For amyloidogenesis to occur, the TTR tetramer must dissociate into four folded monomers and undergo partial denaturation in order to subsequently misassemble into a spectrum of aggregate structures including cross-β-sheet amyloid fibrils.

A "hot spot" for amyloidogenic mutations is located in the 45-58 region thet contains the C strand, C-D loop, and D strand which are located at the edge of each dimer (Serpell *et al*. 1995). Several studies have shown that mutant TTR form high molecular weight oligomers more readily than wild-type TTR, and that further aggregation leads to the formation of amyloid fibrils (Kayed *et al*. 2003). There is a good correlation between the rate of aggregation of TTR *in vitro* and the extent or severity of the disease (Hurshman *et al*. 2008; Lashuel *et al*. 1999; Quintas *et al*. 1997). In particular, my work dealt with the L55P mutation, that produces a significantly more aggressive amyloidosis than the more common V30M mutation, and *in vitro* studies have shown that L55P TTR aggregates much more readily than V30M (Quintas *et al*. 1997; Lashuel *et al*. 1998, 1999; Pokrzywa *et al*. 2007). The structure of the highly amyloidogenic and clinically aggressive L55P variant crystallizes in a different space respect to wt TTR and other variants (Quintas *et al*. 1997). Analysis of the 3D structure suggests that strands C and D are disrupted, altering the hydrogen bonds between the AB loop of one dimer and strand H of the other dimer (Sebastião *et al*. 1998), in an area that defines weak, native dimer-dimer interactions. These observations suggest a significant destabilisation of the L55P tetramer with the formation of undefined intermediate species that subsequently aggregate further to form fibrils. It has not been determined whether these destabilised

intermediates serve a dual purpose, as seeds for further polymerisation and aggregation and as soluble, toxic oligomeric species responsible for FAP pathogenesis. Since the L55P variant is clinically aggressive, it has been the focus of much of my work which investigated the mechanisms responsible for the toxicity of L55P in sensory neurons (Gasperini *et al*. 2011)

Studies on the kinetics of amyloid growth indicate that the L55P variant exists in an amyloidogenic conformation at physiological conditions, whereas the wt TTR is stable and non-amyloidogenic. It was observed that amyloid formation from the wild-type protein had an initial rate determining step, not diminished in the presence of pre-formed fibrils, which could be associated with the conformational change of the protein into an amyloidogenic intermediate. However, the kinetics of amyloid formation from the L55P variant showed the absence of this lag time (Bonifacio *et al*. 1996). This could suggest that L55P TTR is already in an amyloidogenic conformation, which assembles immediately into amyloid fibrils, under the conditions tested.

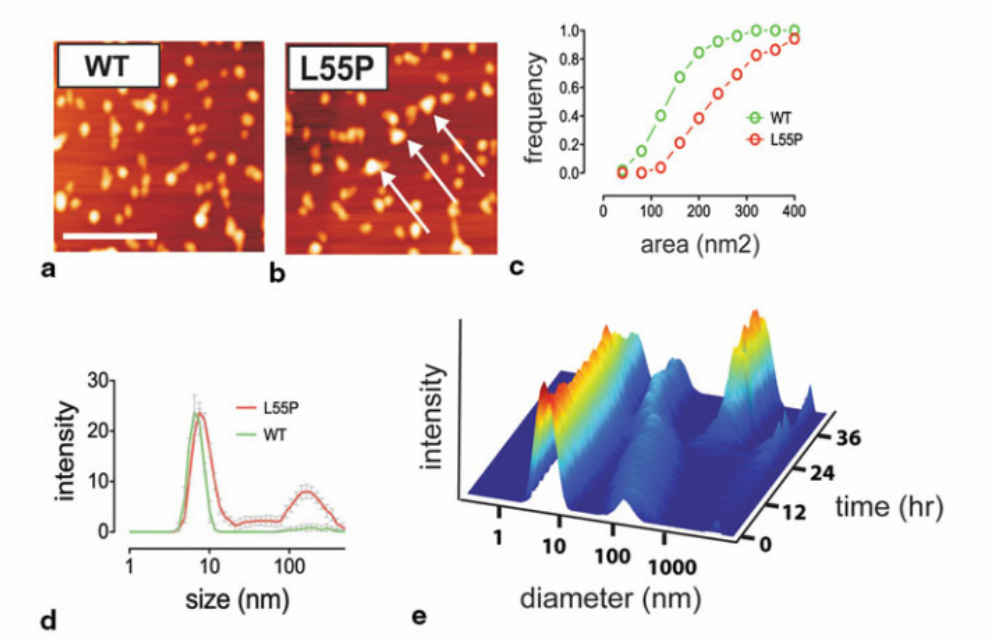

Figure 4. Aggregation of transthyretin *in vitro*. AFM images of freshly prepared a Wild-type and b L55P transthyretin. Arrows denote large, oligomeric aggregates of L55PTTR (scale bar is 100 nm). c When particle cross-sectional areas from the AFM are quantitated, L55P (red) contain a higher proportion of large particles than wild-type preparation (green). d Using a dynamic light scattering technique, L55P (red) contains a population of large, soluble oligomeric aggregates ranging in size from 100–300 nm in diameter. e Qualitatively, when L55P is monitored by DLS at 37◦C over 36 h, these oligomeric species decrease in average size and appear to form much larger (1,000 nm) aggregates, probably protofibrils (Gasperini *et al*. 2011).

The aggregation properties of the L55P variant with wt TTR were investigated by atomic force microscopy (AFM) and dynamic light scattering (DLS). Freshly prepared L55P and wt TTR in physiological buffers contains predominantly globular or amorphous particles ranging in apparent size from 10–50 nm in diameter (Fig. 4a, b). The smallest particles observed by AFM are approximately 10 nm in diameter and are probably tetramers. Significantly, using quantitative image analysis of particle cross-sectional area (Fig. 4c), the average AFM particle sizes of L55P are greater than those of wild-type preparations confirming that L55P is highly unstable at physiological pH and ionic strength (Quintas *et al*. 1997b).

In wt TTR, substantial fluctuations, both locally or globally, which is designated by intrinsic instability/flexibility were seen. At variance, the L55P variant displays significant local structural changes, including the displacement of the Φ angle of Pro55 from -134° to near -69° of Leu55 and the increase of the average C-alpha distance between residue 55 and its native hydrogen bonding partner in the wt TTR, Val14, from 5.2 Å to 6.6 Å (Lei *et al*. 2004). This observation suggests that the local conformation adopted by the L55P variant is thermally accessible to wt TTR. Therefore, the D strand may be intrinsically unstable so that the mutations which destabilize this site will increase the local and global mobility leading to higher tendency towards amyloidogenicity. Earlier spectroscopic analyses and proteolysis sensitivity studies have suggested that C-strand-loop–D-strand rearrangement leads to the formation of a monomeric amyloidogenic intermediate (Lai *et al*. 1996). In addition to the D strand, the alpha-helical region and the strands at the monomer–monomer interface are also intrinsically unstable. The central channel of L55P undergoes opening and closing fluctuations (Fig.5), which may provide an explanation of the fact that while the mutation is far from the channel, the mutant shows a substantial low binding affinity of thyroxine (Lei *et al*. 2004).

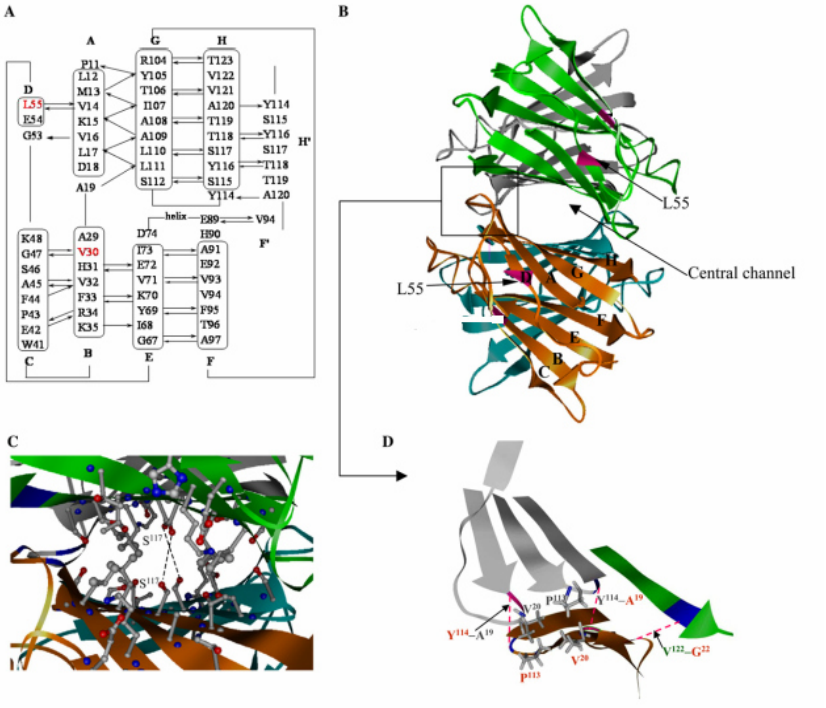

Figure 5. A) Schematic representation of the main-chain hydrogen bonds and β-strands ; B and C) Ribbon diagram of the tetramer and central channel; D) The dimer interface formed by monomer. The residues tht make the hydrofobic contacts are shown with a ball-and-stick model (Lei *et al*. 2004).

TTR most likely disassembles and forms amyloid when its ligands are released to the target organs (White and Kelly 2001). It was proposed that monomers are the building block of fibrils, *in vitro*, whose elementary protofilamentscontain two twisted β-sheets and comprise a single vertical stack of structurally modifed TTR monomers (Cardoso *et al*. 2002; Quintas *et al*. 2001). *In vivo* studies have revealed that TTR might be deposited in a non-fibrillar or pre-fibrillar form in the nerves prior to major nerve fiber degeneration in the early stages of FAP (Sousa *et al*. 2001). N-terminally truncated dimers can also form amyloid fibrils after limited proteolysis (Schormann *et al*. 1998).

The contribution of the inserted amino acid does not alter the overall structure of the protein but may interfere with disease aggressiveness and, affect tetramer stability, dissociation rate and aggregate trafficking to specific tissues such as the peripheral nerves, heart, and meninges.

Although these structural alterations may predict TTR amyloidogenicity, some studies have also shown that because of the presence of cysteine residues (4 per tetramer), TTR is more prone to be post-translationally modified by S-thiolation and S-sulphonation (Nakanishi *et al*. 2010; Lim *et al*. 2003), which have been shown to affect TTR

amyloidogenicity. In addition, only 5-15% of circulating TTR is free of post-translational modifications (Hagen *et al*. 1973). It has also been shown that the interaction of TTR with anionic lipids and cholesterol might accelerate the aggregation process (Hou *et al*. 2008).

TTR aggregation, especially *in vivo*, does not occur without additional proteins. In fact, in addition to the factors mentioned above, there are many other factors involved in TTR aggregation. TTR amyloid fibrils from FAP patient deposits and nearly all amyloid fibrils *in vivo* are found to be co-aggregated with many other molecules such as serum amyloid P (SAP), heparan sulphate, and metalloproteinases, which makes it even more difficult to analyse which one of these molecules actually contributes to TTR aggregation and clearance *in vivo* and *in vitro* (Cardoso *et al*. 2008; Murakami *et al*. 1992). Among the various molecules that co-aggregate with TTR, glycosaminoglycans (GAGs) are able to speed up TTR aggregation *in vitro*, and this phenomenon is dependent on the degree of GAG sulphation. Because GAG composition and concentrations vary among different tissues, this might partly explain the specificity of these aggregates for certain tissues (Bourgault *et al*. 2011).

2.5 Selective Transthyretin Kinetic Stabilizers

Destabilization of the tetrameric fold of TTR is important for protein aggregation which culminates with fibril formation. Many TTR mutations interfere with tetramer stability, increasing the amyloidogenic potential of the protein. A series of 12 different compounds, described in the literature as *in vitro* TTR fibrillogenesis inhibitors, were tested for their ability to inhibit L55P aggregate formation; J. W. Kelly and the company FoldRx, Inc., which he founded, have pioneered the use of small-molecule ligands to stabilize the native homotetrameric TTR (Johnson *et al*. 2005), and their compound, Fx-1006A (tafamidis), is currently in clinical trials (Johnson *et al*. 2008).

Kinetic stabilizers for the treatment of the TTR amyloidoses must be both highly potent and selective. The ligands must not interact with the thyroid hormone receptor (THR), a major concern arises from the similarity of some kinetic stabilizers to triiodothyronine (T3, the primary thyroid hormone) and T4 (the prohormone). Nonsteroidal anti-inflammatory drug (NSAID) activity is also contraindicated to treat TTR amyloidosis

patients; thus, TTR kinetic stabilizers should exhibit minimal NSAID activity, such as salicylic acid (Gales *et al*. 2008), diflunisal (Miller *et al*. 2004), and analogues of flufenamic (Baures *et al*. 1999). While sometimes unpredictable, these activities can usually be minimized by maximizing TTR amyloid inhibition potency, TTR binding affinity and binding selectivity to TTR in human plasma, have been accomplished using a combination of structure-based drug design and assays to evaluate the above mentioned criteria (Johnson *et al*. 2005). A wide variety of TTR kinetic stabilizers have been identified including naturally derived flavonoid and xanthone derivatives (Baures 1998; Maia *et al*. 2005) as well as synthetic compounds belonging to five families including: bisaryloxime ethers, biphenyls, 1-aryl-4,6-biscarboxydibenzofurans, 2-phenylbenzoxazoles and biphenylamines (Petrassi *et al*. 2005; Petrassi *et al*. 2000; Wojtczak *et al*. 1992). More recently, additional ligands, such as isatin (Gonzalez *et al*. 2009) and β-aminoxypropionic acid linked aryl or fluorenyl derivatives have been identified (Palaninathan *et al*. 2009). The primary candidates for the most potent and selective kinetic stabilizers were biphenyls, 2-phenylbenzoxazoles and dibenzofurans, since some bisaryloxime ethers display reduced chemical stability (Johnson *et al*. 2005). This relative lack of selective, structurally diverse TTR kinetic stabilizers is largely due to the fact that, until recently, no systematic optimization had been attempted on the three structural elements composing a typical TTR amyloidogenesis inhibitor (Johnson *et al*. 2008). Optimization of the ideal aryl substituents and their substitution pattern on aromatic rings X and Z, as well as the linker substructure joining the rings, revealed numerous high affinity solutions for the occupancy of thyroxine binding sites (Johnson *et al*. 2009). At present, on the basis of these new SAR data, it is possible to make accurate predictions of which structures will exhibit TTR kinetic stabilizer potency, TTR plasma binding selectivity and the desired binding orientation (Choi *et al*. 2010).

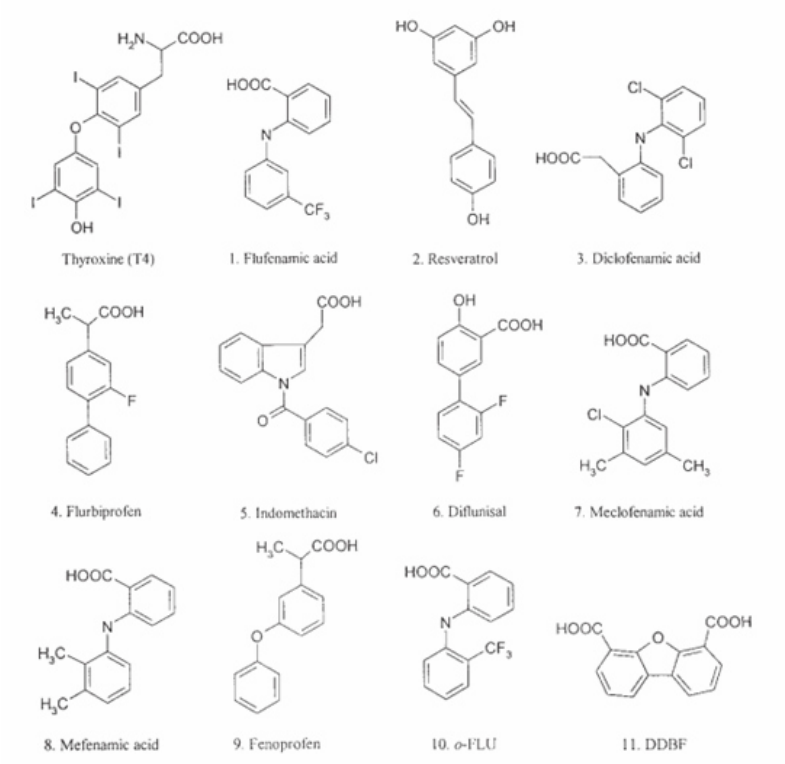

Figure 6. Structures of thyroxine (T4), the natural ligand of TTR, the NSAIDs tested as fibril formation inhibitors, and designed TTR fibril formation inhibitors (10–12). oFLU is o-tri-fluoromethylphenyl anthranilic acid; DDBF is dibenzofuran-4,6-dicarboxylic acid; PHENOX is N-m-trifluoromethylphenyl-phenoxazine-4,6-dicarboxylic acid (Klabunde *et al.* 2000).

Several natural polyphenols have been reported to act on different amyloidogenic proteins inhibiting amyloid formation (see the following section). In particular, for TTR, the attention is focused on some natural polyphenols such as curcumin, nordiidroguaiaretic acid (NDGA), epigallocatechin 3-gallate (EGCG) that have similarities with T4, and have been studied in relation with TTR amyloidogenesis. These studies showed that all these compounds stabilize the TTR and inhibit aggregation by three different means: EGCG strongly suppresses the dissociation of the TTR tetramer maintaining it as a soluble protein; curcumin induces the oligomerization of TTR in a characteristic homogeneous population of non-toxic "off-pathway" small aggregates and NDGA moderately reduces the amount of aggregated TTR (Ferreira *et al*. 2011). Furthermore, the oligomers and the intermediate species formed with the treatment of EGCG and curcumin are not toxic to the neuronal cells (Ferreira *et al*. 2012).

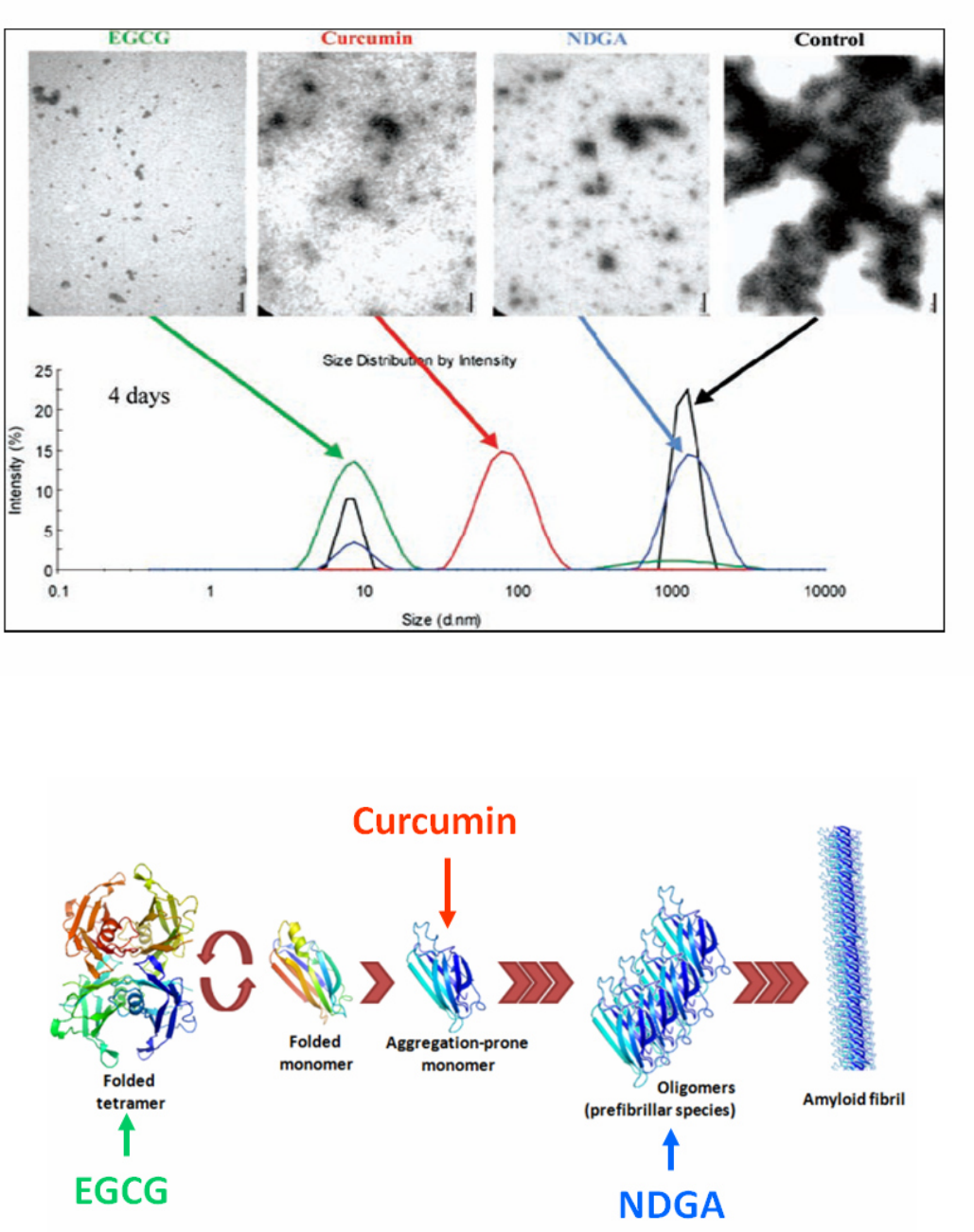

Figure 7. TEM and DLS analysis of aggregation. The proteins was incubated at 37°C under stagnant conditions, in the absence (control) and presence of EGCG, curcumin or NDGA for 4 days. Scale bar = 200 nm. DLS, dynamic light scattering; EGCG, epigallocatechin-3-gallate; NDGA, nordihydroguaiaretic acid; TEM, transmission electron microscopy; TTR, transthyretin. (Ferreira *et al.* 2012).

3 β2-Microglobulin

3.1 β2-Microglobulin structure and functions.

The major histocompatibility complex class I (MHC I) molecule and antigenic peptide are recognized by $CD8^+$ cytotoxic lymphocytes (CTL) during CTL activation and lysis of targets. The heavy chain of the MHCI molecule can interact non-covalently with a number of other molecules to form a CTL activating complex. One of these molecules is β2-microglobulin (β2m), whose role is to serve as a co-receptor for the presentation of the MHC I in nucleated cells for cytotoxic T-cell recognition (Pedersen LO *et al*. 1994). $CD8^+$ and β2m, the non-polymorphic ligands of the MHC I heavy chain, have been shown by X ray crystallography to interact with the immunoglobulin- like α3 domain and the α1α2 domains of the MHC I heavy chain in addition to interacting to each other (Saper *et al*. 1991).

β2-microglobulin is a low molecular weight polypeptide of 11800 Da, synthesized by all nucleated cells, initially as a 119 residue protein and, after processing, secreted as a 99 residue protein. β2m has a β-sandwich fold typical of the immunoglobulin superfamily, and contains seven β-strands (Fig. 1). Three strands form one side of the sandwich and four strands the other. An internal disulfide bond tethers strands 2 and 6 in the folded protein. Its structure resembles that of the constant domains of IgG and it is found on the cytoplasmic membrane of most cells, where it forms the light chain of histocompatibility antigens (Bjerrvm *et al*. 1985). Free β2m is released into the blood and other body fluids during cell membrane turnover and it is freely filtered by renal glomeruli and then catabolized by the tubules (Peterson *et al*. 1972). It has been calculated that approximately 150 mg of β2m is metabolized daily by the normal kidney (Vincent *et al*. 1980), the major site of β2m degradation. In conditions characterized by reduced glomerular filtration rate the serum levels of β2m increase (Wibell *et al*. 1973). Serum levels are also elevated in diseases associated with increased cell turnover and in several benign conditions such as chronic inflammation, liver disease, renal dysfunction, some acute viral infections, and a number of malignancies, especially hematologic malignancies associated with the B-lymphocyte lineage. In uremia, the increase is massive, which is in contrast to the moderately increased values (two- to threefold the normal) seen in some other conditions, e.g., lymphoproliferative (Cassuto

et al. 1978), autoimmune (Maury *et al*. 1982), and hepatobiliary diseases (Rashid *et al*. 1981). Serum β2m level < 4 mcg/mL is a good prognostic factor in patients with multiple myeloma.

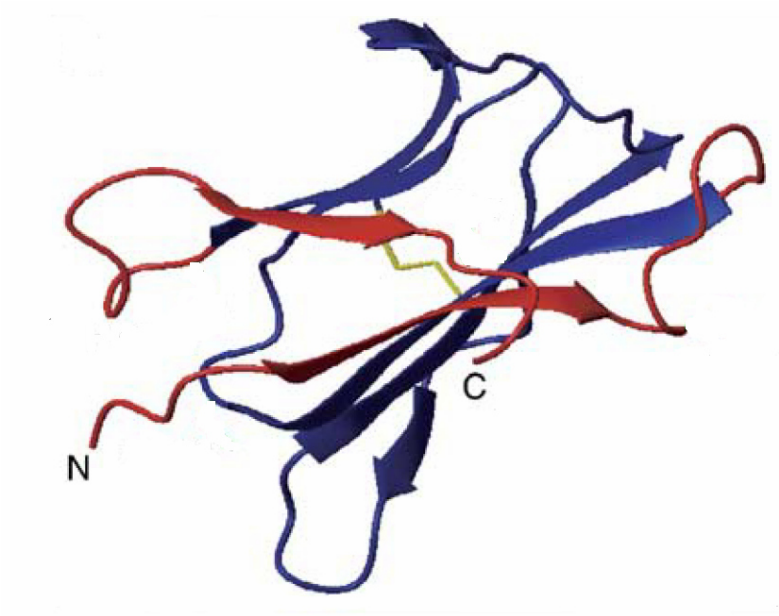

Figure 1 Ribbon structure of β2m. The N- and C-terminal h-strands are shown in red.(P.J. Bjorkman *et al*. 1997).

3.2 β2-Microglobulin amyloidosis

In 1985 Gejyo *et al*. identified a new type of amyloid fibril protein consisting of β2m. The protein was isolated from amyloid-laden tissue from a patient with chronic renal failure and carpal tunnel syndrome (CTS) who had been on regular hemodialysis (HD) treatment for 13 years. The identification of β2m as an amyloidogenic protein has brought a fundamental contribution to the understanding of the mechanisms of amyloidogenesis in general and has further emphasized the complexity of amyloid disease and the diversity of proteins capable of forming, under certain circumstances, congophilic fibrillar deposits in human tissues.

β2m deposition is associated with the syndrome of arthralgias and arthropathy in long-term dialysis patients, although the precise pathogenic role played by amyloid deposits

still needs to be clarified. The chronic arthralgias are usually bilateral and often involve the shoulders initially. Other joints, in particular the knees, wrists and small joints of the hands, may also be involved. Chronic joint swelling is another important feature of the disease, as may be recurrent haemarthrosis and chronic tenosynovitides of the finger flexors.

CTS is a well-recognized complication in HD patients (Warren *et al*. 1975; Brown *et al*. 1986) and is clearly related to the duration of HD (Brown *et al*. 1982). A prevalence of 50% has been reported in patients who have received more than 12 years of HD (Schwarz *et al*. 1984). In HD patients on conventional dialyzers mean serum β2m levels are of the order 30-50 mg/1 (Hurst *et al*. 1989; Thielemans *et al*. 1988) (normal reference range, 0.8-3.0 mg/1). The β2m level appears rather stable in follow-up studies of 2-6 months, but in longer follow-up it tends to increase with the number of years in HD. The serum level of β2m does not discriminate between HD patients who have β2m amyloid and those who do not (Gejyo *et al*. 1986). In patients on continuous ambulatory peritoneal dialysis (CAPD) serum β2m levels are markedly elevated and are of the same order, although slightly lower, than in HD (Ballardie *et al*. 1986; Chanard *et al*. 1986). The slightly lower levels could be explained by the permeability of the peritoneal membrane to β2m (Thielemans *et al*. 1988). In fact, the interaction between the blood and the dialysis membranes triggers the activation of mononuclear cells, which stimulate the production of inflammatory cytokines. The activation depends on the material used for dialysis, which is also considered as an index of biocompatibility. Cytokines, such as interleukin-1 (IL-1), tumor necrosis factor-α (TNF-α), and interleukin-6 (IL-6), can induce an inflammatory state of the base during the process of hemodialysis , connected in acute manifestations, such as increased temperature and hypotension (Piazza *et al* 2006).

Amyloidogenic properties of β2m have been associated to its secondary structure in particular because it contains two antiparallel beta-pleated sheets (Lancet *et al*. 1979). The beta structure has been suggested to be important in the stabilization of the tertiary conformation of heavy chains of class I HLA antigens on the cell surface (Lancet *et al*. 1979) and is obviously involved in the amyloidogenic properties of β2m. Connors *et al*. demonstrated that amyloid fibrils can be created *in vitro* from intact molecules of β2m (Connors *et al*. 1985). This is remarkable, since *in vitro* and in vivo creation of amyloid from precursor proteins usually involves limited proteolysis of the precursor (Glenner *et al*. 1980). Fragments of β2m may also form amyloid as suggested by the presenceof

β2m fragments in synovial amyloid in dialysis patients and amyloid kidney stones of uremic patients (Linke *et al*. 1986).

The current pathogenetic model of β2m amyloidosis has several similarities with the models of the major acquired systemic amyloid diseases, AA and AL amyloidoses (Glenner *et al*. 1980). First, there is a circulating precursor which may be either normal or abnormal. In the case of β2m amyloidosis, the precursor is most probably normal β2m, although some evidence suggests the presence of an abnormal β2m fraction in sera from patients on longterm HD. Second, the level of the circulating precursoris markedly elevated. In β2m amyloidosis, the mean serum level of β2m is about 20- to 30-fold the level found under normal conditions. Third, the precursor is elevated for a long period of time. In the case of β2m amyloidosis the duration of the massive elevation is usually 10 years or more. Finally, not all patients with prolonged elevation of the amyloid precursors develop amyloidosis. The additional factors required for amyloidogenesis to occur are, however, poorly defined. The role of the mononuclear phagocyte system in amyloid precursor proteins processing is probably important. The possible roles of the amyloid P protein (Woo *et al*. 1987), a characteristic component of extracerebral amyloid including β2m amyloid (Gorevic *et al*. 1986), and of amyloid-degrading proteases (Maury CPJ 1988) and amyloid-enhancing factors (Kisilevsky *et al*. 1986) are yet to be assessed. A number of factors that favour the conversion of β2-m fibrils *in vitro* have been identified such as the incubation of highly concentrated β2-m for 5-6 days at physiological pH and at a temperature of 20 °C, in addition, the presence of fibrils can act as a trigger for a rapid aggregation of the protein (Esposito *et al*. 2009). High concentrations of soluble β2-m may play a pathogenic role explaining protein toxicity to HL60 cells by stimulating osteoclastogenesis. Studies with human neuroblastoma cells, SH-SY5Y, showed instead that, although β2-m is potentially neurotoxic, it is unlikely that this protein plays a role in the pathophysiology of cognitive impairment observed in people on hemodialysis because of the protective blood-brain barrier, which keeps low the β2-m concentration in the cerebrospinal fluid (Giorgetti *et al*. 2009).

Although transformation of wild-type β2-m into amyloid fibrils is difficult to achieve *in vitro*, many recombinant β2-m variants have been investigated, and hypotheses have been developed about the mechanisms underlying fibrillogenesis. The most important rearrangements of the protein, with respect to its structure in MHC-I, were observed for strands D and E, the interstrand loop D-E, and strand A, including the N-terminal

segment. Data showed that these modifications can be considered as the prodromes of the amyloid transition that starts at sheet 1 with the rupture of strand A pairing, and leads to polymerization, through intermolecular pairing at strand D and probably strand C, and precipitation into fibrils. Instead two variants of human β2-m were compared with wild-type protein, namely the mutant R3Aβ2-m and the form devoid of the N-terminal tripeptide (ΔN3β2-m), a reduced unfolding free energy was measured compared with wild-type. The results of a systematic investigation on 13 amyloidogenic β2-m mutants have recently been published (Jones *et al*. 2003; Smith *et al*. 2003). Although no correlation was proposed between the location of the mutations and the extent of destabilization with respect to wild-type sequence, a unique role in amyloid formation was envisaged for the N and C-terminal β-strands of β2-m (A and G, respectively) from the increased fibrillogenesis rate at acidic and mildly acidic pH of the variants with mutations in strands A and G. The underlying rationale is based on the loss of local hydrophobic packing by β-strand unpairing, leading to increased population of conformers with exposed assembly-competent surfaces (Corazza *et al*. 2004).

3.3 Asp76Asn Variant β 2 –Microglobulin

Recently the first naturally occurring structural variant, Asp76Asn (D76N), of human β2-m was identified in members of a French family showing an autosomal dominant, inheritable systemic amyloidosis with slowly progressive gastrointestinal symptoms and autonomic neuropathy.

In contrast to patients with dialysis-related amyloidosis, all members of this family had normal circulating concentrations of β2-m and normal renal function. The pathogenic protein was aggressively fibrillogenic *in vitro*, prompting a re-evaluation of previously hypothesized mechanisms of β2-m fibrillogenesis. Extensive amyloid deposits were found in the spleen, liver, heart, salivary glands, and nerves (Valleix *et al*. 2012). Despite the misfolding propensity of the D76N variant and the essential contribution of β2–m to the structure of the HLA class I complex, none of the heterozygotes had clinical evidence of immunodeficiency.

The high-resolution crystal structures of the D76N variant at 1.40 Å, and wild-type β2-m (Protein Data Bank code 2YXF) matched closely, with a root mean square difference of 0.59 Å, as calculated over the whole C-alpha backbone (Esposito G *et al*. 2008). The Asp76Asn β2-m variant was thermodynamically unstable and remarkably fibrillogenic *in vitro* under physiological conditions. The substitution of asparagine to aspartate at residue 76 has two notable effects. First, the Asn76 amide establishes a new hydrogen bond with Tyr78, which consequently moves about 1.5 Å closer to residue 76. In its new position, Tyr78 provides a hydrogen bond to the amide nitrogen of Thr73. Second, the theoretical isoelectric point increases from 6.05 to 6.40, which is of particular interest because the negative Asp76 residue in the wild-type protein partly balances the positive charges of the neighbouring Lys41 and Lys75 residues, whereas this region of the protein has a strong positive charge in the D76N variant (Fig. 2).

The new hydrogen bonds, Asn76–Tyr78 and Tyr78–Thr73, appear to stabilize the 73–78 region of the polypeptide sequence that connects the E and F strands of the protein (E–F loop) (Fig.2A). Indeed, the high B-factors (a measure of the fluctuation of each atom around its position in the crystal) of the E–F loop (165% of the molecularity of native protein folding inferred from the crystal structure) indicate that this is the most flexible part of the structure of wild-type β2-m, whereas the equivalent region of the D76N variant is more rigid, with reduced B factors (120% of average) (Valleix *et al.* 2012).

The D76N substitution allows a fully folded three-dimensional structure almost identical to that of the wild type protein that forms amyloid fibrils in dialysis-related amyloidosis. However, dissection of the mechanism of D76N β2-m fibrillogenesis confirmed the previously established paradigm that the amyloidogenicity of monomeric globular proteins is intimately connected to native fold destabilization (Booth, D. R et al. 1997).

Importantly, a specific intermediate of the folding pathway of wt β2-m which was previously structurally characterized and shown to play a crucial role in priming the amyloid transition (Chiti *et al*. 2001), is abundantly populated in the D76N variant. It is therefore possible that this specific residue substitution facilitates the molecular mechanism responsible for the inherent amyloidogenicity of wt β2-m and thereby enables the variant to cause clinical pathology even at normal plasma concentrations.

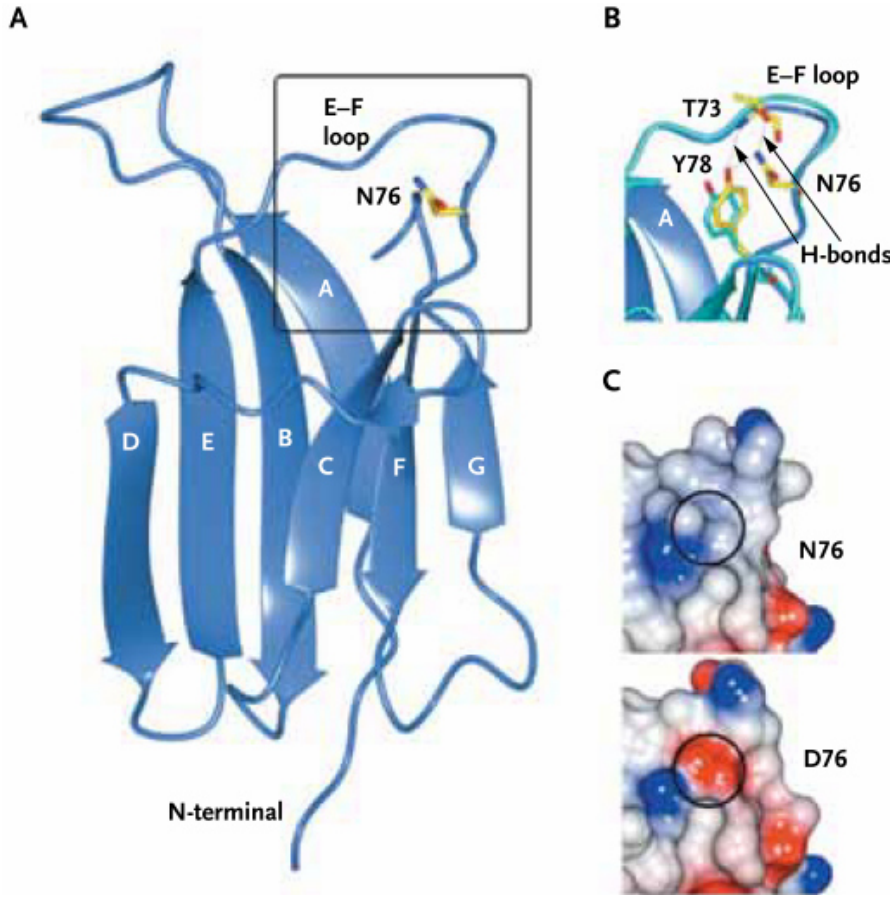

Figure 2. Crystal Structure of D76N Variant β2-Microglobulin.Panel A is a ribbon representation of the D76N variant. Panel B is a close-up view of the E–F loop (residues 70 to 80) shown in Panel A, superimposed on the wild-type β2-microglobulin structure (blue–green). Residues belong-ing to the D76N variant are yellow, and Tyr78 belonging to wild-type β2-microglobulin is blue–green; hydrogen (H) bonds are shown as dashed lines. Panel C shows the surface electrostatic potential of the E–F loop region in the D76N variant (top) and in wild-type β2-microglobulin (bottom); circles indicate the mutated residue. Blue represents positively charged regions, and red negatively charged regions (Valleix *et al.* 2012).

Data suggested that the ability of D76N β2-m to catalyze fibrillogenesis by wt β2-m can be modulated and even blocked by typical chaperones such as crystallin, leading to inhibition of fibrillization that depends on the stoichiometric chaperone/ β2-m ratio. A role for extracellular chaperone-like proteins in the inhibition of wt β2-m amyloidogenesis has been proposed previously (Ozawa *et al*. 2011), and it is plausible that the persistent, extremely high concentration of wt β2-m in renal failure patients on dialysis may overcome the natural protective role of physiological chaperones that otherwise protect against deposition of this weakly amyloidogenic protein when it circulates at its normal serum concentration.

4 Role of Phenols in health and diseases

4.1 Origin

Phenolic compounds are synthesized and act as secondary metabolites in plants. The biosynthesis of phenolic compounds in plants requires complex metabolic processes encompassing the flavonoids, shikimate and phenylpropanoid pathways. In contrast with primary metabolities (e.g. phytosterols, acyl lipids, nucleotides, amino acids and organic acids), which have a clear and essential role associated with principal events of plant metabolism (photosynthesis, respiration, growth or development), secondary metabolites have long been neglected. Nevertheless, secondary metabolites, with a wide variety of molecular structures and irregular distribution throughout the plant kingdom, have several functions involving defence and survival strategies, such as plant protection against herbivores and microbial infections, action as signal molecules in the interaction between plants and their environment, protection against UV radiation or action as attractants for pollinators and seed-dispersing animals. Phenolic compounds are sometimes accumulated at high concentration in plant tissues and other structures and are thus abundant micronutrients of our diets (Duthie *et al*. 2003).

4.2 Classification

Polyphenols can be classified into different classes, according to the number of phenolic rings in their structure, the structural elements that bind these rings each other, and the substituents linked to the rings (Fig.1). Phenolic compounds have at least one aromatic ring with one or more hydroxyl groups and are classified as flavonoids and nonflavonoids. Processed foods and beverages, such as black tea, matured red wine, coffee and cocoa, may contain phenolic transformation products that are best described as derived polyphenols. Crozier and coworkers that proposed the flavonoids and non-flavonoids classification, describe dietary non-flavonoids as characterized by C_6-C_1 phenolic acids, with gallic acid as the precursor of hydrolysable tannins, hydroxycinammates (C_6-C_3) and their conjugated derivates, and stilbenes (C_6-C_2-C_6). Despite this, the classification omits a sub-class of phenolic compound named lignans (-(C_6-C_3)$_n$), a phenolic family of compounds formed by two phenylpropanoid units linked

by a hydrogen bridge, these being the monomeric and dimeric forms of hydroxycynammic acid and cynammic alcohol. Flavonoids are polyphenolic compounds comprising 15 carbons with two aromatic rings connected by a three-carbon bridge. Flavonoids are charecterized by a C15 phenylchromane core, composed of two aromatic rings cnnected by a three carbon bridge (Crozier *et al*. 2009; Passamonti *et al*. 2009). The main subclasses of these compounds are the flavones, flavonols, flavan-3-ols, isoflavones, flavanones, and anthocyanidins. Other flavonoid groups that provide less dietary components are the chalcones, dihy- drochalcones, dihydroflavonols, flavan-3,4-diols, coumarins, and aurones. The basic flavonoid skeleton may have numerous substituents. The majority of flavonoids occur naturally as glycosides rather than aglycones. The presence of methyl groups or isopentyl units may give a lipophilic character to flavonoid molecules (Crozier *et al*. 2009). Moreover, most flavonoids in foods are conjugated to a carbohydrate moiety, representing a wide range of combinations depending on the flavonoid, its linkage and the linked mono- and disaccharide (Passamonti *et al*. 2009).

Among the nonflavonoids of dietary significance are the phenolic acids. Gallic acid is the commonest phenolic acid, and occurs widely in complex sugar esters in gallo-tannins, such as 2-O-digalloyl-tetra-O-galloyl-glucose, which are minor dietary components. The related ellagic acid-based ellagitannins, such as sanguiin H-6 and punicalagin, are found in a variety of fruits, including raspberries (Rubus idaeus), strawberries (Fragaria ananassa), blackberries (Rubus spp.), and many others, including pomegranate (Punica granatum) and persimmon (Diospyroskaki), as well as walnuts (Juglans regia), hazelnuts (Corylus avellana), and oak-aged wines where they are leached from the oak during maturation of the wines (Landete JM. 2011.). The ellagitannin content of some food products can be high (e.g. a glass of pomegranate juice plus 100 g serving of raspberries provide 300 mg, while four walnuts provide 400 mg) (Larrosa *et al*. 2012). The C_6–C_3 hydroxycinnamates occur mainly as conjugates, for example, with tartaric acid or quinic acid, and collectively are referred to as chlorogenic acids. Chlorogenic acids, principally 3-O-, 4-O-, and 5-O-caffeoylquinic acids, form 10% of green robusta coffee beans (Coffea canephora). Regular consumers of coffee may experience a daily intake exceeding 1 g of chlorogenic acid, and it constitutes for many people the major intake of dietary phenolics. Accumulating in the flesh of grapes, caftaric acid is the main hydroxycinnamate in both red and white wines produced from Vitis vinifera and well as Concord grape juice, which is a product of

grapes of Vitis lambrusca. Stilbenes have a C_6-C_2-C_6 structure and are phytoalexins produced by plants in response to disease, injury, and stress (Langcake P and Pryce RJ 1977.). Although only extremely minor dietary components, the main stilbene is resveratrol (3,5,4¢-trihdroxystilbene), which occurs as cis and trans isomers as well as conjugated derivatives, including trans-resveratrol-3-O-glucoside (trans-piceid). The woody root of the noxious weed Polygonum cuspidatum (Japanese knotweed or Mexican bamboo) contains unusually high levels of trans-resveratrol and its glucoside with concentrations of up to 377 mg/100 g dry weight (Vastrano *et al*. 2000). Red wines contain a diversity of stilbene derivatives, but invariably in very low concentrations compared to the levels of other (poly)phenolic components (Crozier *et al*. 2010).

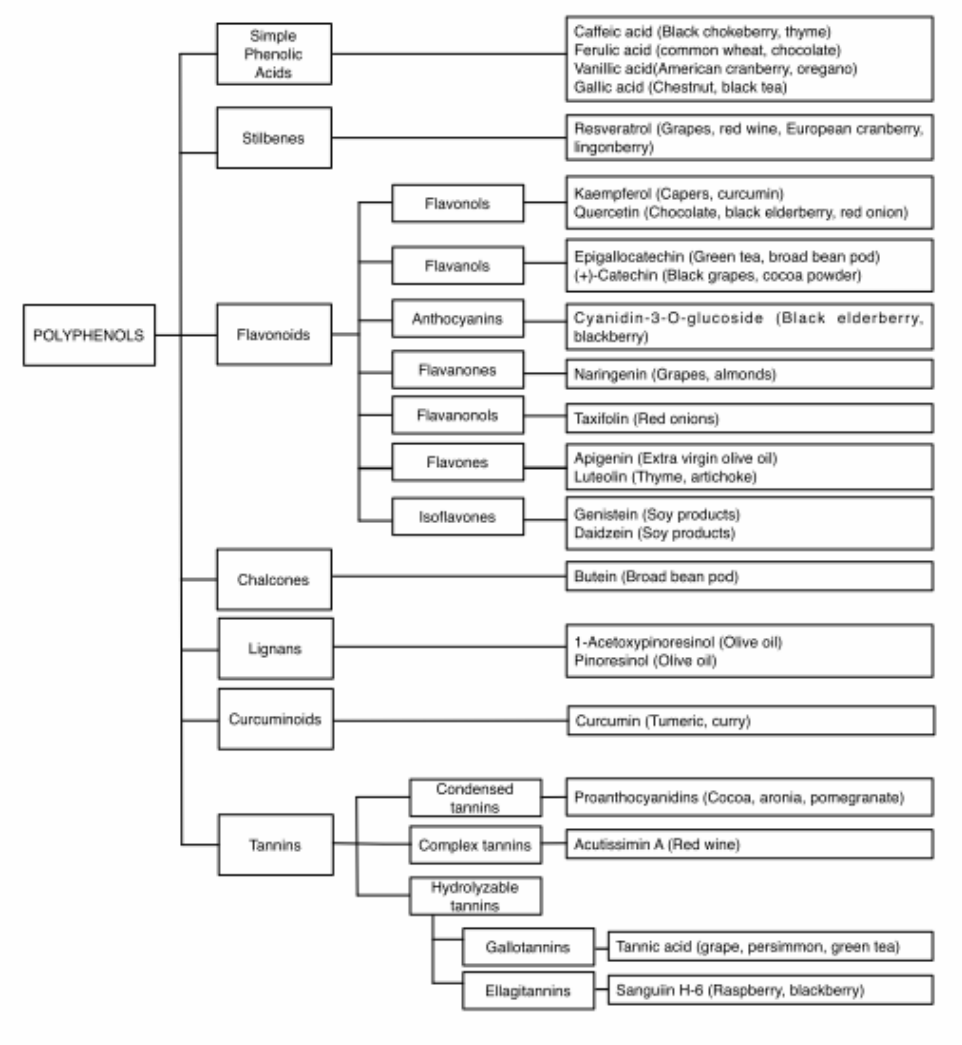

Figure 1. Classification of common dietary polyphenols, with characteristic examples of each phenolic compound.

4.3 Nutrition and prevention of disease

The importance of nutrition for disease prevention has been recognized since the days of Hippocrates 460-377 B.C. who said: “Let food be your medicine and medicine be your food”. Nutrition is one of the lifestyle factors that can contribute to the development and progression of chronic diseases such as diabetes, cancer, atherosclerosis, cardiovascular disease and neurodegenerative diseases (Virmani *et al*. 2006; Lillycrop *et al*. 2012).

In the early 1990s, various research groups started talking about use of antioxidants (e.g., melatonin, resveratrol, green tea, lipoic acid) and metabolic compounds (e.g., nicotinamide, acetyl-L-carnitine, creatine, coenzyme Q 10) as possible candidates in neuroprotection. Apart from providing proof of efficacy for a particular health claim, other factors such as finding the right dosages, the safety profile, and especially the level of purification and presence of solvents and contaminants, heavy metals, bacteria, fungi, etc. are all issues needed to be considered as their use becomes widespread (NIH Office of Dietary Supplements (2012); Gold *et al*. 1999). Considering recent advances in research, especially nutrigenomics, it can be shown that they are intimately linked, via evolution and genetics, to cell health status an ability to modulate apoptosis, detoxification, and appropriate gene response. Nutritional deficiency and disease, especially lack of vitamins and minerals, were well known and associated with specific disease conditions, major examples being lack of vitamin C and scurvy or lack of niacin (vitamin B3) and pellagra (Jukes TH 1989). The classical mechanism for the actions of minerals, vitamins, and nutrients as substrates and cofactors in various enzyme- or receptor-related activities is well known. Studies suggest that many natural compounds such as curcumin, carotenoids, acetyl-L-carnitine, coenzyme Q10, vitamin D and other nutraceuticals have the potential to target multiple pathways. Additional functions have been found for these compounds when used in times of particular stress and deficiency states and/or at higher than normal dosages, in particular, their ability to modulate cell health status, inducing for example apoptosis or detoxification, especially in response to free radical stress, e.g., reactive oxygen species (ROS) and reactive nitrogen species (RNS) or both (Roberts *et al*. 2009). Epidemiological studies suggest that high dietary intake of polyphenols is associated with decreased risk of a range of diseases including cardiovascular disease (CVD), specific forms of cancer (Kuriyama *et al*. 2006) and neurodegenerative diseases (Checkoway *et al*. 2002).

Many of the anti-cancer properties associated with green tea are believed to be mediated by the flavanol epigallocatechin gallate (EGCG), which has been shown to induce apoptosis and inhibit cancer cell growth by altering the expression of cell cycle regulatory proteins and the activity of signaling proteins involved in cell proliferation, transformation and metastasis (Khan *et al*. 2006). In addition to flavonoids, phenolic alcohols, lignans and secoiridoids (all found at high concentration in olive oil) are also thought to possess anti-carcinogenic effects (Owen *et al*. 2000) that have been reported in large intestinal cancer cell models, in animals (Bartoli *et al*. 2000) and in humans (Owen *et al*. 2000). These effects may be mediated by the ability of olive oil phenolics to inhibit the initiation, promotion and metastasis in human colon adenocarcinoma cells (Hashim *et al*. 2008) and to down-regulate the expression of COX-2 and Bcl-2 proteins that have a crucial role in colorectal carcinogenesis (figure 2) (Llor *et al*. 2003).

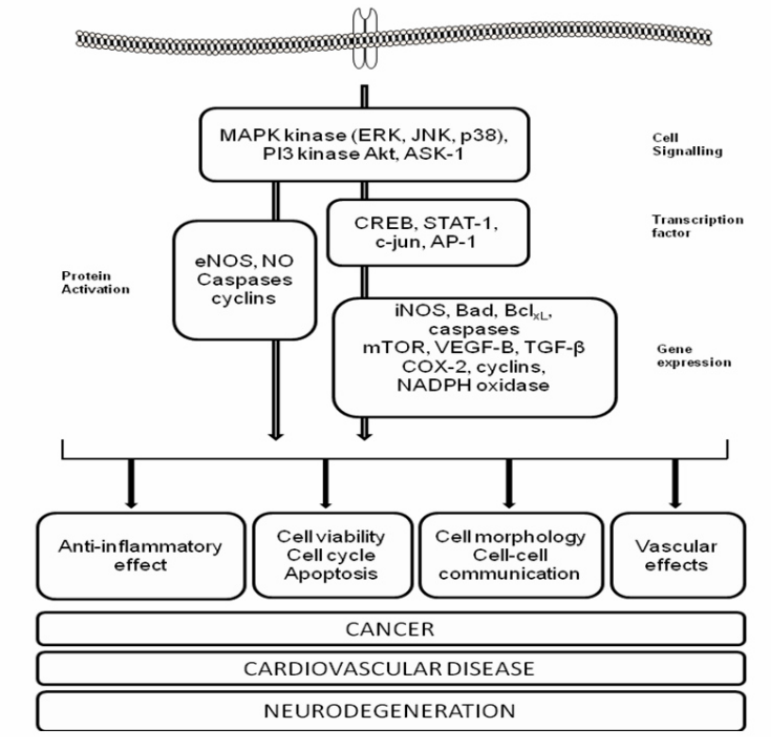

Figure 2. The interaction of polyphenols with cellular signaling pathways involved in chronic disease. Flavonoid-induced activation and/or inhibition of MAP kinase and PI3 kinase signaling leads to the activation of transcription factors which drive gene expression. For example, activation of ERK/Akt and the downstream transcription factor CREB by flavonoids may promote changes in neuronal viability and synaptic plasticity, which ultimately influence neurodegenerative processes. Polyphenol-induced inhibition of mthe JNK, ASK1 and p38 pathways leads to inhibition of both apoptosis in neurons and a reduction of neuroinflammatory reactions in microglia (reduced iNOS expression and NO•release). Alternatively, their interaction with signaling may lead to direct activation of proteins such as eNOS, which controls nitric oxide release in the vasculature and thus influences CVD risk (Vauzour *et al*. 2010).

Cardiovascular disease (CVD), in particular coronary heart disease and stroke, is a major cause of mortality in developed nations. CVD is a chronic, multi-factorial disease in which a range of genetic and environmental factors plays a role in its initiation, progression and development. For example, smoking, high saturated fat diets and physical inactivity are well known environmental factors that are known to increase the risk of CVD (Ambrose *et al*. 2004). Prospective studies have indicated a correlation between the intake of flavonols, flavones and flavanols and a reduced risk of coronary artery disease (Arts *et al*. 2005) and anthocyanin and flavanone intake and reduced CVD related mortality (Mink *et al*. 2007).

Various human, animal and cell studies have suggested that polyphenols may exert beneficial effects on the vascular system via an induction of antioxidant defenses (Wan *et al*. 2001), by lowering blood pressure, improving endothelial function (Papamichael *et al*. 2004), inhibiting platelet aggregation (Erlund *et al*. 2008), lower density lipoprotein oxidation and reducing inflammatory responses (Schramm *et al*. 2003). One suggested mechanism for the action of polyphenols on vascular function involves their ability to modulate the levels and activity of nitric oxide synthase (eNOS) and therefore, nitric oxide (NO) bioavailability to the endothelium (Figure 2) (Leikert *et al*. 2002). Neurodegenerative conditions such as Parkinson's (PD) and Alzheimer's (AD) diseases, multiple sclerosis (MS) and other neurodegenerative disorders appear to be triggered by multi-factorial events including neuroinflammation, glutamatergic excitotoxicity, increases of oxidative stress, iron and/or depletion of endogenous antioxidants. Flavonoids such as quercetin, puerarin, narinigenin and ginistein protect dopaminergic neurons against oxidation and apoptosis (Mercer *et al*. 2005). Recent data show that regular dietary intake of flavonoid-rich foods and/or beverages has been associated with 50% reduction in the risk of dementia (Commenges *et al* 2000), a preservation of cognitive performance with ageing (Letenneur *et al* 2007; Morris *et al*. 2006), a delay in the onset of Alzheimer's disease (Dai *et al*. 2006) and a reduction of the risk of developing Parkinson's disease (Checkoway *et al*. 2002).

In the brain, free radical production induces inflammatory processes called neuroinflammation, and in this condition antioxidants exert a protective action.

Indeed, in pathologies like AD or PD, flavonoids can exert positive actions (Virmani *et al*. 2013) since they:

- attenutate the release of cytokines as IL1β;
- exhibit inhibitory actions against the production of iNOS

- inhibit the activation of NADH oxidase and ROS
- have a regulatory activity on the action of NFkB
- can modulate the MKKK network

For example, one of the main components of green tea, EGCG, demonstrates neuroprotective actions via MAPK, Akt, and Proteinase C. Indeed, EGCG acts via alpha secretases to allow the amyloid beta peptide processing typical of AD (Mandel *et al*. 2005).

In the context of Parkinson's disease, the citrus flavanone tangeretin has been observed to maintain nigro-striatal integrity and functionality following lesioning with 6-hydroxydopamine, suggesting that it may serve as a potential neuroprotective agent against the underlying pathology associated with Parkinson's disease (Datla, K.P *et al*. 2001).

In addition to the neuroprotection elicited by flavonoids, phenolic compounds such as caffeic acid and tyrosol have also been shown to protect against 5-S-cysteinyl-dopamine (Vauzour *et al*. 2010) and peroxynitrite neurotoxicity *in vitro* (Vauzour *et al*. 2007).

There is also a growing interest in the potential of polyphenols to improve memory, learning and general cognitive ability (Spencer *et al*. 2008). Human investigations have suggested that fruits and vegetables may have an impact on memory (How *et al*. 2007) and depression (Krikorian *et al.* 2010) and there is a large body of animal behavioural evidence to suggest that berries, in particular blueberries and strawberries, are effective in reversing age-related deficits in spatial working memory (Joseph *et al*. 1998) in improving object recognition memory (Goyarzu *et al*. 2004) and in modulating inhibitory fear conditioning (Ramirez *et al.* 2005).

4.4 Mediterranean diet and polyphenols

The present concept of Mediterranean diet (MeDi) is based on the recent traditional Mediterranean diet that was studied in the 1950s to 1960s in the South of Europe during the Seven-Country study (Keys 1997).

MeDi is based on the point of view that nutrition is considered a paradox: that although the people living in Mediterranean countries tend to consume relatively high amounts of fat and salt (Leclercq and Ferro-Luzzi Mar 1991), they have far lower rates of cardiovascular disease than in countries like the United States, where similar levels of

fat consumption are found. The MeDi often is cited as beneficial due to its low content of saturated fats and high content of monounsaturated fats and dietary fiber. One of the main explanations is thought to be the health effects of olive oil included in the Mediterranean diet. The inclusion of red wine is considered a factor contributing to health as it contains flavonoids with powerful antioxidant properties (Baron-Menguy *et al*. 2007). MeDi is extremely rich in polyphenols from various foods and beverages, and there is no doubt they provide protection against various diseases. A meta-analysis published in *BMJ* in 2008 showed that following strictly the Mediterranean diet reduced the risk of dying from cancer and cardiovascular disease as well as the risk of developing Parkinson's and Alzheimer's disease. The results report 9% and 6% reduction in overall, cardiovascular, and cancer mortality respectively. Additionally a 13% reduction in incidence of Parkinson's and Alzheimer's diseases is to be expected provided strict adherence to the diet is observed (Sofi *et al*. 2008). Similarly, a 2007 study found that adherence to the MeDi may affect not only risk for Alzheimer disease (AD) but also subsequent disease course with lower mortality rate. A recent randomized Spanish trial of diet pattern published in *The New England Journal of Medicine* in 2013 followed almost 7,500 individuals over around 5 years: they found that individuals on a MeDi supplemented with mixed nuts and olive oil had a 30% reduction in risk of having a major cardiovascular event and a 49% decrease in stroke risk. Subjects followed one of three different diets. They included either a low fat diet, a Mediterranean diet with 50 ml of extra virgin olive oil daily or a Mediterranean diet with 30 grams of mixed nuts. The nuts were primarily walnuts which have a high amount of omega-3 fatty acids (Estruch *et al* 2013). Recently, an observational study published, November 5, 2013, in *Annals of Internal Medicine* concluded that following a Mediterranean diet might help middle-aged women to live longer and thrive. The study was a 15 years long observational study done to examine the association between dietary patterns at midlife and health in aging. The participants in this study were 10,670 women with dietary data and no major chronic diseases between 1984 and 1986. In addition, all women were in their late 50s and early 60s. After reviewing the data of 15 years, researchers in this study calculated the outcomes and reported that middle-aged women who followed the Mediterranean diet had a 40% more chance to live up to age 70, compared with other participants who followed a dissimilar eating style (Samieri *et al*. 2013).

4.5 Inhibition of amyloid fibrils formation by polyphenols

Natural compounds from medicinal plants are capable of binding to different targets implicated in AD and thereby exert neuroprotective effects. Previous studies have demonstrated that certain medicinal plants such as *Gingko biloba*, *Huperzia serrata*, *Salvia officinalis* and *Melissa officinalis* exert neuroprotective effects by preventing membrane lipid oxidation, reducing inflammation, inhibiting Aβ aggregation and attenuatining apoptosis (Wang *et al*. 2006; Izzo and Capasso 2007). Certain phytochemicals such as romarinic acid, curcumin and xanthone (Lim *et al*. 2001; Izzo and Capasso 2007) have also shown multipotent neuroprotective effects (Youdim and Buccafusco 2005; Van Der Schyf *et al*. 2006; Ji and Zhang 2008). Self-assembly of amyloid proteins into toxic oligomeric and fibrillary aggregates is considered the main cause in amyloid disease. Consequently, the research for new compounds interfering with aggregation of amyloid proteins is considered a rewarding strategy to develop new therapeutic compounds. Natural polyphenols have been extensively studied for their multiple biological activities, which make them interesting compounds in the prevention and pathological tissue reactions related to deposits of amyloidogenic proteins (Sgarbossa A *et al*. 2012; Bhullar *et al*. 2013). Lansbury and coworkers screened 169 compounds for *in vitro* inhibition of α-synuclein, an amyloidogenic protein that is found to accumulate in Lewy bodies in the brain of Parkinson's disease patients. Using thioflavin T assay, the researchers identified 15 inhibitory catecholamine compounds, including the polyphenols dobutamine and apomorphine (Conway KA *et al*. 2001). The mechanism of inhibition of amyloid formation is not the same for all natural polyphenols. They can act on various assembly pathwaysinteracting with different amyloid forms, such as monomeric, oligomeric or fibrillary aggregates. Some compounds inhibit the formation of oligomers, but promote fibril formation, others inhibit fibrils, but not oligomers formation , others inhibit both. Other polyphenols, like EGCG redirect amyloid fibril formation from fibrillogenic forms to non-fibrillogenic oligomers.

The initial hypothesis about the role of aromatic interactions in amyloid fibril formation was based on the remarkable occurrence of aromatic residues in many amyloid-related proteins and short peptide fragments (Gazit *et al*. 2002), and the well-known role of aromatic stacking in self-assembly processes in chemistry and biochemistry (Aggeli A. et al. 1997). This hypothesis led to the suggestion that stacking of aromatic residues

may play a role in assembly acceleration in many cases of amyloid fibril formation. Stacking interactions may provide an energetic contribution as well as directionality and orientation that are facilitated by the restricted geometry of planar aromatic stacking (Platt *et al* 2005). Natural polyphenols are characterized by the presence of aromatic rings and one or more phenolic rings which may interact with the aromatic residue present in amyloidogenic proteins (Porat *et al*. 2006; Wu *et al*. 2006), inhibiting the self-assembly process in amyloid fibril formation. Examples (Table 3) are: curcumin, resveratrol, rosmarinic acid, tannic acid, baicalein, piceid, oleuropein, ferulic acid, EGCG, salvianolic acid B, silibinin, keampferol, myrecetin, quercetin, morin, catechin and epicatechin. All these polyphenols have at least one aromatic ring with hydroxyl groups responsible for hydrophobic interactions with the proteins. According to some data, the mechanism of inhibition is due to the interaction between phenolic rings of polyphenols and aromatic residue of amyloidogenic proteins which prevent the π-π interaction disturbing π-stacking between protein units within the β-structure and block the self assembly leading to amyloid fibril formation. (Porat *et al*. 2006; Cheng *et al*.2013).

Polyphenols	Amyloid protein target	Effect
Curcumin	Aβ α-syn TTR, Lysozyme hIAPP	- Destabilizes preformed fibril amyloid - Inhibits fibril formation
EGCG	Aβ α-syn TTR Huntingtin	– Suppresses TTR tetramer dissociation – Inhibits Aβ and α-synuclein aggregation – Inhibits the aggregation of mutant huntingtine protein
Revesratrol Piceid	Aβ hIAPP	– Inhibits the formation of hIAPP fibrils – Inhibits Aβ oligomeric cytotoxicity – Destabilizes preformed Aβ fibrils
Myricetin, Morin, Quercetin, Catechin, Epicatechin, Kaempferol	Aβ hIAPP α-syn	– Inhibits Aβ and α-syn fibril formation – Destabilized preformed Aβ and α-syn fibrils – Inhibits hIAPP amyloid formation
Tannic acid	Aβ α-syn	– Inhibits Aβ and α-syn fibril formation, destabilizes preformed fibril amyloid
Rosmarinic acid	Aβ hIAPP	– Inhibits Aβ aggregation pathway – Inhibits hIAPP amyloid formation, destabilizes preformed hIAPP fibrils
Ferulic acid	Aβ A-syn hIAPP	– Inhibits fibrils formation and extension of Aβ, α-syn – Destabilizes preformed Aβ and α-syn fibrils – Represses amylin amyloid formation
Oleuropein	hIAPP	– Interferes with amylin aggregation
Salvionolic acid B	Aβ hIAPP	– Inhibits Aβ fibril formation, disaggregates preformed fibrils – Inhibits hIAPP fibril formation
Baicalein	Aβ A-Syn hIAPP	– Inhibits fibrillation of α-syn, disaggregates preformed fibrils – Inhibits formation of amylin β-sheet structure
Silibinin	Aβ hIAPP	– Inhibits Aβ aggregation – Inhibits hIAPP fibrillization

Table 3. Some polyphenols with anti-amyloidogenic effects (Viviane L. Ndam Ngoungoure *et al*. 2014).

4.6 Oleuropein aglycone: Olive oil phenol

Olea europaea is native to the Mediterranean region and, both the oil and the fruit are amongst the main components of the Mediterranean diet. The main active constituents of olive oil include oleic acid, phenolic constituents, and squalene. The main phenolic compounds, hydroxytyrosol and oleuropein, give extra-virgin olive oil its bitter, pungent taste. The pharmacological properties of olive oil, the olive fruit and its leaves have been recognized as important components of medicine and a healthy diet because of their phenolic content (Visioli *et al*. 2002). Oleuropein belongs to the secoiridoid class, compounds abundant in Oleaceae, Gentianaceae, Cornaleae, as well as in many other plants. Iridoids and secoiridoids are usually glycosidically bound and are produced from the secondary metabolism of terpenes as precursors of various indole alkaloids. The secoiridoids in Oleaceae are usually derived from the oleoside type of glucosides (oleosides), which are characterized by an exocyclic 8,9-olefinic functionality, a combination of elenolic acid and a glucosidic residue. Oleuropein is an ester of 2-(3,4-dihydroxyphenyl)ethanol (hydroxytyrosol) and has the oleosidic skeleton that is common to the secoiridoid glucosides of Oleaceae (Soler-Rivas *et al*. 2000), it is deglycosylated by a β-glucosidase released from olive fruits during crushing giving rise to oleuropein aglycone (Ole*A*) which, due to its high hydrophobicity, is retrieved in olive oil (Fig.3).

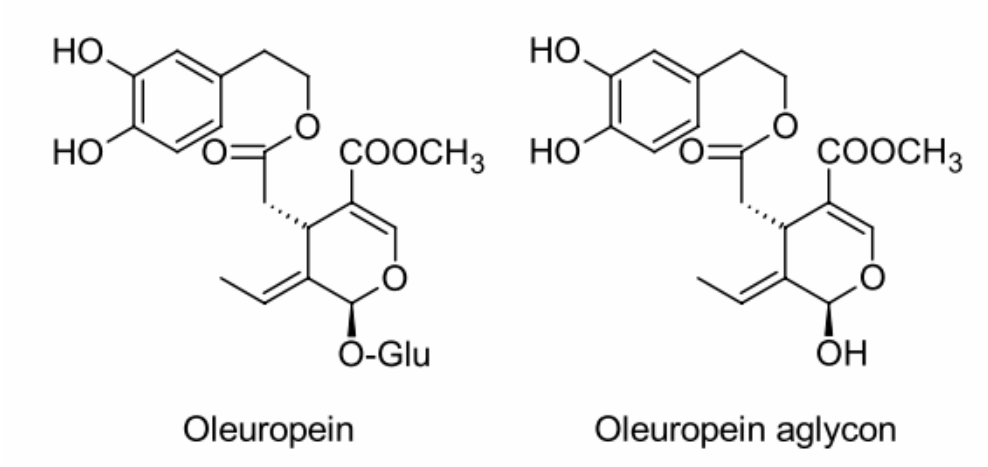

Figure 3. Structures of oleuropein and oleuropein aglycone

In the development of the olive fruit, three phases are usually distinguished: a growth phase, during which accumulation of oleuropein occurs; a green maturation phase that coincides with a reduction in the levels of chlorophyll and oleuropein; and a black maturation phase that is characterized by the appearance of anthocyanins and during which the oleuropein levels continue to fall (Amiot *et al*. 1989).

The content of OLE in olive drupes depends on the cultivar and the time of ripening; in addition, the recovery of the de-glycosylated oleuropein derivative depends on the way the fruits are processed to obtain EVOO. Finally, the content of OLE in EVOO depends on oil ageing, as the molecule undergoes degradation (mainly oxidation) with time. In a recent review Cicerale *et al*. report for the aglycone concentrations up to 351.7 mg/kg in EVOO, while a value of 2.0 mg/kg is reported for oleuropein (Cicerale *et al*. 2009).

Oleuropein has several pharmacological properties (Fig. 4); these include antioxidant (Visioli *et al*. 2002), anti-inflammatory (Visioli *et al*. 1198), anti-atherogenic (Carluccio *et al*. 2003), anti-cancer (Owen *et al*. 2000), antimicrobial (Tripoli *et al*. 2005), and antiviral (Fredrickson *et al*. 2000) properties, and for these reasons, it is commercially available as food supplement in Mediterranean countries. In addition, oleuropein has been shown to be cardioprotective against acute adriamycin cardiotoxicity (Andreadou *et al*. 2007) and has been shown to exhibit anti-ischemic and hypolipidemic activities (Andreadou *et al*. 2006).

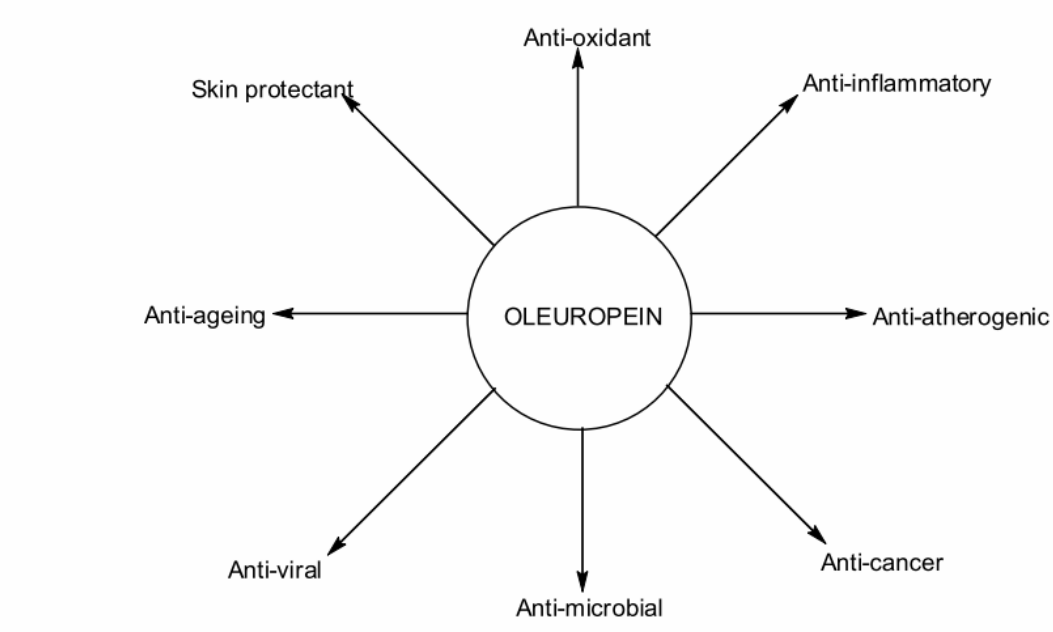

Figure 4. Pharmacological effects of oleuropein and oleuropein aglycone.

The aglycone is able to cross the plasma membrane acting inside the cells and is better absorbed in the intestine because is more hydrophobic than the glycated form. Another important aspect to be considered is that Ole*A* interaction with cell membranes would increase its local concentration; this is particularly relevant when considering the beneficial effects that would be attained above critical concentration of the molecule. Moreover, Ole*A* acts not only as an antioxidant, rather, it seems to be able to interact with molecular targets, in some cases with high specificity. A number of studies, including the ‘‘Three city study’’ (Bazoti *et al*. 2008) have clearly shown a strict association between most of the protective effects of the MeDi and the sustained consumption of EVOO, a basic component of the MeDi. In particular, a number of polyphenols and secoiridoids found in EVOO, including oleocanthal, hydroxythyrosol and Ole*A*, have been considered potential candidates as key responsible of the protective effect of EVOO (Mori *et al*. 2012). Most of the research on oleuropein as an aggregation inhibitor was performed on its aglycone derivative, which was shown to interfere with both hIAPP and Aβ42 aggregation (Rigacci *et al*. 2010; Rigacci *et al*. 2011), skipping the appearance of toxic oligomers and promoting peptide aggregation into aggregates devoid of cytotoxicity (Link CD 1995). Studies *in vivo* show an Ole*A* protection against Aβ42 aggregation in tissue, which generates the plaque deposits found in AD, using *C. elegans* as a simplified invertebrate model of AD (Wu *et al*. 2006). Finally, we recently showed that dietary supplementation of OLE strongly improved the cognitive performance of the TgCRND8 mouse model of AD; mice showed remarkably reduced plaque deposits, microglia migration to the plaques for phagocytosis. Data obtained with cultured cells confirmed that Ole*A* is able to induce autophagy, possibly by acting on the mTOR pathway (Grossi *et al*. 2013). Also, Ole*A* was more effective than oleuropein and hydroxytyrosol (that, anyway, were also active) as an inhibitor of Tau fibrillization (Kostomoiri *et al*. 2013). Oleuropein was also shown to modify APP processing, increasing the formation of the non-amyloidogenic and neuroprotective sAPPα fragment and to decrease Aβ oligomers in HEK695 cell supernatants by increasing matrix metalloproteinase-9 (MMP-9) secretion (Pitt, J *et al*. 2009). These results are very promising and pave the way to a more extensive investigation of Ole*A* ability to inhibit toxic amyloid aggregation of other proteins too, given the high similarity of amyloid aggregates originated from different protein/peptides.

5 Transthyretin and hyperhomocysteinemia

5.1 Homocysteine and Hyperhomocysteinemia

Homocysteine is a homologue of the amino acid cysteine, from which it differs by an additional methylene bridge (-CH_2-), and it is biosynthesized from methionine. Homocysteine is metabolized through two pathways: methionine receives an adenosine group from ATP, a reaction catalyzed by S-adenosyl-methionine synthetase, to give S-adenosyl methionine (SAM). L-Homocysteine has two primary fates: conversion via tetrahydrofolate (THF) back into L-methionine or conversion to L-cysteine (Champe *et al*. 2008). Remethylation requires folate and B12 coenzymes; trans-sulfuration requires pyridoxal-5'-phosphate, the B6 coenzyme (Selhub 1999). In kidney and liver, homocysteine is also remethylated by the enzyme betaine homocysteine methyltransferase (BHMT), which transfers a methyl group to homocysteine via betaine demethylation to dimethylglycine (DMG). The trans-sulfuration pathway requires the enzyme cystathionine-synthase (CBS) and vitamin B6 (pyridoxal-5'-phosphate). Once formed from cystathionine, cysteine can be used in protein synthesis and glutathione production.

The above pathway yields cysteine, which is then used by the body to make glutathione, a powerful antioxidant that protects cellular components against oxidative damage. Blood levels of total homocysteine increase throughout life in men and women (Selhub *et al*. 1999). Prior to puberty, both sexes enjoy optimal healthy levels (about 6 µmol/L). During puberty, levels rise, more in males than females reaching, on average, almost 10 µmol/L in men and over 8 µmol/L in women (Ganji *et al*. 2006). For reasons not yet clear, homocysteine levels tend to be higher in males incrasing with age, smoking habits, and caffeine consumption. As we grow old, mean values of homocysteine continue to rise and the concentrations usually remain lower in women than in men (Ganji *et al*. 2006). The higher total homocysteine concentrations seen in the oldest individuals may be caused by many factors including defects in absorption of vitamin B12 or a suboptimal intake of B-vitamins (especially vitamin B12) due to reduced kidney function, medications that reduce the absorption of vitamins (Ruscin *et al*. 2002) or increase the catabolism of the vitamins (Wulffele *et al*. 2003). Certain diseases are associated with higher homocysteine levels, similarly to lifestyle factors such as coffee

consumption (Temple *et al*. 2000) and excessive alcohol intake (Sakuta *et al*. 2005). Lack of exercise, obesity, and stress are also associated with hyperhomocysteinemia.
Homocysteine can both initiate and potentiate atherosclerosis. For example, homocysteine-induced injury to the arterial walls is one of the factors that can initiate the process of atherosclerosis, leading to endothelial dysfunction and eventually to heart attacks and strokes (Gallai *et al*. 2001, Papatheodorou *et al*. 2007). Several studies have shown that homocysteine can inflict damage to the arterial wall via multiple destructive molecular mechanisms (Zeng *et al*. 2003, Hofmann *et al*. 2001). The risk associated with homocysteine appears to increase throughout the normal range of concentrations; each 1 micromolar rise in the blood concentration corresponding to an increase of about 10% in cardiovascular risk. Homocysteine can be directly toxic to blood vessels — similarly to oxidized LDL andcholesterol it disrupts the healthful function of the cells lining the blood vessels— it seems likely that homocysteine is not merely a marker for some other pathogenic (disease causing) factor. It is therefore highly desirable to develop and implement safe measures for minimizing serum homocysteine levels.

5.2 Homocysteine and alteration on protein structure

The problem of Hcy toxicity has attracted a great deal of interest. At molecular level, several potential mechanisms were proposed, including those involving ROS formation (McDowell and Lang, 2000), hypomethylation (Hultberg *et al*. 2000), induction of unfolded protein response and protein N-homocysteinylation. One of proposed homocysteine toxicity mechanisms includes endoplasmatic reticulum stress and the unfolded protein response. The cellular consequence of protein modification with homocysteine is endoplasmatic reticulum (ER) stress, a condition in which unfolded proteins accumulate in the ER (Kaufman, 1999).
It was found that homocysteine decreases extracellular superoxide dismutase (EC-SOD) (a glycoprotein that protects the vascular wall from oxidative stress), mRNA expression and protein secretion. Moreover, homocysteine induces the expression of GRP78 mRNA and activates PERK in vascular smooth muscle cells, responses observed during ER stress (Nonaka *et al*. 2001). Vascular endothelial growth factor (VEGF) expression

is increased by exposure to chemical inducers of ER stress (Abcouwer *et al*. 2002). Homocysteine increases VEGF expression 4.4-fold due to ATF4-dependent activation of VEGF transcription in the retinal-pigmented epithelial cell line ARPE-19. HTL and DTT induce VEGF expression 7.9 and 8.8-fold, respectively (Roybal *et al*. 2004).

Homocysteine forms stable disulfide bonds with cysteine residues which may alter or impair protein function (Jacobsen *et al*. 2005). Homocysteine exhibits the greatest (comparing to cysteine and glutathione) tendency to generate disulfide bonds with protein thiols groups involved in the function of many enzymes, structural proteins and receptors; accordingly, the interaction with these groups might disrupt cellular metabolism (Hultberg *et al*. 1998). Binding of homocysteine to plasma protein is biphasic. The first reaction, involving displacement of cysteine from plasma proteins, is rapid and oxygen-independent, while the second reaction is a slower, oxygen dependent thiol oxidation (Togawa *et al*. 2000). S-homocysteinylated proteins (S-Hcy-proteins) are present in human plasma. Major components of the S-Hcy-protein pool in human plasma are albumin, containing about 1 homcysteine molecule per 100 protein molecules, and γ-globulins, containing about 3.4 molecules per 100 protein molecules. Other proteins contain >10-fold less S-Hcy/protein than albumin (Jakubowski, 2002b). Human serum albumin is the major plasma protein, making up more than 50% of the total plasma protein. *In vitro* and *in vivo* studies have shown that post-translational homocysteine incorporation into proteins via S-homocysteinylation may impair protein function (Hajjar *et al*. 1998; Undas *et al*. 2001; Majors *et al*. 2002). Homocysteinylated proteins are prone to multimerization and undergo structural changes that lead to their denaturation. Homocysteine thiolactone may also inactivate enzymes by other mechanisms. For example, lysine oxidase, an important enzyme responsible for posttranslational collagen modification essential for the biogenesis of connective tissue matrices, is inactivated by Hcy thiolactone, which derivatizes the active site tyrosinequinone cofactor (Liu *et al*. 1997). In addition to a loss of function, protein homocysteinylation can also generate modified proteins that are physiologically detrimental in other ways. For example, homocysteinylated LDL has been recently shown to elicit immune response in rabbits (Ferguson *et al*. 1998). Protein homocysteinylation is a novel example of protein damage that may explain the involvement of Hcy in the pathology of human vascular diseases.

5.3 Transthyretin and Homocysteine: post-translational modifications and TTR amyloidogenesis

It is not known whether posttranslational modifications of TTR occur intracellularly or extracellularly. However, in plasma, the reduced, oxidized, and protein-bound forms of homocysteine, cysteine, cysteinylglycine, and glutathione interact by redox and disulfide exchange reactions. These interactions may play an important role in the extracellular antioxidant defence system (Ueland *et al*. 1996). Sulfitolysis of disulfide bonds in proteins produces S-sulfonated proteins. The reaction involves the nucleophilic attack of the sulfite ions on disulfide bonds in proteins (Cecil and Wake 1962). For example, S-sulfonation of albumin and fibronectin is well documented. Formation of S-sulfonated proteins may disrupt the redox thiol status in plasma, allowing excessive reactive oxygen species to oxidize proteins. The levels of oxidized proteins increase with age, possibly due to the increase of ROS generation (Berlett and Stadtman 1997). Post-translational modification of human TTR at Cys10 alter protein structure of. Monomeric TTR has a single cysteine residue at position 10. In the normally folded tetrameric protein, the Cys10 residues are in exposed sites at the beginning of the helical regions and can conjugate with cysteine and other sulfur-containing ligands. According to the crystal structure of wild-type TTR, the Cys10 residue is located at the edge of β-strand A and its sulfur atom could form a sulfur-hydrogen bond (Terry *et al*. 1993). When the Cys10 residue is post-translationally modified, the sulfur atom of Cys10 is no longer available to form hydrogen bond, and the distruption of this bond may alter TTR structure causing it to adopt a different conformation. Modifications are heterogeneous, with S-sulfonation or S-thiolation (cysteine or cysteineglycine) most commonly reported. Cys10 modification reportedly affects TTR stability. S-cysteinylation destabilizes TTR at both low pH (Zhang and Kelly, 2003) and high pH, whereas S-sulfonation stabilizes against aggregation under acidic conditions and at pH 9 (Kingsbury *et al*. 2008). Kishikawa *et al*. reported that S-sulfonation enhanced the amyloidogenicity of TTR (Kishikawa *et al*. 1999). The formation of TTR fibrils was studied with three different preparations: unmodified TTR (with thiol compounds bound to Cys10 and containing approximately 20% S-sulfonated protein), DTT-treated TTR (with a free sulfhydryl group at Cys10), and TTR conjugated with sulfite (S-sulfonate TTR). At pH 4.0 there was a 3-fold enhancement of fibril formation with S-sulfonate

TTR compared to unmodified TTR while reduced TTR had very low ability to fibrillize. These results show that sulfonation of Cys10 in TTR might increase the fibrillization potential of the protein, which could lead to a more rapid progression of familial TTR amyloidosis or senile systemic amyloidosis. Interestingly, a higher percentage of S-conjugated TTR to the unmodified form has been reported in patients with symptomatic amyloid disease (Suhr *et al*. 1999). Likewise, the Cys33 residue is within a structured region of TTR and its post-translational modification may interrupt normal folding. Interestingly, only one other Cys substitution (at position 114) has been described by DNA sequence analysis. However, no data have been reported on the post- translational modification of Cys114.

Protein conformational changes resulting from amino acid substitution and posttranslational modification may affect the rate of protein degradation. Degradation of extracellular proteins involves pinocytosis and specific receptor-mediated endocytosis. Through these processes, extracellular proteins are taken inside the cell for degradation in lysosomes. The mechanism of TTR cellular uptake and degradation is not well understood. However, cellular uptake of TTR has been shown to be receptor-mediated, and the structure of the TTR can affect receptor recognition (Sousa and Saraiva 2001). Post-translational modifications, in addition to amino acid substitution, can affect TTR structure and thus its ability to bind these receptors.

TTR undergoes homocysteinylation at its single cysteine residue (Cys 10) both *in vitro* and *in vivo* (Lim *et al*. 2003). The ratios of TTR-Cys10-S-S-homocysteine and TTR-Cys10-S-S-sulfonate to that of unmodified TTR increased with increasing homocysteine plasma concentrations, whereas the ratio of TTR-Cys10-S-S-cysteine to that of unmodified protein decreased. Recent data show that L-homocysteine reacts with TTR in the human plasma to form a stable covalent adduct both *in vitro* and *in vivo*. TTR is the third plasma protein, after albumin (Refsum *et al*. 1985; Sengupta *et al*. 2001) and fibronectin (Majors *et al*. 2002), to be identified as a carrier of homocysteine *in vivo*.

Aim of the study

AIM OF THE STUDY

During my PhD I have focused my attention different aspects of the Aggregation pathway of TTR and β2-microglobulin variant, D76N as well as on the study of possible inhibitors of the fibrillogenesis process.

1. Oleuropein Aglycone: a natural polyphenol which protects against the cytotoxicity associated with Transthyretin fibrillogenesis

In addition to liver and heart transplantation, there is no effective medical treatment to improve or blocks the progression of the diseases; it is therefore evident the importance of studying strategies to inhibit the formation of TTR amyloid fibrils or to delineate appropriate therapeutic interventions. Recent data show that some compounds, natural and not, stabilize the TTR native state and inhibit fibril formation, suggesting the possibility of medical treatment for TTR-amyloidosis associated. In particular it has been shown that natural compounds, such as curcumin, rosmarinic acid, EGCG or Resveratrol Can have a protective effect on the aggregation of TTR. On the basis of these results, we decided to investigate the effects of OleA on TTR aggregation and cytotoxicity. In order to study the effects of OleA I have used various various analysis *in vitro* techniques, such as Intrinsic Fluorescence, FT-IR, DLS, protein digestion with PK, and TEM, and *in vivo* analysis on HL-1 cardiomyocytes by the MTT cytotoxicity assay and immunofluorescence.

2. Wild-type and Leu55Pro Transthyretin Homocysteynilation, worsening of cardiomiopathy onset

The problem of Homocysteine (Hcy) toxicity has become of great interest considering that Hcy can form stable disulfide bonds with proteins cysteine residues, which may alter or impair the function of the protein itself. Protein homocysteinylation is a novel example of protein damage that may explain the involvement of Hcy in a series of human cardiovascular.

Recently the binding of cysteine and homocysteine with wt-TTR have been found in human serum. Considering the mass-spectrometry data already available on about the

binding of wt-TTR and Hcy, we performed made some *in vitro* and *in vivo* experiments to study the effect of Hcy on wt- and L55P-TTR in physiological conditions. In particular on L55P, that it induces ~~a~~ cardiomiopathy in patients, and we tested the samples on HL-1, cardiomyocyte cell line.

3. Molecular insights into membrane interaction of a new amyloidogenic variant of β2-microglobulin

I have investigated the cytotoxicity of D76N-β2m on neuroblastoma cell line SH-SY5Y with particular emphasis on the correlation between the structural aspects of the aggregates and their cytotoxic effect. Studies with human neuroblastoma cells, SH-SY5Y showed that β2-m is not neurotoxic, because the protective blood-brain barrier keeps the protein at lower concentration in the cerebrospinal fluid. The pathogenic protein was aggressively fibrillogenic *in vitro*, prompting a revaluation of previously hypothesized mechanisms of β2-m fibrillogenesis. Extensive amyloid deposits were found in the spleen, liver, heart, salivary glands, and nerves. So resulted be important characterize the way by the aggregates resulted be cytotoxic. Preliminary results indicate that the pre-fibrillar species of D76N are toxic and appear to interact preferentially with the extensions of SH-SY5Y cells, confirming the neurodeposition of these aggregates observed in patients. These observations have led to carry out a series of experiments on SH-SY5Y cells differentiated by treatment with retinoic acid. In addition to vitality and cellular localization of the aggregates we analyzed cellular apoptosis, the intracellular calcium flux and ROS production.

Materials and Methods

1. Oleuropein Aglycone: a natural polyphenol which protects against the cytotoxicity associated with Transthyretin fibrillogenesis

Oleuropein deglycosilation. Oleuropein was purchased from Extrasynthese and deglycosilated by almond β-glycosidase (EC 3.2.1.21, Fluka, Sigma-Aldrich) as previously described (Rigacci *et al*. 2010). Briefly, a 10 mM solution of Oleuropein in 310 µl of 0.1 M sodium phosphate buffer, pH 7.0, was incubated with 9 IU of β-glycosidase overnight at room temperature. The reaction mixture was centrifuged at 18,000 rpm for 10 min to precipitate the oleuropeina aglycon, which was dissolved in DMSO (dimethylsulfoxide) (Rigacci *et al*. 2010). The complete oleuropein deglycosylation was confirmed by assaying the glucose released in the supernatant with Glucose (HK) Assay kit (SIGMA), the 100mM stock was protected from light and used by the day it was prepared.

TTR samples. Lyophilized TTR was dissolved in buffer 30mM sodium phosphate pH 7.5 and the aggregation was induced by added of 100mM sodium acetate pH 4.0.TTR fibrils were obtained by incubating wt-TTR at 37°C and pH 4.4 for 72h whereas the L55P fibrils were grown upon incubation at 37°C and pH 5.5 for 96h, as previously reported (Bonifacio *et al*. 1996; Lai *et al*. 1996). Aggregation kinetic was followed by FT-IR. To study the interference of OleA with aggregation, wt-TTR and L55P were incubated with 3XOleA for 72h and 96h, respectively; disaggregation experiments were carried out using pre-formed fibrils incubated with OleA for different time lengths.

Congo Red Assay. Congo Red (CR) is used to demonstrate the presence of amyloidal deposits in tissue. CR appears red at normal light but yellow/green between crossed polarisers. Binding the amyloid induces a characteristic shift in CR maximal optical absorbance from 490nm to 540 nm (Frid *et. al.* 2007). The assay was performed as previously described (Nilsson *et al*. 2004), 7,14 µM of TTR incubated in the presence or in absence of 3x Ole during the aggregation. Ole was added also with pre-formed fibills of TTR for 10 minutes and 5 hours. Fibrills and native wt-TTR were incubated with 5mM Sodium phosphate buffer, 150 mM NaCl, pH 7.4 contained 20µM of CR. The spectrum was recorded in the 400-700 nm region using Jasco V-630 Spectrophotometer. Blank spectra were acquired for CR alone, in the presence or in absence of Ole, and subtracted to each sample spectrum. Spectral difference was obtained by substracting

the spectrum of CR with buffer of TTR aggregation, CR with Ole and TTR in aggregation buffer without CR.

Transmission Electron Microscopy. Five microliter aliquots from TTR in presence and absence of Ole were withdraw at different time points and were loaded onto a formvar/carbon-coated 400 mesh nickel grids (Agar Scientific, Stansted, UK) and negatively stained with 2.0% (w/v) uranyl acetate (Sigma-Aldrich). The grid was airdried and examined using JEM 1010 trasmission electron microscope at 80kV excitation voltage.

Isolation and culture of HL-1 cardiomyocyte. Mouse atrial myocytes HL-1 were obtained from Dr W. C. Claycomb (Louisiana State University Health Science Center, New Orleans, LA, USA) and grown in T25, gelatin- fibronectin coated flasks, as previously described (Sartiani *et al*. 2002). The cells were maintained in Claycomb Medium (JRH Biosciences), supplemented with 10% fetal bovine serum (Sigma-Aldrich), 2.0 mM L-glutamine (Sigma-Aldrich), 0.1 mM noradrenaline (Sigma-Aldrich) and 100U/mL penicillin-streptomycin (Sigma-Aldrich). Every three days the cells were detached and re-plated at a 1:3 dilution in a new T25 flask or in 96 well plates (70-90% confluent) and used for experimental measurements.

MTT Assay. The MTT assay is based on the protocol described for the first time by Mosmann (Mosmann T, 1983). The assay was optimized for the cell lines used in the experiments. To test if the drug was able to reduce the toxicity of amyloid aggregates of TTR was used a test of cell viability using the 3-(4,5-dimethylthiazol-2-y1)-2,5-dipheniltetrazolium-bromide (MTT). This product is of yellowish colour in solution. Mitochondrial dehydrogenases of viable cells cleave the tetrazolium ring, leading to the formation of purple crystals which are insoluble in aqueous solutions. The crystals are re-dissolved in isopropanol and the resulting purple solution is measured spectrophotometrically. An increase or decrease in cell number results in a concomitant change in the amount of formazan formed, indicating the degree of cytotoxicity caused by the test material. This assay is used to assess the viability of cells subjected to appropriate treatments compared to control cells. HL-1 cells were seeded into 96-well plates at a density of 6000 cells/well in fresh complete medium and grown fro 48h.Cells were treated with 20μM of wt-TTR and L55P in presence and absence of 3X Ole, also with pre-fibrillar aggregates incubated with Ole. After 24h of incubation, the culture

medium was removed and the cells were incubated with 100 µl of serum-free DMEM without phenol red, containing 0,5 mg/ml MTT for 1h at 37°C. Then, 100 µl of cell lysis solution (20% SDS, 50% N, N-dimethylformamide) was added to each well and the samples were incubated at 37 °C to allow complete lysis. The absorbance of the blue formazan was read at 570 nm using a spectrophotometric microplate reader automatically. The final values of absorption were calculated by averaging of each sample in triplicate and subtracting from this the average of the white, consisting of 100µl of MTT solution and 100 µl of lysis solution. All data were expressed as mean ± deviation standard.

Confocal Immunofluorescence. Subconfluent HL-1 cells grown on glass coverslips were treated for 24h with the different samples of wt-TTR and L55P (20µM). After incubation the cells were washed with PBS and cell surfaces GM1 labeling was performed by incubating the cells with 10 ng/ml CTX-B Alexa488 in complete medium for 10 min at room temperature. Then fixed in 2.0% buffered paraformaldehyde for 10 min and permeabilized by treatment with 50% acetone 50% ethanol for 4 min at room temperature, washed with PBS and blocked with PBS containing 0.5 % BSA and 0.2 % gelatine. The cells were incubated 1.0 h at room temperature with a rabbit polyclonal antibody raised against TTR diluted 1:600 in the blocking solution; then the cells were washed with PBS for 30 min under stirring. The immunoreaction was revealed with Alexa568-conjugated anti-rabbit secondary antibody (Molecular Probes) diluted 1:100 in PBS. Finally, the cells were washed twice in PBS and once in redistilled water to remove non-specifically bound antibodies. Cell fluorescence was visualized using a confocal Leica TCS SP5 scanning microscope (Leica, Mannheim, Ge) equipped with a HeNe/Ar laser source for fluorescence measurements. The observations were performed using a Leica Plan 7 Apo X63 oil immersion objective, suited with optics for DIC acquisition.

Fluorescence resonance energy transfer (FRET). Fluorescence resonance energy transfer (FRET) misuring a distance-dependent physical process by which energy is transferred non radiatively from an excited molecular fluorophore (the donor) to another fluorophore (the acceptor). The analysis was based on the immunoreaction between GM1 (donor) and TTR (acceptor) aggregates labeled with Alexa FLUO-488 and Alexa

FLUO-568, respectively. 3D volume renderings were obtained by using OsiriX software (http://www.osirix-viewer.com).

Dynamic light scattering (DLS). DLS is a well-established technique for measuring the size and size distribution of molecules and particles typically in the submicron region, and with the latest technology lower than 1nm. Typical applications of dynamic light scattering are the characterization of particles which have been dispersed or dissolved in a liquid. The Brownian motion of particles or molecules in suspension causes laser light to be scattered at different intensities. Analysis of these intensity fluctuations yields the velocity of the Brownian motion and hence the particle size using the Stokes-Einstein relationship. The basic principle is simple: The sample is illuminated by a laser beam and the fluctuations of the scattered light are detected at a known scattering angle θ by a fast photon detector. Simple DLS instruments that measure at a fixed angle can determine the mean particle size in a limited size range. More elaborated multi-angle instruments can determine the full particle size distribution. From a microscopic point of view the particles scatter the light and thereby imprint information about their motion. Analysis of the fluctuation of the scattered light thus yields information about the particles. Experimentally one characterizes intensity fluctuations by computing the intensity correlation function g2 (t), whose analysis provides the diffusion coefficient of the particles (also known as diffusion constant). The diffusion coefficient D is then related to the radius R of the particles by means of the Stokes-Einstein Equation:

$$D = \frac{kT}{6\pi R\eta}$$

Where k is the Boltzmann-Konstant, T the temperature and η the viscosity. The correlation of the intensity can be performed by electronic hardware or software software analysis of the photon statistics. Because fluctuation is typically in the range of nanoseconds to milliseconds, electronic hardware is typically faster and more reliable at this job.

FT-IR spectroscopy. These experiments were made in collaboration with the University of Milan, the Department of Physyscs, briefly aliquots of lyophilized protein were resuspended at a final concentration of 80μM in deuterated 30 mM phosphate buffer, with and without Oleuropein, at different pD. Deuterated buffers containing Oleuropein

were prepared from a stock solution of Oleuropein 50 mM in DMSO. Fourier transform infrared (FTIR) spectra were collected and analyzed as previously described (Ami *et al*. 2012). In particular, a volume of 15 µl of the protein solution was placed in a temperature-controlled transmission cell (Wilmad, USA) with BaF2 windows and an optical path made by a Teflon spacer of 100 µm. FTIR spectra were collected in transmission mode during incubation at 37°C for 72 hours in the transmission cell. A Varian 670-IR spectrometer (Varian Australia Pty Ltd., Mulgrave VIC, AU) was employed under the following conditions: 2 cm-1 spectral resolution, 5 KHz scan speed, triangularapodization, and 256 and 1000 scan coadditions. After 72 hour at 37°C, the same solution was heated up to 100°C at a rate of 0.2°C/min. Buffer subtraction, vapor correction (when necessary), and the second derivative of the absorption spectra (Susi *et al*. 1986; Natalello *et al*. 2012) were performed using the Resolutions-Pro software (Varian Australia Pty Ltd., Mulgrave VIC, AU).

Acrylamide Quenching. Aliquots of the protein solutions were drawn at various time points during the course of fibrillation and mixed with increasing concentrations of acrylamide, from 0 to 0.6 M in buffer phosphate pH7 followed by mixing and incubation for 5 minutes in the dark. The intrinsic fluorescence was recorded before and after addition of the quencher. Excitation wave-lenght was set to 280 nm and emission intensity was scanned from 300 to 450 nm. Fluorescence intensities were further corrected for diluition because of the step-wise addition of acrylamide. Quenching data were analysed by fitting to the Stern-Volmer equation that describes collisional quenching processes:

$$(I0/I)=1 + Ksv[Q]$$

where I0 is the fluorescence intensity prior to the addition of the quencher, I is the intensity after quencher addition, and [Q] is the molar quencher concentration. High Ksv values indicate a high degree of quenching and therefore high Trp accessibility. Stern-Volmer plots for the TTR were fitted with the equation:

$$F0/F = (1 + Ksv\text{-}[A]) \exp(Kst)[A])$$

where F0 and F are the intrinsic fluorescence intensities in the absence and presence of acrylamide, respectively, [A] is the concentration of the acrylamide, Ksv is the Stern-

Volmer constant for dynamic quenching, and Kst is the static component of the quenching process (Souillac *et al*. 2003).

Protease Digestion. Samples of TTR fibrils in presence and absence of Ole was treated with 50X of Proteinase K at different times (Bateman *et al*. 2010). Aliquots of these samples were taken at defined times and analyzed by SDS-PAGE using 15% (w/v) polyacrilamide gels. The progressive digestions were monitored observing a progressive intensity change of the corresponding bands.

***Intrinsic fluorescence*.** The fluorescence emission spectra were normalized to an intensity of 1.0 at the observed λmax using FLwinlab software (Perkin-Elmer Instrument Corporation, Wellesley, MA) prior to derivatization. Trp emission scan normalization was essential to compare the intensities and the positions of various bands appearing in the second derivatives of the fluorescence emission scans. The average of five scans was then subjected to smoothing using a 11-point smoothing average and a Savitzky-Golay algorithm using Omnic-software (Nicolet Inc., Madison, WI). Finally, the second derivatives of the smoothed spectrum were obtained using the same software. A smoothing step of the normalized data was required to reduce the noise in the second derivative. The smoothing criteria meet the need that the overall shape and intensity of the raw emission scan is not affected following smoothing and at the same time the overall shape of the bands in the second derivative is preserved and the excess noise is removed.

Statistical Analysis. Statistical analysis of the data was performed by using one way analysis of variance (ANOVA) and Bonferroni test to determine differences in cytotoxicity.

2. Wild-type and Leu55Pro Transthyretin Homocysteynilation, worsening of cardiomiopathy onset

Materials. All reagents were of analytical grade or of the highes tpurity available.bovine serum albumin (BSA), fetal bovine serum (FBS), were from Sigma-Aldrich (Milan, Italy), unless otherwise stated. Fluo3-AM, calcein-AM and CM-H2 DCFDA (Life Technologies, CA, USA) were prepared as stock solutions in dimethylsulfoxide (DMSO), dried under nitrogen and stored in light-protected vessels at −20 °C until use.

Isolation and culture of HL-1 cardiomyocytes. How said above, for these experiments I have used HL-1 mouse atrial myocytes and grown in T25, gelatin- fibronectin coated flasks. The cells were maintained in Claycomb Medium (JRH Biosciences), supplemented with 10% fetal bovine serum (Sigma-Aldrich), 2.0 mM L-glutamine (Sigma-Aldrich), 0.1 mM noradrenaline (Sigma-Aldrich) and 100U/mL penicillin-streptomycin (Sigma-Aldrich).

TTR samples. Lyophilized L55P-TTR was dissolved in buffer 30mM sodium phosphate pH 7.4. To study the interference of Hcy with aggregation, L55P was incubated with Hcy in a molar ratio 1:2 (TTR tetramer:Hcy) in 10min-7days range.

SDS-PAGE. Proteins were separated by SDS-PAGE. SDS is an anionic detergent applied to protein sample to linearize proteins and to impart a negative charge to linearized proteins. In most proteins, the binding of SDS to the polypeptide chain imparts an even distribution of charge per unit mass, thereby resulting in a fractionation by approximate size during electrophoresis. Sample were dissolved in Laemmli sample buffer (62.5mM Tris-HCl, pH 6.8, 2% SDS, 25% glycerol, 0.01% bromphenol blue). The 0.1% of 2-βmercaptoethanol (BME) was added before the boiling (10 min, 95 °C) in a water bath, a 10µl sample was applied onto the 15% SDS-PAGE gel. The visualization was carried out using Coomassie Brilliant Blue dye.

Native-PAGE. "Native" or "non-denaturing" gel electrophoresis is run in the absence of SDS. While in SDS-PAGE the electrophoretic mobility of proteins depends primarily on their molecular mass, in native PAGE the mobility depends on both the protein's charge and its hydrodynamic size. The electric charge driving the electrophoresis is governed by the intrinsic charge on the protein at the pH of the running buffer. This

charge will, of course, depend on the amino acid composition of the protein as well as post-translational modifications such as addition of sialic acids. Running Buffer 5x, Leammli 2x and 12% Acrylamide gel without SDS. The samples were not boiled and the visualization was carried out using Coomassie Brilliant Blue dye.

Dot-blot assay. Accordingly to Abcam protocol, briefly, 2µl of samples were spotted onto the nitrocellulose membrane and this latter was air-dried and blocked with PBS containing 5% BSA (Bovine Serum Albumin, SIGMA, Aldrich). Following incubation with anti-TTR primary antibodies (1:600) or A11 anti-oligomer antibodies (a gift from Glabe C.) (1:1000), peroxidase-conjugated anti-rabbit antibodies and a chemiluminescent substrate, the image was acquired with a ChemiDoc system (Bio-Rad).

Turbidimetric Assay. According to Arsequell T and co-workers (Arsequell *et al*. 2012) we monitored turbidity in a 96 multiwells contained 5 µM L55P- TTR and 10 µM Hcy (1:2) in buffer sodium phosphate at pH 7.0 and were carried out at 37 °C without stirring. The absorbance was determined at 400nm with an automatic plate reader (Bio-Rad).

Transmission Electron Microscopy. 5 µl aliquots of the TTR in presence and absence of Hcy were withdraw at different time points, loaded onto a formvar/carbon-coated 400 mesh nickel grids (Agar Scientific, Stansted, UK) and negatively stained with 2.0% (w/v) uranyl acetate (Sigma-Aldrich). The grid was air-dried and examined using JEM 1010 trasmission electron microscope at 80kV excitation voltage.

MTT Assay. The MTT assay was optimized for the cell lines used in the experiments. Briefly, HL-1 cells were seeded into 96-well plates at a density of 6000 cells/well in fresh complete medium and grown for 48h. Then the cells were treated for 24 h with 5µM L55P-TTR (tetramer) at different times of aggregation in the presence or in the absence of Hcy (10 µM). HypF-N oligomers were formed in according to protocol of Campioni and co-workers (Campioni *et al*. 2010). Native proteins were diluted to a final concentration of 12µM into the same media. Oligomers were then incubated in the appropriate media for 1 h at37 °C while shaking, in the absence or presence of each TTR, and then added to cultured cells or subjected to biophysical/biochemical analysis. The protein : TTR molar ratio was 10:1 (Cascella *et al*. 2013).

Circular Dichroism spettroscopy. The spectra were recorded with a Jasco J-810 spectropolarimeter equipped with a thermostated cell holder attached to a Thermo Haake C25P water bath. The spectra were acquired with a 2 cm/min scan speed and data points were collected from 260 to 190 nm at 25 ° C with a 1 mm path length quartz cell. The final concentration of all samples was 40 μM. All spectra were blank-subtracted and converted to molar ellipticity per residue.

Dynamic light scattering (DLS). DLS measurements were performed using a Zetasizer Nano S DLS device from Malvern Instruments (Malvern, Worcestershire, UK), thermostated with a Peltier system and using a low-volume (45 μl), ultramicro cell (code 105.251-QS) from Hellma Analytics (Müllheim, Germany). Size distributions by intensity and total light-scattering intensity were determined at regular time-intervals over a period of 10 min. The temperature was maintained at 37 °C and the parameters were set manually on the instrument to allow the same settings in the various distributions acquired at different time-values. These included ten acquisitions each of 10 second duration, with cell position 4.2 cm and attenuator index 7. The reported data are the average of three consecutive measurements.

Resveratrol binding assay. Fluorescence studies were based on Tatyana *et al* 2008 (Tatyana *et al*. 2008; Choi *et al*. 2010). Briefly, Resveratrol was excited at 320nm and Emission spectra were recorded over a range of 350–450 nm. Free resveratrol has a fluorescence maximum at 390 nm. Fluorescence intensity increased substantially upon binding to TTR. All data have been obtained in presence of 10μM Resveratrol and 10μM Hcy incubated with 5μM TTR in native condition (sodium phosphate buffer pH 7.5).

Statistical Analysis. Statistical analysis of the data was performed by using T-student test to determine differences in cytotoxicity.

3. Molecular insights into membrane interaction of a new amyloidogenic variant of β2-microglobulin

Cell Culture. Human neuroblastoma SH-SY5Y is a dopaminergic neuronal cell line which has been used as an in vitro model for neurotoxicity experiments (Chand *et al*. 2002). Briefly, SH-SY5Y cell were cultured with complete medium (50% HAM, 50% DMEM, 10% fetal bovine serum, 3.0mM glutamine, 100units/ml penicillin and 100 µg/ml streptomycin), in a humidified, 5% CO2, 37°C incubator. 48 hour after seeding, serum levels of the medium were reduced to 3% with RA (10µM) for differentiation for four days prior to treatment (Yuen-Ting *et al*. 2009). All the materials used for cell culture were from Sigma.

Cell viability assay. The toxicity of the different forms of D76N aggregates (5µM) by the MTT assay. The assay was optimized for the cell lines used in the experiments. This product is of yellowish colour in solution. In all of the MTT-experiments, SH-SY5Y cells were plated at a density of 10000 cells per well on 96-well plates in 100µl of culture medium. After the treatment the absorbance value of blue formazan were determined at 595nm with automatic plate reader (Bio-Rad). The final values of absorption were calculated by averaging of each sample in triplicate and subtracting from this the average of the white and all data were expressed as mean ± deviation standard.

Reactive oxygen species (ROS) measurement. Intracellular ROS levels were determined using the fluorescent probe 2', 7'–dichlorofluorescin diacetate, acetyl ester (CM-H2 DCFDA) from Molecular Probes. CM-H2 DCFDA is a cell-permeant indicator for reactive oxygen species that is nonfluorescent until removal of the acetate groups by intracellular esterases and oxidation occurs within the cell. Oxidation of these probes can be detected by monitoring the increase in fluorescence. SH-SY5Y cells were plated at a density of 10000 cells per well on 96-well, like MTT-Assay, after 24h of treatments, DCFDA 10µm in DMEM without phenol red was added.

After 30 min the fluorescence values at 538nm were detected by Fluoroscan Ascent FL (Thermo-Fisher).

Intracellular Free Ca^{2+} levels. The cytosolic levels of free Ca^{2+} were measured using fluorescent probe Fluo-3 acetoxymethyl ester (Fluo-3 AM) from Molecular Probes. Fluo-e posses an absorption spectrum compatible with excitation at 488nm by argon-ion laser sources, and a very large fluorescence intensity increase upon Ca^{2+} binding. Subconfluent SH-SY5Y cells cultured on glass coverslips were incubated at 37°C for 5 min with 5.0μM Fluo-3 AM prior to D76N addition. Then the cells were fixed in 2.0% buffered paraformaldehyde for 10 min. Cell fluorescence was visualized using a confocal Leica TCS SP5 scanning microscope (Leica, Mannheim, Ge) equipped with a HeNe/Ar laser source for fluorescence measurements. The observations were performed using a Leica Plan 7 Apo X63 oil immersion objective, suited with optics for DIC acquisition.

Apoptosis Detection. The apoptosis effects induced by D76N aggregates were detected by Annexin V-FITC Apoptosis detection kit (Sigma-Aldrich). Also Propidium Iodide Solution with Annexic V-FITC were used to discriminate among viable, apoptotic and secondary necrotic cells. Briefly, after the treating for 24h with the most toxic D76N aggregates, cells are incubated with Annexim V-FITC and propidium iodide for 10 min, at room temperature. The cells are analyzed by flow cytometry, annexinV-FITC is detected as a green fluorescence and propridium iodide is detected as a red fluorescence.

Confocal Immunofluorescence. Subconfluent SH-SY5Y cells grown on glass coverslips were treated for 24h with the different D76N aggregates (5μM). How said previously, cell surfaces GM1 labeling was performed by incubating the cells with 10 ng/ml CTX-B Alexa488 in complete medium for 10 min at room temperature. Then fixed in 2.0% buffered paraformaldehyde for 10 min and permeabilized and blocked with PBS containing 0.5 % BSA and 0.2 % gelatine. The cells were incubated 1.0 h at room temperature with a rabbit polyclonal antibody raised against β2-microglobulin diluted 1:600 in the blocking solution; and the immunoreactions was revealed with Alexa 568-conjugated anti-rabbit secondary antibody (Molecular Probes) diluted 1:100 in PBS. Finally, the cells were washed twice in PBS and once in redistilled water to remove non-specifically bound antibodies. Cell fluorescence was visualized using a confocal Leica TCS SP5 scanning microscope (Leica, Mannheim, Ge) equipped with a HeNe/Ar laser source for fluorescence measurements. The observations were performed

using a Leica Plan 7 Apo X63 oil immersion objective, suited with optics for DIC acquisition.

Single particle imaging and tracking. Briefly, living cells previously exposed to aggregates were incubated in phenol red-free Leibovitz's L-15 medium 10% FBS at 37 °C first with anti-β2m (1:600) for 20 min, then for 5 min with anti-mouse Alexa 488 (1:500) and 10 µg/ml biotinylated CTX-B, and finally with streptavidin QDs (Invitrogen) in QD binding buffer for 1 min. QDs emitting at 655 nm were used at a 1:10000 dilution. Cells were monitored with a custom-made wide-field epifluorescence microscope equipped with an oil-immersion objective (Nikon Plan Apo TIRF 60x/1.45), a Reliant 150 Select argon ion laser (excitation line 488 nm) and a heating chamber. A FF499-Di01-25 dichroic, and FF01-655/15-25 (for QDs) and FF01-530/43-25 (for Alexa 488) emission filters (Semrock) were used. 250 or 100 consecutive frames were acquired with an integration time of 10 ms, respectively, with an Electron Multiplying Charge-Coupled iXon Ultra camera (Andor). Recording sessions did not last more than 30 min. Tracking of single QDs, which were identified by their fluorescence intermittence, was performed with MATLAB (MathWorks, Natick, MA) using a homemade macro that accounts for blinking in the fluorescence signal.

Quantitative analysis of diffusion coefficient. The mean square displacement (MSD) analysis allows to calculate the initial diffusion coefficient (D) of each particle. Briefly, physical parameters can be extracted from each trajectory (x(t),y(t)) by computing the MSD, determined from the following formula:

$$MSD(ndt) = \frac{1}{N-n} \sum_{i=1}^{N-n} [(x_{(i+n)} - x_i)^2 + (y_{(i+n)} - y_i)^2]$$

where xi and yi are the coordinates of a particle on frame i, dt is the time between two successive frames, N the total number of frames of the trajectory and ndt the time interval over which the displacement is averaged. This function enables the analysis of the lateral dynamics on short (initial diffusion coefficient) and long (types of motion) time scales. Different types of motion can be distinguished from the time dependence of the MSD. The initial diffusion coefficient (D) is determined by fitting the initial 2 to 5 points of the MSD against time plot with MSD(t) = 4D2-5 t + b. The cumulative probability C (d) of D defines the probability that D is less that d. We compared

cumulative probability distributions and median instead of mean values because D values were spread over four orders of magnitude. Images were threshold with ImageJ software, creating binary masks corresponding to amyloid aggregates.

GM1 depletion. To reduce cell membrane GM1, the plated SH-SY5Y cells were treated by inhibiting cell glucosylceramide synthase by supplementing the cell culture medium with 25μM D-threo-1-phenyl-2-decanoylamino-3-morpholino-1-propanol (PDMP; Matreya, LLC, Bellefonte, PA) for 48 hours at 37°C in complete medium (Tamboli *et al*. 2005). The pre-treatment was made for a MTT-Assay and Immunofluorescence.

Statistical Analysis. Statistical analysis of the data was performed by using T-student test to determine differences in cytotoxicity. For QDs: Comparisons between the different cumulative distributions were performed by Kolmogorov-Smirnov test. A p value < 0.05 was considered statistically significant. SPT data were collected from 10 cells from three independent experiments.

Results

1. Oleuropein Aglycone: a natural polyphenol which protects against the cytotoxicity associated with Transthyretin fibrillogenesis

Ole is cytoprotective against TTR toxicity. Ole exhibits a wide range of pharmacological properties. In the current study, we first investigated Ole for its protective effects against cytotoxicity on human HL-1 cells induced by wt-TTR and L55P-TTR amyloid aggregates. The wt-TTR and L55P-TTR were incubated with Ole in a 1:3 (TTR monomeric:Ole molar ratio) ratio for 30 min at 37 °C and then the pH was raised to 4.4 and 5.0, respectively, to start the aggregation process. At different times, aliquots of protein solutions were taken to test them on HL-1 cells by the MTT assay. The cells were treated with 20 μM protein solutions for 24 h (monomeric TTR concentration). No toxic effect of treatment with Ole alone was observed. As shown in Figure1, the wt-TTR and L55P-TTR, after 72 h (wt-TTR-*i*72h) or 96 h (L55P-TTR-*i*96h*)* of acid-treatment were cytotoxic and the exposed cells displayed about 35%±6,8 and 50%±3,32 toxicity, respectively, compared to vehicle-exposed cells. However, the aggregates of both proteins grown in the presence of Ole*A* (wt-TTR/Ole*A*-*i*72h and L55P-TTR/Ole*A*-*i*96h) were much less toxic, in fact, cell sufferance was abrogated completely for wt-TTR/Ole*A* (Fig.1A) and partially for L55P-TTR/Ole*A* (80%±8,5) (Fig.1B). We also checked whether the phenol could modify the toxicity of wt-TTR and L55P pre-formed fibrils. To this aim the preformed fibrils, corrisponding to wt-TTR/Ole*A*-*i*72h and L55P-TTR/Ole*A*-*i*96h, of either protein were incubated with Ole*A* 1:3 monomer TTR:Ole*A*, molar ratio for 10 min (wt-TTR/Ole*A*-*dis*10min and L55P-TTR/Ole*A*-*dis*10min, respectively) or 5 h (wt-TTR/Ole*A*-*dis*5h and L55P-TTR-Ole*A*-*dis*5h, respectively). The resulting MTT assay showed a decrease of toxicity to values of 85±8.5% for wt-TTR/Ole*A*-*dis*10min and 95±4.54% for wt-TTR/Ole*A*-*dis*5h (Fig.1A), while the cell viability values were about 80±5.6% for both L55P-TTR/Ole*A*-*dis*10min and L55P-TTR-Ole*A*-*dis*5h samples (Fig.1B). Finally, we determined whether Ole*A* inhibited the toxicity of TTR aggregates or increased cell resistance by exposing the cardiomyocytes to the phenol before the addition of TTR aggregates. The results of these experiments (data not shown) showed that cell pre-incubation with Ole*A* for 24 h did not enhance cell viability. These findings suggest that Ole*A* protection does not result from any stimulation of cell defences; rather it could arise from some interference with the protein aggregation process or with the association of TTR-toxic species with

the exposed cells. Therefore, we sought to characterize the effect of Ole*A* on the aggregation of either wt-TTR or the L55P mutant. These preliminary results could indicate that Ole could be an efficient compound for protection against cell death induced by TTR fibrils .

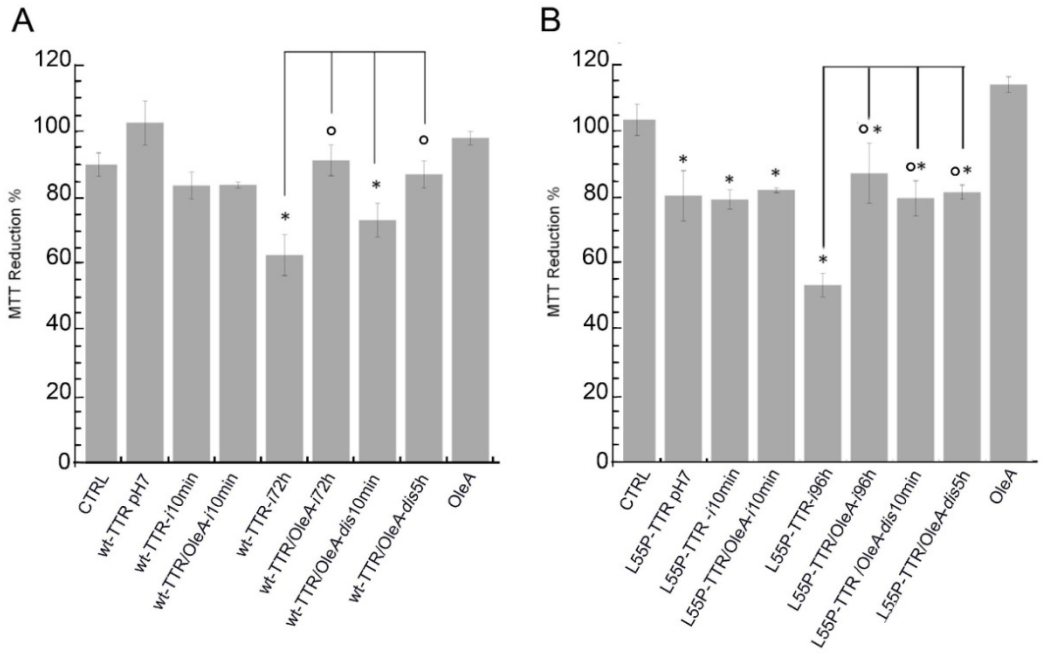

Figure 1. ***Effects of Ole on TTR induced cytotoxicity.*** Cells were treated with TTR (20μM) for 24h in the absence or presence of Ole (1:3 ratio). Cell viability was assessed by MTT reduction assay. Error bars indicate the standard deviation of triplicate independent experiments. A) $F_{8,36}$= 14.74; * p< 0.01 vs control ; ° p< 0.01 vs wt-TTR-*i*72h. B) $F_{8,36}$= 27.21; *p<0.01; ° p<0.01 vs L55P-TTR-*i*96h.

Confocal analysis. To determine whether aggregate toxicity was related to their ability to interact with the plasma membrane of HL-1 cells, we looked for the presence of the fibrillar aggregates on the cell surface. Confocal fluorescence microscopy experiments were performed using a polyclonal antibody raised against recombinant TTR. The cell membranes were counterstained with Alexa-488 conjugated CTX-B, a probe that specifically binds the monosialoganglioside GM1, a common lipid raft marker. Then wechecked whether the structural changes induced by Ole*A* in TTR fibrils might alter their interaction with elements of cell plasma membrane. Confocal images show evidence of wtTTR-*i*72h and L55P-TTR-*i*96h fibril clustering on HL-1 cell membrane (Fig.2A, E). The interaction with HL-1 plasma membrane of wt-TTR fibrils grown in the presence of Ole*A* (wt-TTR/Ole*A*-*i*72h) was suppressed (Fig.2B) whereas L55P-TTR fibrils grown in the presence of Ole*A* (L55P-TTR/Ole*A*-*i*96h) displayed only sporadic events of clusterization onto the surface of the exposed cells (Fig. 2F).

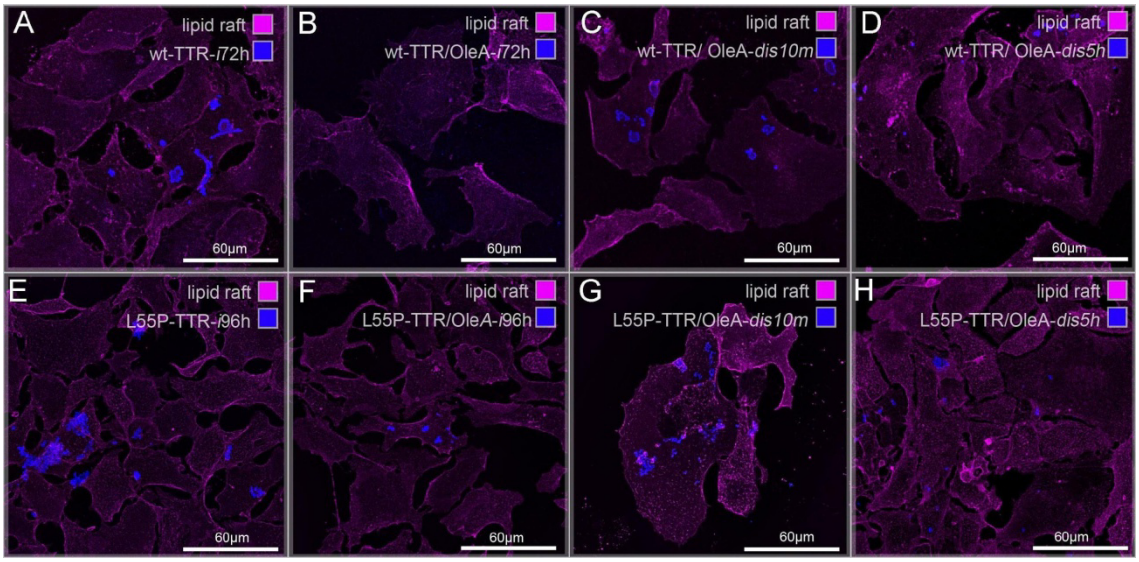

Figure 2. ***Ole effects on fibril clustering on HL-1 cells.*** Confocal Z-projections of HL-1 cells exposed to WT-TTR and L55P-TTR fibrils (blue) stained to reveal GM1 (magenta). (A) WT-TTR fibrils and (E) L55P-TTR fibrils grown in aggregation medium for 72 and 96 h, respectively; (B)wt-TTR/Ole-*i*fibrils and (F) L55P-TTR/Ole-*i* (3:1, Ole: monomer TTR).

Then, we performed a 3D analysis, to assess whether fibrils could affect membrane integrity, and sensitized FRET analysis, to monitor fibril interaction with GM1. Both wt- and L55P-TTR untreated fibrils interacted with the cell membrane (Figs. 3A, C and E, G). However, while the former were found only in surface depressions enclosed by intact plasma membrane (Fig.3A, inserts 1 and 1a), the latter were found also inside cell cytoplasm (Fig.3C, inserts 3 and 3a), suggesting that the two species interact differently with cell membrane components. These data were confirmed by the sensitized analysis of FRET between TTR immunofluorescence and stained GM1 fluorescence. In fact, FRET signal in L55P-TTR*i*96h appeared more defined and homogeneously distributed (Fig.3G), and its efficiency was higher when compared to wt-TTR (Fig.3E). Figure 3B shows a HL-1 cell treated with wt-TTR/Ole*A*-*i*72h fibrils: despite the absence of evident aggregates we found diffused dots of TTR immunofluorescence signal characterized by a low efficiency FRET with GM1 fluorescent staining. When present, clusters of L55P-TTR/Ole*A*-*i*96h on the plasma membrane were characterized by a higher FRET efficiency than wt-TTR/Ole*A*-*i*72h fibrils (Fig.3D, H). Of note, a diffused staining of fluorescence dots, with low FRET efficiency was evident also in this sample (Fig.3D, H and insert 4).

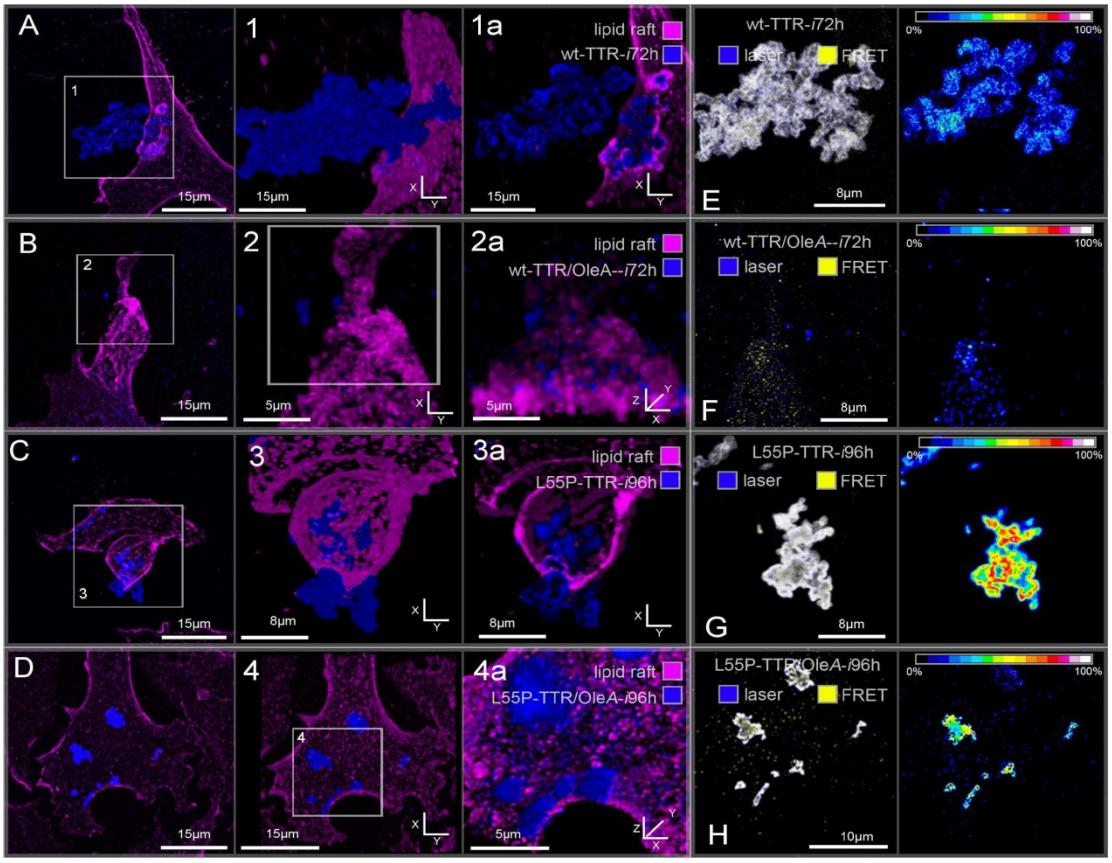

Figure 3. ***3D and FRET confocal analysis of fibrils interaction with HL-1 cell plasmamembrane***. (A) Z-projection of wt-TTR immunostaining (blue) and GM1 (magenta) on HL-1 cell plasmamembrane; (1 and 1a) 3D-volume renderings of regions selected in A show details of cell surface (1) and cytoplasmic area (1a) obtained by performing a volume crop on *z*-axis. (B and 2) Analysis of FRET between GM1 staining and fibril immunostaining; FRET (Yellow) and 543 nm laser (Blue) excited fibril immunofluorescence are shown in (B), FRET efficiency is shown in 2. (C) wt-TTR/Ole-*i*fibrils on HL-1 cells. (3 and 3a) 3D-volume renderings of the corresponding selected regions; TTR aggregates on cell surface are indicated by arrows in 3a. (D) FRET analysis between GM1 staining and wt-TTR/Ole-*i*fibrils immunostaining; FRET efficiency is shown in 4. (E) L55P-TTRfibrilson HL-1cells. (5 and 5a) 3D-volume renderings of regions selected in E show details of cell surface (5) and cytoplasmic area (5a). (F) FRET analysis between GM1 staining and L55P-TTRfibrils immunostaining; FRET efficiency is shown in 6. (G) L55P-TTR/Ole-*i*fibrilson HL-1cells. (7 and 7a) 3D-volume renderings of the corresponding selected regions; TTR aggregates on cell surface are indicated by arrows in 7a. (H) FRET analysis between GM1 staining and L55P-TTR/Ole-*i*fibrils immunostaining.

Finally, we analyzed the effect of Ole*A* on the interaction of preformed fibrils with the cell membrane. wt-TTR/ and L55P/OleA-dis10m immunofluorescent fibrils were seen as aggregates with a low FRET emission localized principally in their internal portions and as immunofluorescent diffused dots with low FRET signal (Figs.4A, C and E, G). Interestingly, dots of fluorescent wt- and mutant-TTR increased with the time of fibril treatment with Ole*A* (Figs.4B, D and F, H). Overall, all these data, along with those on aggregate cytotoxicity and TEM analyses reported in Figures 2 and 8, suggest that Ole*A* may remodel fibrils to less-toxic, smaller aggregates that interact with the cell membrane without affecting its integrity.

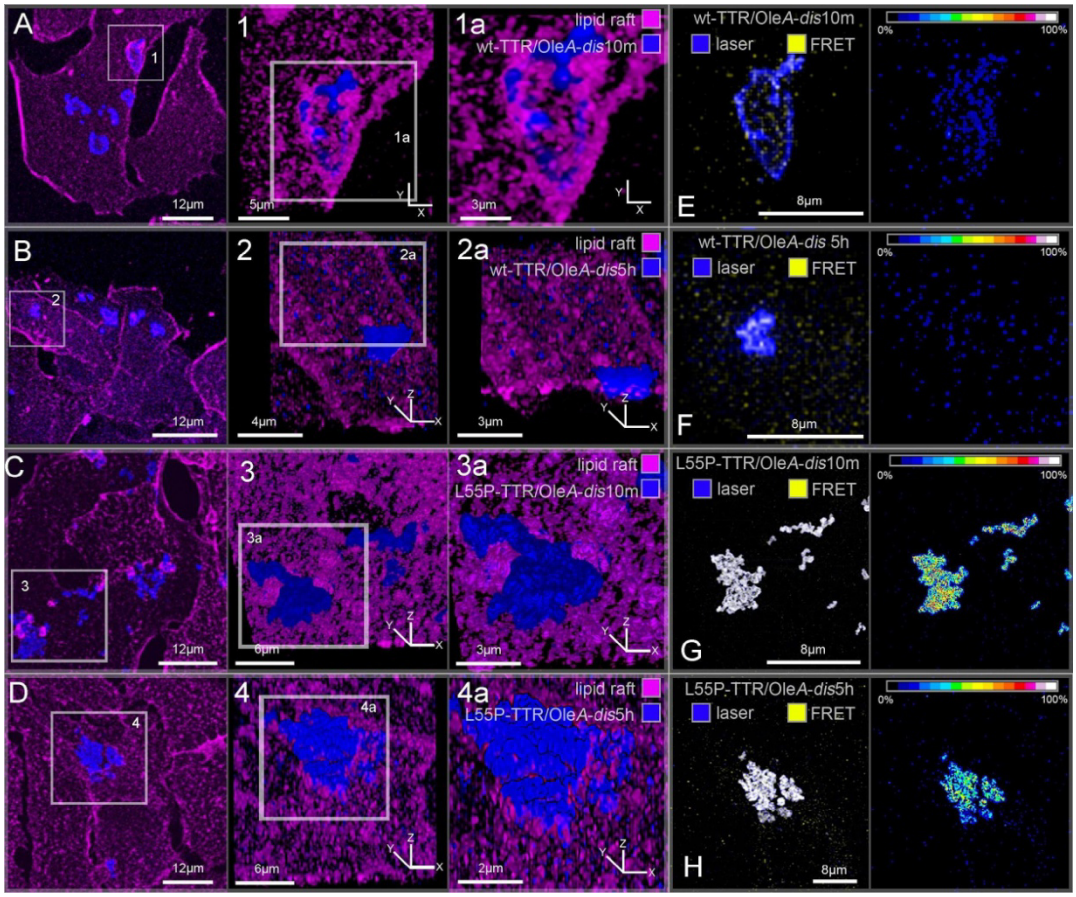

Figure 4. OleA effect on fibrils and following changes of fibril/membrane interaction. (A) Z-projection of wt-TTR/Ole*A*-*dis*10m fibril immunostaining (blue) and GM1 (magenta) on HL-1 cell plasmamembrane; (inserts 1 and 1a) 3D-volume renderings of corresponding selected regions show increasing magnifications of amyloid TTR aggregate interacting with GM1 on cell surface. (B and insert 2) Analysis of FRET between GM1 staining and fibril immunostaining; FRET (Yellow) and 543 nm laser (Blue) excited fibril immunofluorescence are shown in (B), FRET efficiency is shown in insert 2. (C) wt-TTR/Ole*A*-*dis*5h fibrils on HL-1 cells. (inserts 3 and 3a) 3D-volume renderings of regions selected in C showing amyloid aggregates interacting with GM1 on cell surface (3); dots TTR aggregates on cell surface are indicated by arrows in 3a. (D) FRET analysis between GM1 staining and wt-TTR/Ole*A*-*dis*5hfibrils immunostaining; FRET efficiency is shown in insert 4. (E and inserts 5 and 5a) L55P-TTR/Ole*A*-*dis*10mfibrilson HL-1cells. (5 and 5a) 3D-volume renderings of the selected regions showing details of cell surface; arrows indicate diffused TTR aggregates on cell surface. (F) FRET analysis between GM1 staining and L55P-TTR/Ole*A*-*dis*10mfibrils immunostaining; FRET efficiency is shown in 6. (G) L55P-TTR/Ole*A*-*dis*5hfibrilson HL-1cells; (7 and 7a) 3D-volume renderings of selected regions showing details of cell surface; arrows indicate diffused TTR aggregates on cell surface. (H) FRET analysis between GM1 staining and L55P-TTR/Ole*A*-*dis*5hfibrils immunostaining; FRET efficiency is shown in 8.

Congo Red Assay and DLS analysis. Considering the cytoprotective effects of Ole*A* we decided to investigate *in vitro* these effects on TTR aggregation by spectroscopic and fluorimetric techniques. To disclose the structural bases of Ole*A* cytoprotection we first assessed whether it inhibited protein aggregation. To explore the effects of Ole*A* on TTR fibrillogenesis, we compared the Congo Red (CR) absorption spectra of TTR samples in the presence or in the absence of Ole*A*. At pH 7.0 both wt-TTR and L55P-

TTR were not stained with CR, as shown in Fig 4A and B. The absorption maximum at 490 nm of non-bound CR displayed a red-shifted to a higher wavelength (550 nm) when it bound amyloid material present in the samples of wt-TTR and L55P-TTR at acidic pH. At these conditions, the presence of Ole*A* reduced significantly CR optical absorbance and its red-shift, indicating a decrease in the formation of amyloid fibrillar species associated with increased cross β-pleated sheet.

In parallel, the same samples were analysed by dynamic light scattering (DLS) for additional characterization of the protein species in the sample. At pH 7 the TTR sample contained particles of about 7 nm apparent hydrodynamic diameter (D_H), which is consistent with previous reports relative to soluble TTR molecules (Fig.5C) (Pires *et al.* 2012). After 72 h in aggregation medium, the D_H increased to about 1700 nm. The wt-TTR/Ole*A*-*i*72h sample was a homogenous population with D_H around 400 nm, corresponding to TTR smaller aggregates (Fig.5C). L55P-TTR after 30 min of incubation at pH 7.0 in aggregating buffer contained a particle population corresponding to a soluble protein also in the presence of the phenol (Fig. 5D). The presence of Ole*A* did not prevent fibril formation after 96 h of aggregation, even though particle size was lower than that found in phenol-untreated samples (Fig.5D).

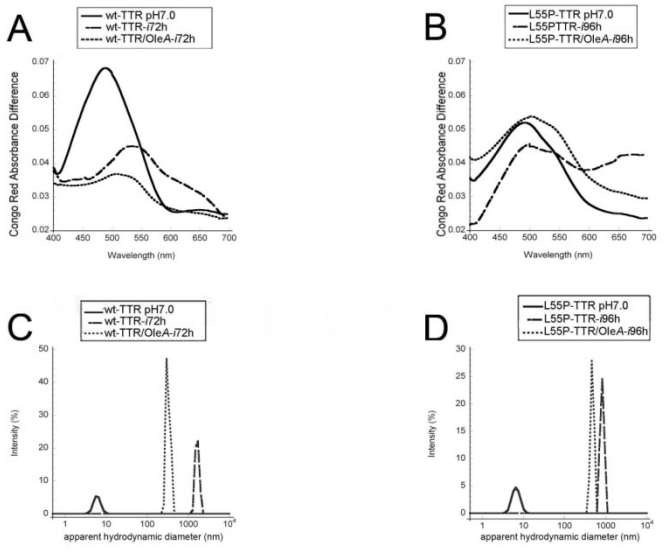

	Hydrodynamic diameter (nm)
Sample	72h aggregation
wt-TTR pH7.0	6.879±0.21
wt-TTR-*i*72h	1181.7
wt-TTR/Ole*A*-*i*72h	327.8

	Hydrodynamic diameter (nm)
Sample	96 h aggregation
L55P-TTR pH7.0	6.597±0.27
L55P-TTR-*i*96h	1295.5
L55P-TTR/Ole*A*-*i*96h	511.9

Figure 5. ***Congo red and DLS analysis*** **.** Absorption spectra of CR and wt-TTR (A) and L55P-TTR (B) in native or amyloidogenic conditions in presence or absence of Ole*A*. DLS spectra of wt-TTR (C) and L55P-TTR (D) in native or amyloidogenic conditions in presence or absence of Ole*A*.

FTIR-analysis. To investigate more in depth the interference of Ole*A* with TTR aggregation, the protein secondary structure and thermal stability was analyzed by FTIR spectroscopy in collaboration with the Department of Physics "Giuseppe Occhialini at the University of Milan, . The FTIR spectra are highly descriptive of the intra- and intermolecular modifications in a peptide/protein sample undergoing aggregation, in particular by showing the occurrence of intra- or intermolecular beta-sheets. Fig. 6A and Fig. 7A show the FTIR spectra of wt-TTR and L55P-TTR at pH 7.0, collected at different times during sample incubation at 37 °C for 72 h; the spectra were recorded in the Amide I region, where absorption results from C=O stretching vibration of the peptide bonds. The spectra are dominated by a component at 1628 cm^{-1} that can be assigned to the β-sheet structure of the native protein, in agreement with previous FTIR studies (Cordeiro *et al.* 2006; Zandomeneghi *et al.* 2004). The second derivative of the absorption spectra disclosed a second β sheet component around 1689 cm^{-1} togheter with additional components assigned to protein secondary structures, as indicated in Fig. 6B and Fig. 7B (Cordeiro *et al.* 2006; Zandomeneghi *et al.* 2004). Only minor structural changes of wt-TTR were revealed by FTIR analysis during 72 h of incubation (Fig. 6C); these were mainly due to the hydrogen/deuterium exchange of the native protein (Natalello *et al.* 2012), whereas a partial unfolding of the L55P mutant was indicated by a decrease of the 1628 cm^{-1} component (Fig. 7C). After the incubation, the same solutions were heated up to 100 °C at a rate of 0.2 °C/min, and transmission spectra were collected at 1.7 °C steps (Fig. 6C and Fig. 7C). At these conditions, wt-TTR but not L55P-TTR displayed a very high thermal stability, in agreement with previously reported findings (Cordeiro *et al.* 2006; Ami *et al.* 2012). Indeed, in the wt-TTR second derivative spectrum the 1628 cm^{-1} peak of native β-sheet retained about 50% of its initial intensity, whereas in L55P-TTR this component was lost. Furthermore, a peak around 1615 cm^{-1}, typical of amyloid aggregates (Cordeiro *et al.* 2006; Natalello *et al.* 2012), appeared and steadily increased in the wt-TTR and L55P-TTR second derivative spectra. This peak, was present also after sample cooling from 100 °C to 37 °C (Fig. 6C and 7C), indicating that unfolding and aggregation are irreversible processes. The same study was also carried out in acidic conditions in the absence or in the presence of Ole*A* (Fig. 6D-I and Fig.7D-I). The FTIR absorption spectra collected at different times of acid incubation and their second derivatives showed several spectral features (Fig. 6E, D and 7E, D) indicating loss of native

secondary structure and consequent amyloid aggregation of both wt- and mutant proteins independently of Ole*A* presence or absence in the aggregation medium. In particular, the native β-sheet components decreased in intensity and two amyloid-related peaks around 1615 cm^{-1} and 1682 cm^{-1}appeared in the spectra (Fig. 6E, H and 7E, H). Heating of protein solution resulted in the complete disappearance of the native spectral components with further aggregation of both proteins (Fig. 6F, I and 7F, I), indicating that Ole*A* was not able to inhibit their heath-induced misfolding.

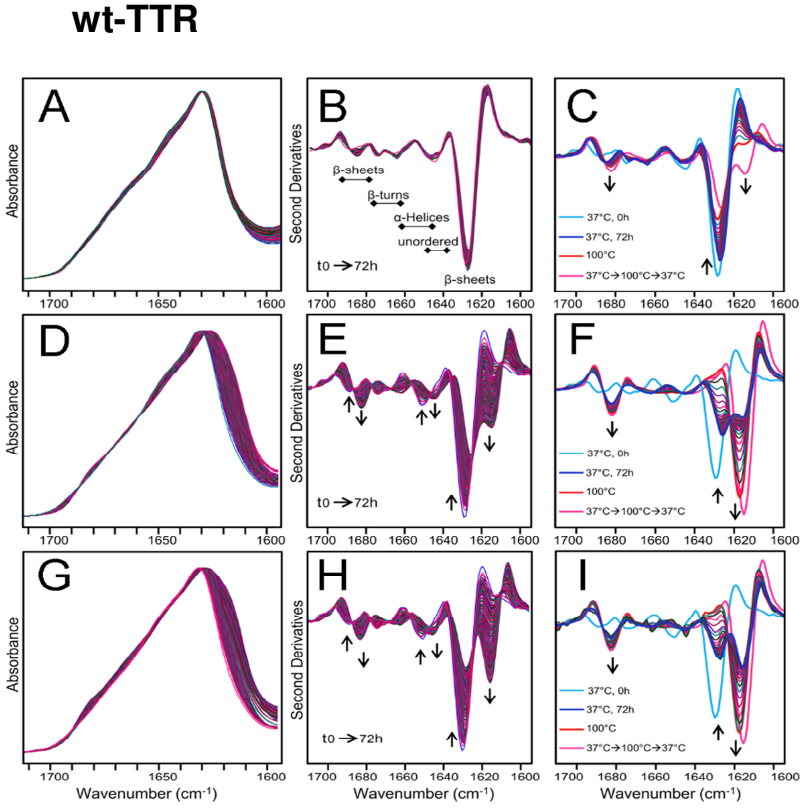

Figure 6. ***FTIR characterization of WT TTR.*** (A) FTIR absorption spectra of wt-TTR at pH 7.5 collected at different times of incubation up to 72 hours at 37 °C. (B) Second derivatives of the absorption spectra reported in (A). Band assignments to protein secondary structures are indicated. (C) Second derivatives of the absorption spectra of WT TTR at pD7.5 collected during heating from 37°C to 100°C and after sample cooling to 37°C. (D) FTIR absorption spectra of wt-TTR at pD3.5 collected at different incubation times up to 72 hours at 37°C. (E) Second derivatives of the absorption spectra reported in (D). (F) Second derivatives of the absorption spectra of wt-TTR at pD3.5 collected during heating from 37°C to 100°C, and after sample cooling to 37°C. G-H) Absorption (G) and second derivative spectra (H) of wt-TTR at pD3.5 in the presence of Ole*A*. Spectra were collected at different incubation times up to 72 hours at 37°C.I) Second derivatives of the absorption spectra of WT TTR at pD3.5 in the presence of Ole*A* collected during the thermal treatment from 37°C to 100°C,and after cooling the sample to 37°C.The arrows point to the spectral changes occurring at increasing incubation times (E, H) or temperature (C, F, I).

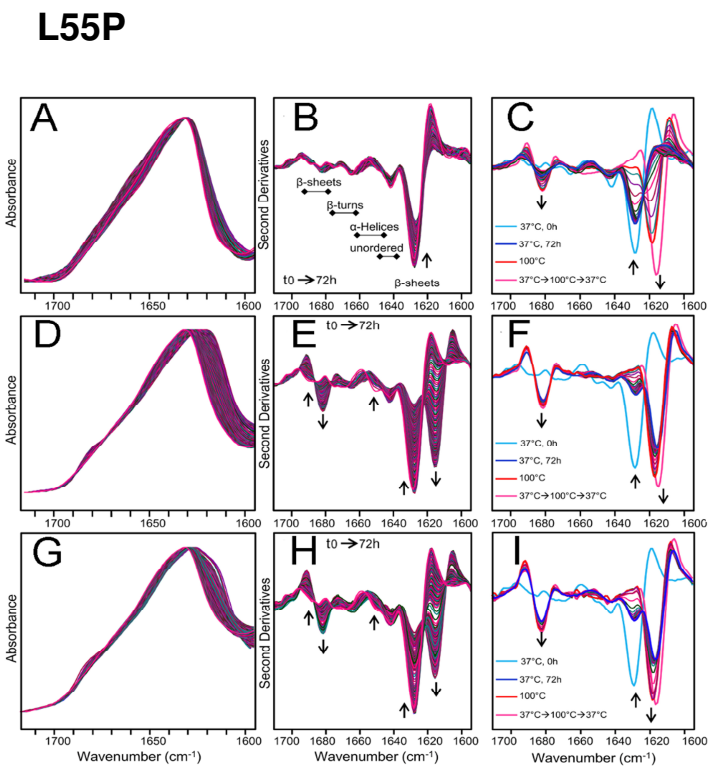

Figure 7. FTIR characterization of the L55P mutant. (A) FTIR absorption spectra of L55P mutant at pH 7.5 collected at different times of incubation at 37°C up to 72 hours. (B) Second derivatives of the absorption spectra reported in (A). The band assignments to the protein secondary structures are indicated. (C) Second derivatives of the absorption spectra of L55P at pD7.5 collected during heating form 37°C to 100°C, and after sample cooling to 37°C. (D) FTIR absorption spectra of L55P at pD 5.0 collected at different incubation times up to 72 hours at 37°C. (E) Second derivatives of the absorption spectra reported in (D). (F) Second derivatives of the absorption spectra of L55P at pD5 collected during the heating form 37°C to 100°C, and after sample cooling to 37°C. G-H) Absorption (G) and second derivative spectra (H) of L55P at pD5 in the presence of Ole*A*. Spectra were collected at different incubation times up to 72 hours at 37°C. (I) Second derivatives of the absorption spectra of L55P at pD5 in the presence of Ole*A* collected during heating from 37°C to 100°C, and after sample cooling to 37°C. The arrows point to the spectral changes occurring at increasing incubation times (E, H) or temperature (C, F, I).

Intrinsic autofluorescence. The aggregation of TTR in the presence or in the absence of Ole*A* was investigated by monitoring the fluorescence emission maximum of its intrinsic autofluorescence. Fig 5B shows that incubation of TTR at pH 4.4 induced a red shift of the emission maximum, suggesting that autofluorescence elements moved to a relatively more polar environment in the ongoing aggregation process. A red shift was also seen in Ole*A*-treated samples (Fig.8B). To enhance the resolution of tryptophan (Trp) emission spectrum during wt-TTR aggregation in the presence or in the absence of Ole*A*, we performed spectrum derivatization against wavelength. In the second derivative plots three main peaks at 320, 340 and 350 nm were observed, corresponding

to increasing polarity of the Trp environment. The 320 nm peak was evident after 10 min of aggregation and gradually decreased at later times reaching its minimum in 72 h-old fibrils (Fig.8). Accordingly, the 350 nm peak corresponding to the highest polarized environment started to rise with aggregation and was particularly evident after 48 h. Moreover, at this time a further 335 nm peak appeared. After 72 h of incubation in aggregation medium the 350 nm component decreased while the 335 nm peak was more evident. These data connect the highest value of 72 h-old amyloid TTR toxicity to a higher exposure to the solvent of aromatic residues. The addition of Ole*A* in the aggregation medium inhibited such a transition since the 320 nm peak retained almost completely its initial values in all samples and the 335 nm peak was inhibited (Fig.8B).
Interestingly, the L55P-TTR emission spectra showed a blue-shift during the aggregation time (Fig.8C). These data indicate that the substitution consistently alters the conformation of amyloid TTR aggregates, as previously reported (Keetch *et al.* 2005).. However, the blue-shift was inhibited by Ole*A* addition to the aggregating medium. The analysis of the second derivative plots of the untreated mutant revealed a shift of the 350 nm peak, evident after 10 min of aggregation, to 335 nm in the cytotoxic 96 h-old sample. These data associate the onset of cytotoxicity of both wt- and L55P-TTR to the appearance of this autofluorescent component. Of note, these alterations were not observed in phenol-treated samples (Fig.8D). The effects of Ole*A* on the emission spectra of wt-TTR and L55P fibrils are shown in Fig.7. We found that Ole*A* treatment rapidly affected fibrils autofluorescence, and after 10 min fibril emission spectra appeared superimposed to those obtained from fibrils grown in the presence of Ole*A*. Accordingly, the second derivative plots showed a recover of the 320 nm peak together with the decline of the 335 nm component (Fig.8). These data suggest that similar binding sites on both oligomeric and fibrillar conformation are involved in the interaction between the phenol and wt- or L55P-TTR.

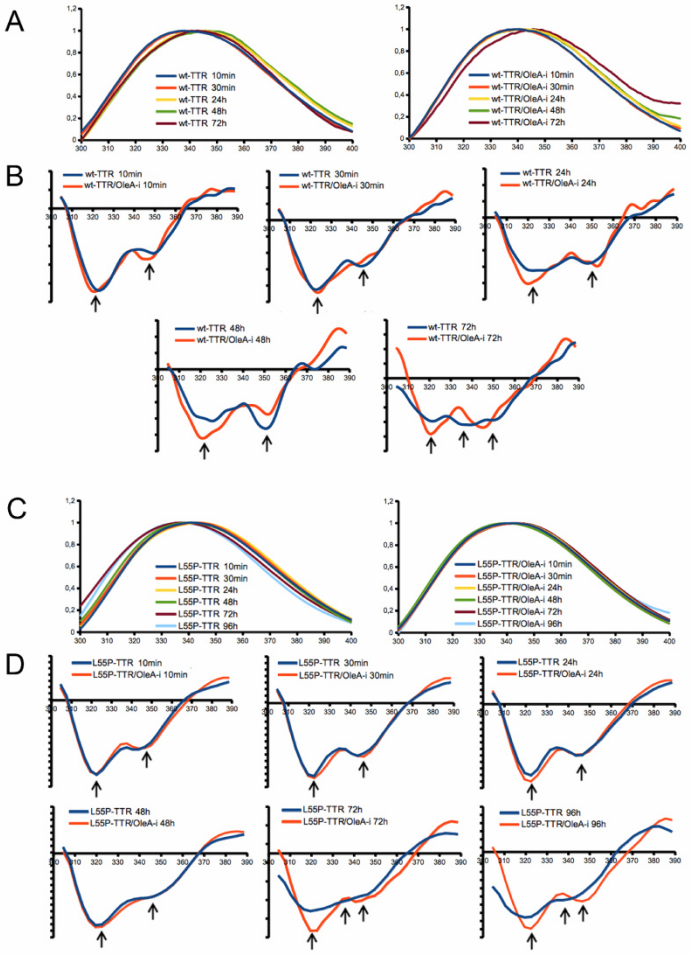

Figure 8. ***Effect of OleA on fluorescence emission of TTR***. (A, C) Intrinsic fluorescence emission spectra of wt-TTR (A) and L55P-TTR (C), alone (left) and Ole*A* treated (right) at different times of acid aggregation. The spectra were normalized to fluorescence intensity of 1.0 at λmax, λexc = 280 nm. (B, D) Time point comparison of second derivatives obtained from emission spectra reported in A and C. The arrows point to the spectral changes occurring at increasing incubation times.

Fluorescence quenching measurements and Proteinase-K digestion. Acrylamide quenching has been used to provide insights into conformational changes of proteins by probing solvent accessibility of fluorescence moieties (Tallmadge *et al.* 1989). To perform these experiments, aliquots of the wt- or L55P-TTR samples were withdrawn from the aggregation solution at various aggregation times and mixed with acrylamide to measure solvent exposure of aromatic residues. Time-dependent changes of intrinsic fluorescence quenching were observed (Fig.8A and 8B). In detail, we found a significant increase of acrylamide quenching that reached its highest values after 48 h and 48/72 h of aggregation for wt- and L55P-TTR, respectively. A similar behaviour was observed for the native structure, confirming the presence of eight solvent -exposed Trp residues in the tetrameric structure. L55P-TTR showed a highest quenching effect

due to structural destabilization induced by the mutation. These changes possibly correspond to some increased availability to the quencher of the aromatic residues in meta-stable intermediate states of the aggregation process. Addition of Ole*A* to the aggregation medium reduced the increase of acrylamide quenching, especially at the aggregation times corresponding to the highest quenching values of untreated fibrils (Fig. 9A and 9B). These data suggest that Ole*A* may reduce the exposure of aromatic residues to the solvent.

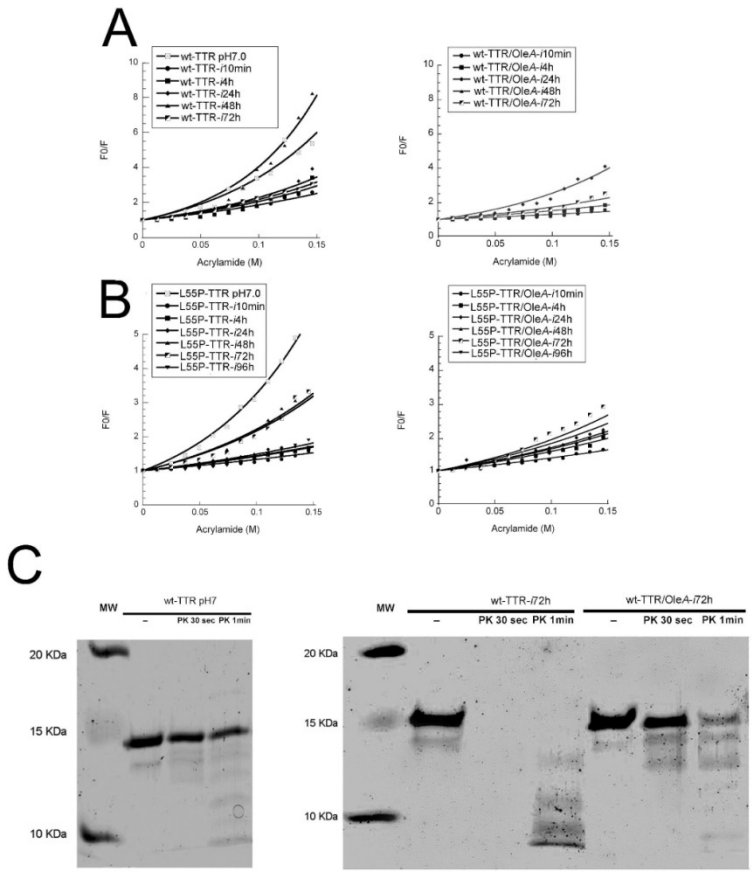

Figure 9. ***OleA affects surface contacts of TTR amyloid assemblies.*** Acrylamide quenching of intrinsic fluorescence of wt-TTR (A) and L55P (B) at increasing times of aggregation. Proteins were incubated in the aggregation medium in the absence (left) or in the presence of Ole*A* (right). PK digestion of native TTR (left). Amyloid fibrils (right) obtained upon incubation of wt-TTR at pH 4.0 for 72h in the absence (columns 2-4) or in the presence of Ole*A* (columns 5-7) were treated with Proteinase-k at 37 °C for 30 sec (columns 3 and 6) and 1 min (columns 4 and 7). Samples were analyzed by SDS-PAGE;*MW,* molecular mass.

Given that hydrophobic interactions are known to be relevant factors in protein aggregation, we checked whether Ole*A* interaction with exposed hydrophobic sites of wt- and L55P-TTR altered their interaction with Proteinase-K (PK), an endoprotease known to cleave peptides preferentially after hydrophobic residues. Resistance of TTR

fibrils to Proteinase-K digestion has been previously analyzed by Betaman and colleagues (Bateman *et al.* 2011). In particular they noticed that TTR amyloid deposits are more sensitive to PK catalysis than native TTR. At our experimental conditions, treatment with PK for 30 s and 1 min resulted in a complete degradation of amyloid aggregates of both wt-TTR and L55P-TTR (Fig.9). By contrast, wt-TTR/Ole*A-i72h* and L55P*/OleA-i96h* showed high resistance to PK digestion (Fig.9), similarly to the natively folded protein. These data suggest that Ole*A*protects TTR aggregates from Proteinase K cleavage by binding to hydrophobic sites of both wt- and L55P- TTR peptides.

EM Analysis of Inhibition of Fibril Formation. EM was used to examine samples of TTR incubated with and without Ole*A,* as described under "Material and Methods." wt-TTR (0.28 mg/ml) incubated for 24 h at 37 °C were predominantly composed of typical fibrils with branchings and bumps (Fig.10A). Moreover, annular units with a diameter compatible with TTR oligomers (about 30-50 nm) were recognizable as components of the fibrillar structure (Fig.10A and inserts 1,2). After 72 h of incubation, wt-TTR appeared more bundled and oligomer-like subunits were crowded and tightly packed (Fig.10B and insert 3). Uniform fibrillar structures were not seen in the L55P-TTR (0.28mg/ml) incubated for 96h at pH 5.5; rather, oligomer-like components similar to those found in the wt-TTR sample were present at these conditions. In the presence of Ole*A*, the fibrillar structures were absent and only unstructured aggregates were detectable for all TTR species (Fig.10D-F). Moreover, a thin layer of non-aggregated oligomer-like subunits was detectable in all samples (Fig.10E-F and inserts 5-7).

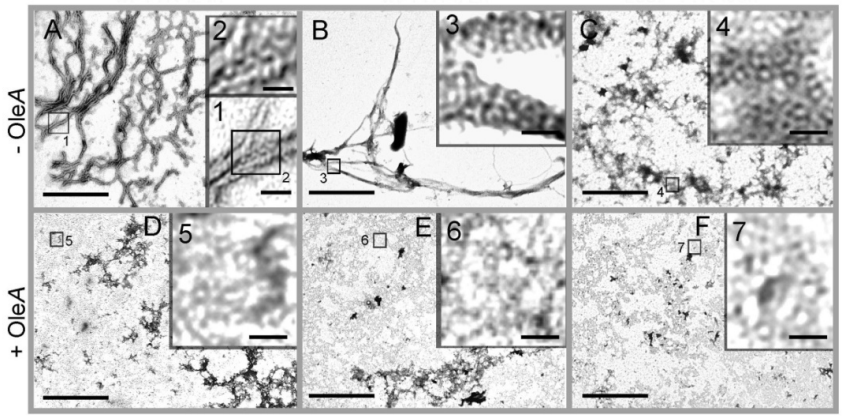

Figure 10. ***Ultrastructural analysis of TTR amyloid assemblies***. TEM micrographs of wt-TTR and L55P-TTR, alone (A-C) and Ole*A* treated (D-F) at different times of acid aggregation. (Inserts 1-7) Details of the corresponding selected ROIs showing oligomers-like structures polimerized inside aggregates (Inserts 1-4) or dispersed on the formvar surface (Inserts 5-7).

2. Homocysteynilation of Wild-type and Leu55Pro TTR, worsens the onset of cardiomiopathy

wt-TTR Homocysteinylation TTR undergoes homocysteinylation at its single cysteine residue (Cys10) both *in vitro* and *in vivo*. The effect of homocysteinylation on the wt-TTR tetramer (1:2; tetramericTTR:Hcy ratio), was analysed by native- and SDS-PAGE, Resveratrol binding and DLS.

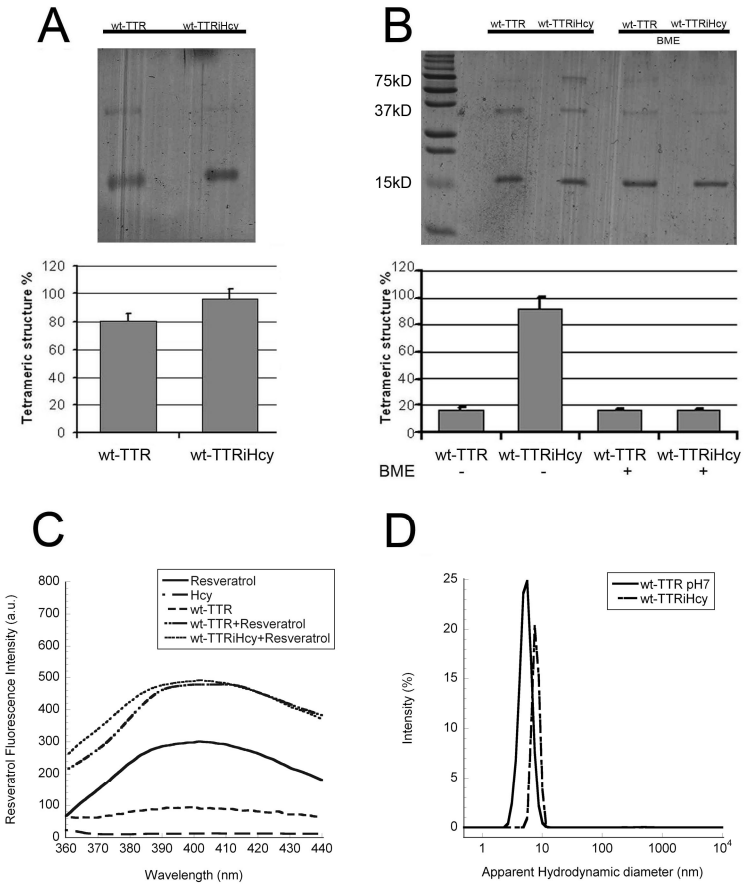

Figure 1. Effects of Hcy on wt-TTR. A) Native and (B) SDS-PAGE gel of wt-TTR in presence and absence of Hcy;(bottom) quantification of the tetramer band with respect to the total bands in the gels. C) Spectra of Resveratrol binding assay after 24h of incubation of TTR with Hcy and addition of Resveratrol for 10min before the lecture. D) Dinamic Light Scattering of wt-TTR in presence and absence of Hcy.

When analyzed in native conditions, the wt-TTR samples incubated with Hcy displayed a 20% increase of the tetramer/total TTR ratio with respect to untreated TTR (Fig.1A). In SDS-PAGE the wt-TTR sample displayed two bands corresponding to the monomer and the dimer. Incubation of wt-TTR with Hcy decreased the level of the monomer and the dimer band and resulted in the appearance of a new band approximately at 75 kDa corresponding to the size of tetrameric TTR. This band was not observed in the

presence of the reducing agent 0.1% 2-β-mercaptoethanol (BME) (Fig.1B). Resveratrol is a polyphenol known to bind and to stabilize the TTR tetramer. trans-resveratrol displays a specific emission spectrum with a maximum fluorescence peak about 390 nm when it is excited at 320 nm (Figueiras *et al*. 2011); moreover, it displays an increase in its fluorescence quantum yield upon binding the TTR tetramer. Using this binding assay we observed that the TTR-Hcy complex maintains the same ability to bind this polyphenol as well as the wt-TTR (Fig.1C).The DLS analysis revealed that upon incubation up to 24 h at pH 7.0, both wt-TTR and wt-TTR-Hcy were present in the sample as particles with an apparent hydrodynamic diameter (D_H) about 7 nm consistent with a native tetrameric fold (Fig.1D). From these data we hypothesize that wt-TTR homocysteinylation produced a stabilization of the TTR tetrameric fold and wondered whether this covalent modification could produce the same effects on the highly amyloidogenic variant L55P-TTR.

L55P-TTR Homocysteynilation. To gain insight into the structural alterations induced by Hcy binding to L55P-TTR, we performed a far-UV CD spectroscopic study. The CD spectra, recorded at 25 °C were obtained at different times of aggregation of L55P incubated at pH 7.0 for 10 days in the absence or in the presence of Hcy (tetrameric L55P-TTR:Hcy; 1:2 ratio) as described in Materials and Methods (Fig.2B). After 30 min of incubation with Hcy, the CD analysis showed some structural changes of the tetrameric fold attributable to Hcy binding to the Cys10 of L55P-TTR. Nevertheless, a highest β-sheet content was observed in all samples of L55P-TTR incubated with Hcy, as suggested by the signal at 216 nm, (in particular after 96h of incubation (Fig.3B) and it was maintained in the subsequent incubation times. These effects are not present on the spectra of wt-TTR treated with Hcy (Fig.2A), confirming a stabilization by Hcy of the tetrameric form of wt-TTR. Figure 3C shows time-dependent turbidity and the absorbance at 400 nm recorded at different times of treatment of L55P-TTR with Hcy. At each incubation time, the L55P-TTR/Hcy complex showed a higher turbidity value suggesting that Hcy favoured aggregation of L55P-TTR but not of wt-TTR. DLS analysis of L55-TTR at pH 7 showed the presence of particles with an D_H at 7.987 nm (Fig.3D). In the first hour of protein incubation with homocysteine the sample was nearly homogenously populated by particles with a D_H value corresponding to that of the natively folded protein (Fig.2E). After 96 h of L55P-TTR incubation at pH 7.0 the

homocysteynilated sample resulted mainly populated of particles with D_H about 4.7 nm (Fig. 3D,E) with respect to the sample without Hcy. It is known that the aggregation process requires disassembly of tetrameric TTR into monomers, in particular the variant L55P requires subtle conformational changes within the monomeric subunit to undergo self-assembly. After 96 h of incubation with Hcy, the average particle size was reduced to 4.7 nm indicating disassembly of the quaternary structure of the protein; in fact this value is compatible, within the experimental error, with previously reported values by Pires and co-workers of R_H 1.9nm (Pires *et al*. 2012). From these data we can hypothesise that L55P-TTR homocysteinylation could result in some increase of the number of monomeric species prone to aggregate.

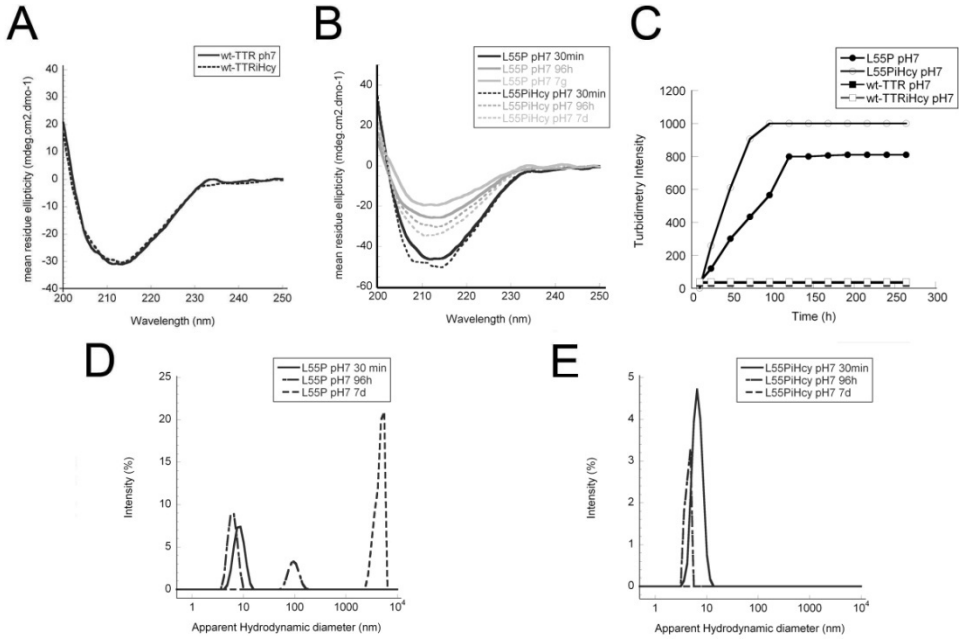

	Hydrodynamic diameter (nm)		
Sample	**30min**	**96h**	**7 days**
L55P pH7	**6.595±0.21(Area100%)**	**4.516±0.23(Area10.9%) 136 (Area89.1%)**	**5443(Area100%)**
L55PiHcy pH7	**6.879±0.3(Area100%)**	**4.615±0.27 (Area100%)**	**2.59^{e+04}(Area100%)**

Figure 2. Secondary structure Analysis. CD spectra of wt- and L55P-TTR recorded in presence and absence of Hcy. A) Spectra are shown for the protein at 37°C in the absence (solid black line) and in the presence (dashed black line) of Hcy. Buffer spectra was subtracted from TTR alone, while CD spectra of Hcy in buffer were subtracted from TTR with Hcy. B) CD spectra of L55P and L55PiHcy at different time of aggregation. C) Turbidimetryc Plot of L55P-TTR in presence of Hcy (packed diamond line) and in absence (packed circles line), and wt-TTR in absence (empty circles line), and in presence of Hcy (empty diamond line). D,E) Hydrodynamic diameter of L55P (D) at different time of incubation with Hcy (E).

The morphology of L55P-TTR aggregates in the absence or in the presence of Hcy was observed by transmission electron microscopy (TEM). When L55P-TTR was incubated

with Hcy (Fig.3B) a larger number of small oligomers and monomeric structures were present on the formvar dish whereas in the absence of Hcy the sample was composed by unstructured aggregates and the monomeric species was not detectable (Fig.3A). After 7 days of aggregation, the TEM images of L55P-TTR*i*Hcy showed the presence of fibrils (Fig.3D), as confirmed by DLS analysis, which revealed a D_H around 2,59e+04.

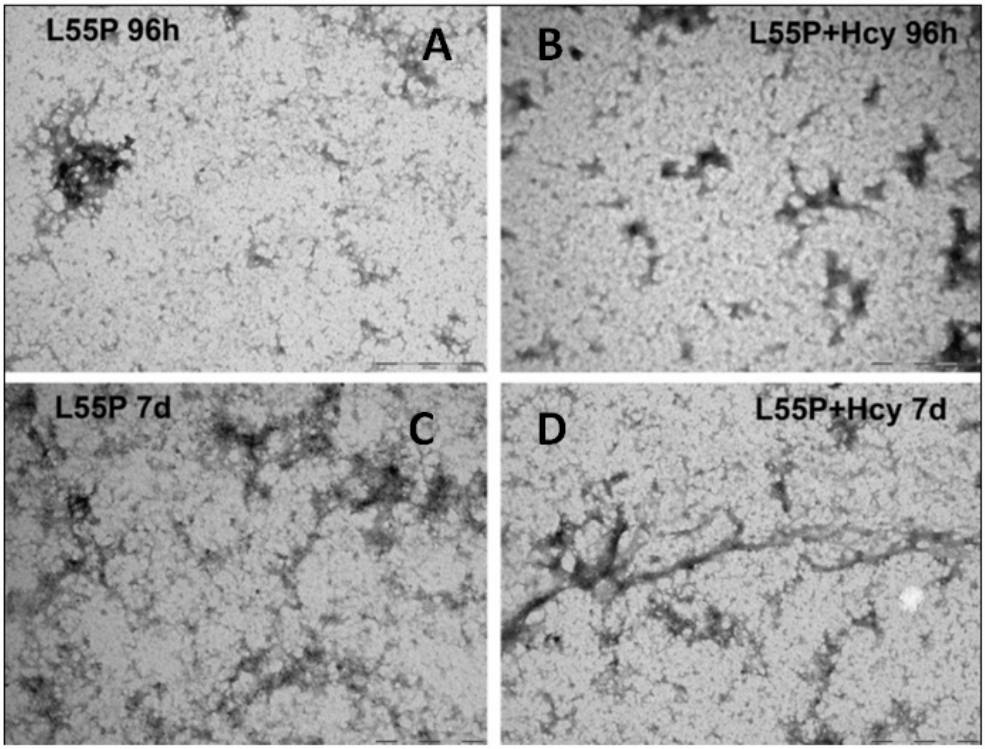

Figure 3. EM images. TEM micrographs of L55P-TTR, alone (A-C) and Hcy treated (D-F) at different times of incubation.

The L55P-TTR samples obtained at different incubation times at pH 7.0 with or without Hcy were analyzed by a conformational antibody (A11) specific for amyloid oligomeric structure; in particular A11 recognizes generic epitopes that do not depend on a particular amino acid sequence but on the presence of the amyloid signature (Kayed *et al*. 2007). Figure 4A showed that the sample incubated in the presence of Hcy was recognized by A11 antibodies with higher affinity with respect to untreated L55P-TTR, suggesting that the presence of Hcy resulted in a higher amount of amyloid species . In addition, the resveratrol binding assay confirmed a L55P-TTR destabilization induced by Hcy (Fig.4B). In fact, incubation with Hcy during mutant aggregation resulted in a reduced ability to bind resveratrol, thus confirming protein destabilization.

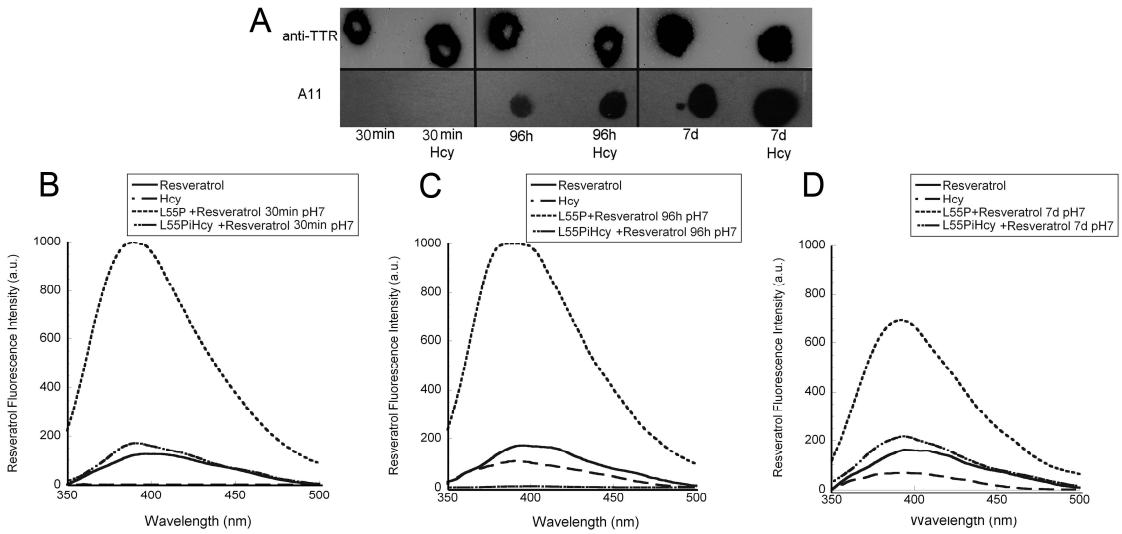

Figure 4. DOT-BLOT and Resveratrol Binding Assay. A) L55P in presence and absence of Hcy labeled by anti-TTR and anti-conformational antibodies, A11. B,C and D) Resveratrol binding assay of L55P treated with Hcy at different times.

Cytotoxicity. All the structures formed in the presence or in the absence of Hcy were screened for cytotoxicity by the MTT Assay. It is known that L55P-TTR amyloid aggregates are cytotoxic to human HL-1 cells; therefore, aliquots of proteins solutions were withdrawn at different times to test their cytotoxicity to HL-1 cells. The cells were treated for 24h with 5μM L55P-TTR incubated at different times in the presence or in the absence of Hcy under physiological pH. After 96h of incubation with Hcy, the L55P-TTR showed a significant toxicity and it induced a 35% of cell sufferance (Fig.5A), whereas the same L55P-TTR species grown in the absence of Hcy were much less toxic, in fact the cell sufferance was completely abrogated. After 7d of aggregation, cell sufferance was the same upon cell treatment with both protein samples confirming the toxicity induced by L55P-TTR and L55P-TTRiHcy fibrils; interestingly, the latter were less toxic than the pre-fibrillar forms, probably the covalent modification led to a transient stabilization and enrichment of the monomeric form which proceeds in any case towards the formation of less toxic fibrils. These data confirm that Hcy destabilized the L55P-TTR, which assembled into more toxic species, with enrichment of monomeric forms.

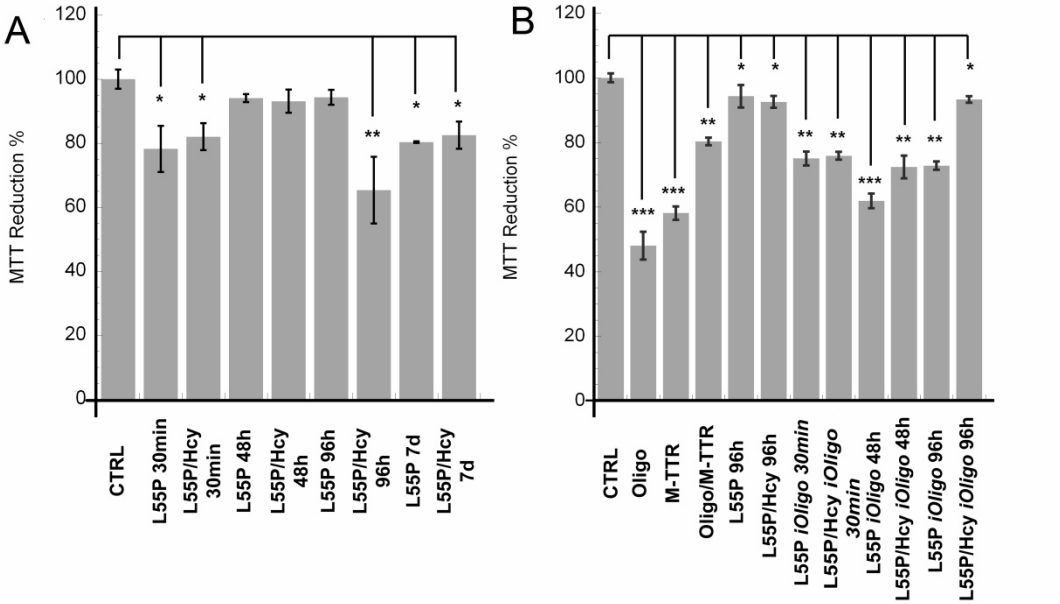

Figure 5. MTT Assay. A) MTT at different time of incubation of L55P with Hcy. B) MTT of L55P/iHcy in presence and absence of HypF-N toxic oligomers. Error bars indicate the standard deviation of triplicate independent experiments. T student analysis: * p<0.005; ** p<0.001;***p<0.0001.

In 1993 it was reported that amyloid fibril formation *in vitro* by Aβ40 was inhibited by human CSF (Wisniewski *et al*. 1993); subsequently the protein responsible of this effect was found to be TTR, which formed stable complexes with Aβ40. Recently it has been observed that TTR is able to suppress the toxicity of extracellularly added oligomers formed by two different peptides/proteins, namely Aβ42 and HypF-N (Li *et al*. 2011). A stable monomeric M-TTR engineered by introducing two methionine substitutions (F87M and L110M) disrupts the subunit interfaces of the TTR tetramer. (Jiang *et al*. 2011). This derivative protects SH-SY5Y neuroblastoma cells and rat primary neurons against oligomer-induced cytotoxicity, and the interaction between M-TTR and HypF-N/Aβ42 oligomers was found to involve further clustering of the oligomers. Based on these data we performed an MTT assay to confirm that Hcy induced the formation of monomeric structure of TTR. Figure 5B showed that 96 h of incubation of L55P-TTR with Hcy resulted in an increase of monomeric structures able to suppress the cytotoxicity induced by HypF-N oligomers, similarly to M-TTR. In this case we did not observe cell sufferance induced by the sample grown after 96 h of incubation with Hcy because the final concentration was reduced 10 times.

3. Molecular insights into membrane interaction of a new amyloidogenic variant of β2-microglobulin

Characterization of D76N aggregation. After dilution in phospahte buffer, the D76N self-assembly process was monitored over time by the ThT fluorescence assay. Since its first description in 1959, the fluorescent dye Thioflavin-T (ThT) has become among the most widely used "gold standards" for selectively staining and identifying amyloid fibrils both *in vivo* and *in vitro*. ThT fluorescence of amyloid is typically measured using an excitation wavelength of 440 nm, giving an emission maximum at ~482 nm. Recent data showed that under physiologic solvent conditions, the D76N variant is converted into fibrils displaying the classic amyloid-like properties within 48 h, whereas the wt protein does not aggregate at all. Fibril formation by the variant was markedly enhanced by shaking the protein solution, a recognized treatment that promotes β-sheet aggregation by overexposing the protein to the water–air interface, which mimicks the in vivo environment at the interface between polar and non-polar surfaces (Valleix S. et al. 2012).

D76N aggregation was characterized by a time-dependent increase in the ThT fluorescence intensity suggesting a transformation of the “native-like” protein into aggregates rich in cross-beta structure. A measurable “lag time” of ca. 3 h was observed and the ThT fluorescence intensity reached its maximum value by ca. 24 h after which there was no significant change in fluorescence intensity (Figure 1A-B). Next, we performed a DLS analysis of the same samples for additional characterization of the species present in the protein sample. The native D76N sample was composed of particles with an apparent hydrodynamic diameter (D_H) of about 8 nm (Fig.1C). During the aggregation time at physiological pH we observed an increase of D_H which confirmed aggregation. To ascertain that the aggregates formed by the protein display cross-beta structure, we used the well-established Congo red binding assay (CR). Amyloid aggregates with cross-beta conformation exhibit a characteristic red shift in their absorption spectrum upon binding to Congo red. Free Congo red solution and native D76N at pH 7.0 exhibited absorption spectra with absorption maxima at 490 nm. After 48 h of aggregation, D76N showed an absorption maximum at higher wavelength. The absorption shift was even more evident from the difference spectrum (bound CR minus free CR) which exhibit an absorption maximum at 550 nm (Fig.1D). These results are consistent with the presence of cross-beta structures in the aggregates formed

by D76N after 48 h of aggregation and with the kinetics of aggregation followed by the ThT fluorescence assay.

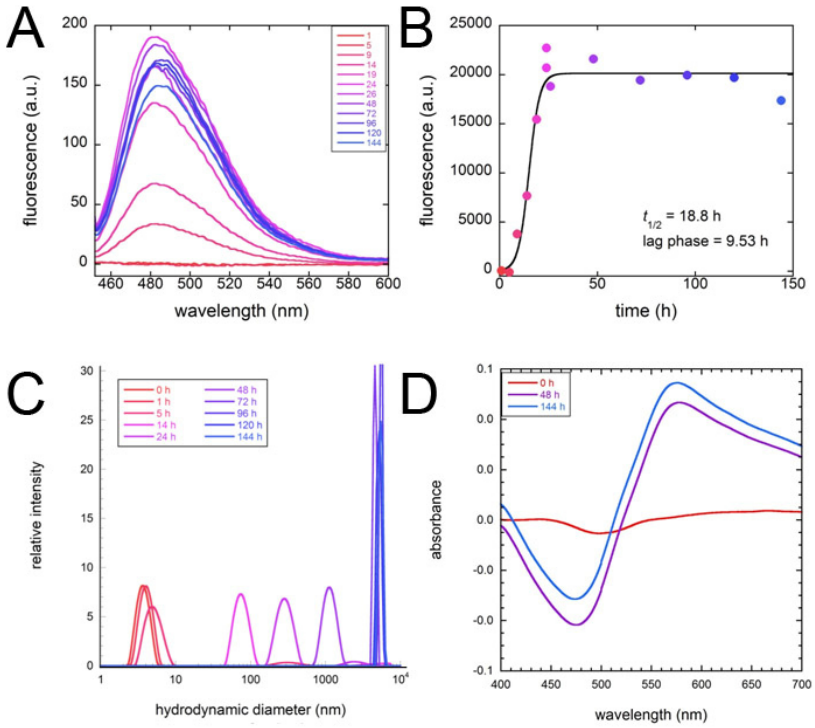

Figure 1. Characterization of D76N aggregates. A,B) Tht fluorescence intensity profile for aggregation of D76N. C) DLS analysis of the aggregates. D) CR difference absorbance spectra.

Cytotoxicity of D76N aggregates. Considering the times of aggregation and the amyloidogenic species obtained under our aggregation conditions,we decided to assess the potential toxicity of these species to SH-SY5Y cells. Human neuroblastoma SH-SY5Y cells are a dopaminergic neuronal cell line widely used as an *in vitro* model for neurotoxicity experiments. To test the toxicity of aggregated D76N we used differentiated SH-SY5Y cells as preliminary data showed that D76N aggregates localized preferentially to neurites. SH-SY5Y differentiation was induced after cell treatment with 10µM *trans*-retinoic acid (RA) for four days. Cell differentiation was confirmed by showing an extensive outgrowth of neurites in the cell sample. The cytotoxicity of D76N aggregates was evaluated by the MTT assay. The aggregates obtained after 144 h of aggregation showed the highest cytotoxicity, with a cells sufferanche of about 80%. The toxicity was evident also at early times of aggregation with a toxicity about 20-30%, in particular when the cells were exposed to D76N species obtained after 96 h of aggregation. Next, we investigated the mechanism of cell damage after cell exposure to D76N aggregates by measuring the intracellular reactive

oxygen species (ROS) and the intracellular free Ca^{2+} levels using the fluorescent probes CM-H_2DCFDA and Fluo-3-acetoxymethyl ester, respectively. The changes in the intracellular redox status and free Ca^{2+} levels in cells exposed to toxic aggregates have been described as crucial events in the impairment of cell function by amyloid aggregates. Figure 2, showed clearly an increase of ROS levels which depending on the aggregation time of D76N (Fig. 2B). The highest ROS induction (3,5-fold increase with respect to untreated cells) was obtained after 24 h cell exposure to a protein sample aged 144 h)144h-aged D76N) which also resulted the most toxic sample according to the MTT results. Confocal analysis of Fluo-3AM fluorescence, a dye able to bind the intracellular free Ca^{2+}, showed that cell exposure to 144 h-aged D76N resulted in a significant increase of the intracellular free Ca^{2+} levels. 1h cell treatment with 96h-D76N and 144h-D76N aggregates induced an increase of fluorescence intensity of about 2-fold and 7-fold, respectively. Cell apoptosis and necrosis could both be triggered by amyloid aggregate toxicity. We therefore investigated whether the changes in ROS production and free calcium levels induced by D76N lead to cell death and, if so, whether activation of apoptosis was involved. Early apoptotic cells are characterized by translocation to the outer membrane leaflet and exposure of a phospholipid normally found in the inner leaflet, whereas necrotic cells undergo membrane rupture. SH-SY5Y cells were treated for 24 h with 144-D76N aggregates and labelled with specific dyes: fluorescein isothiocyante (FITC)-conjugated annexin V to detect phosphatidylserine externalization and propidium iodide (PI) to label the cellular DNA in necrotic cells where the cell membrane integrity has been totally compromised. Such a double labelling allows to discriminate among early apoptotic cells (annexin V-positive, PI-negative), necrotic cells (annexin-V positive, PI-positive), and viable cells (annexin V-negative, PI-negative). Figure 2 shows that cell treatment for 24h with 5µM (monomeric protein concentration) 144 h-aged D76N aggregates caused cell death by necrosis. In fact, while control cells displayed no annexin V-FITC binding and no IP positivity the cells treated with 144h-aged D76N aggregates showed 8.4% cells with only IP positivity, confirming necrotic, rather than apoptotic, death (Fig.2D).

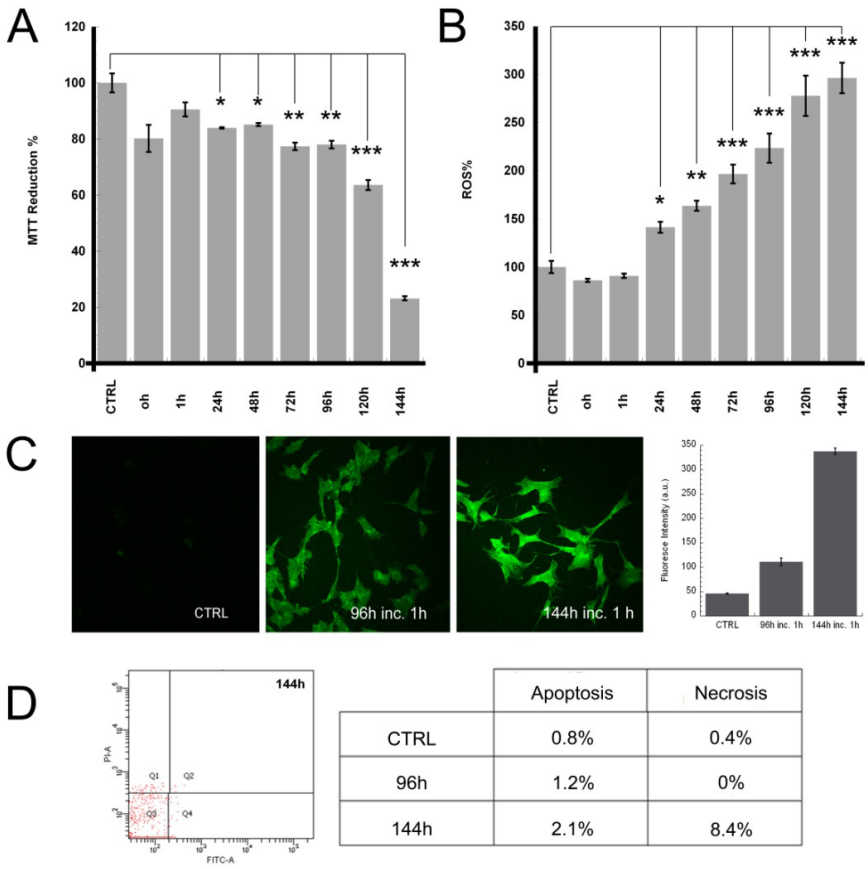

	Apoptosis	Necrosis
CTRL	0.8%	0.4%
96h	1.2%	0%
144h	2.1%	8.4%

Figure 2. Cytotoxicity of D76N aggregates. A,B) MTT assay and ROS% production after 24h of treatment of SH-SY5Y cells with different kind of aggregates at 5μM concentration. Error bars indicate the standard deviation of triplicate independent experiments. T student analysis: * $p<0.005$; ** $p<0.001$;***$p<0.0001$.C) Confocal microscopy imaging of intracellular free Ca^{2+} levels in SH-SY5Ycells exposed for 1h at 96h and 144h time of aggregation. Near the quantification of Ca^{2+} levels respect to untreated cells. D) Gate and cellular percentage stained with Annexin V-FITC, PI, after 24h of incubation with 144h aggregates.

Immunolocalization. The toxicity of amyloid-forming proteins has been hypothesized to reside in the ability of protein oligomers to interact with, and to disrupt, the cell membrane. In order to shed light on the 144h-D76N interaction with the plasma membrane of the exposed cells and to understand whether the toxicity of the different D76N aggregate species was related to their ability to interact with the plasma membrane, we performed confocal microscopy experiments using a polyclonal antibody raised against recombinant β2-m, and Alexa 488-conjugated CTX-B, a probe that specifically binds the monosialoganglioside GM1, a common lipid raft marker. Previous data indicate that cell differentiation increases the presence of GM1, in particular during neurite outgrowth (Ledeen *et al.* 1998). Recent evidence suggests that different amyloid oligomers may exert their deleterious effects through binding to, and causing the aberrant clustering of, lipid raft proteins. The formation of these pathogenic lipid raft-based platforms may be critical for the toxic signalling mechanisms with additional

deleterious effects upon cell function and integrity. Confocal images showed evidences of fibril clustering of 96h- and 144h-D76N at the SH-SY5Y cell membrane (Fig.3A,B,C). Interestingly, our evidences suggest that these aggregates interact preferentially with cell neurites. In particular, the imaged 144 h-D76N aggregates follow the profile of the neurites. Membrane rafts are increasingly recognized to play pivotal roles in favouring protein/peptide aggregation as well as aggregate interaction with the cell membrane. In Figure 3 has been showed a co-localization of the fluorescence signals arising from GM1 and D76N aggregates confirmed also by FRET analysis (Fig.3;1a,2a,3a). As commonly accepted, the presence of FRET indicates a distance <10 nm between the labelled molecules, which strongly supports the occurrence of a direct fibril-GM1 interaction. In addition, a diffused staining of fluorescence dots, with low FRET efficiency, was evident in cells treated with the 144 h-aged aggregates (Fig3,3a). These data suggest that the aberrant localization of these fibrils with the cell membrane at the raft level induces a significant lipid reorganization within the membrane with impairment of cell physiological functions. In addition, these results suggest that the ability of these aggregates to associate with lipids, particularly raft components, causes the uptake of the raft components that, in turn, can affect aggregate morphology.

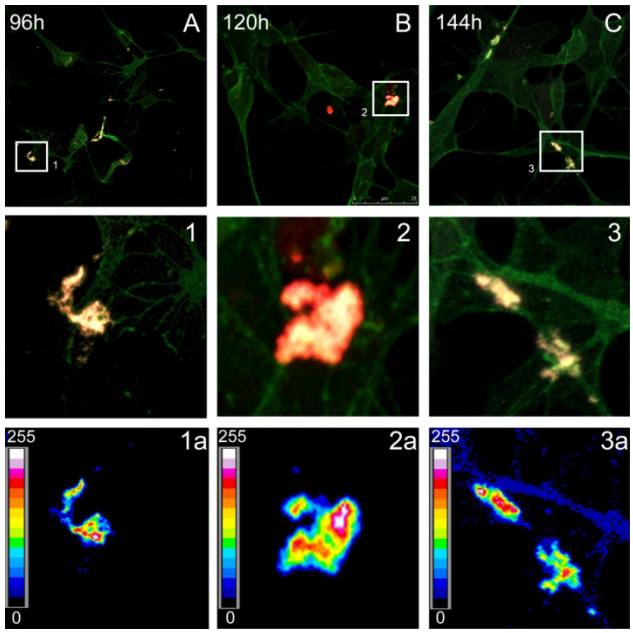

Figure 3. **Immunolocalization of oligomeric and fibrillar D76N on the plasma membrane.** SH-SY5Y cells exposed for 24h to 5μM D76N assemblies that form 96h (A) 120h (B) 144h (C). Cells were stained with CTX-B Alexa 488-conjugated (green fluorescence); protein aggregates were revealed by incubation with anti-β2-m antibodies followed by treatment with Alexa 568-conjugated anti-rabbit secondary antibodies (red fluorescence). The FRET efficiency is shown in 1a,2a,3a for 96h.120h and 144h, respectively.

The importance of GM1 for the aggregate-membrane interaction of. In collaboration with the European Laboratory for Non-Linear Spectroscopy (LENS) were carried out single particle tracking experiments to enhance the interaction of D76N aggregates and GM1 on the plasma membrane of living cells. This tecnique is a sensitive approach to tracking the motion of membrane molecules such as lipids and proteins with molecular resolution in live cells. It makes use of fluorescent semiconductor nanocrystals, quantum dots (QDs), as a probe to detect membrane molecules of interest (Bannai *et al.* 2006). Neuroblastoma SH-SY5Y cells were incubated for 20 min with 5μM preformed D76N aggregates and labeled with anti-β2m/anti-mouse Alexa 488 and CTX-B/QDs 655 (Fig.4A). Trajectories of single GM1 molecules moving tangentially onto the plasma membrane were extrapolated from recordings acquired at 100 Hz and overlaid on thresholded binary images of β2m aggregates. We found that the aggregates did not diffuse significantly during the recording sessions of 2.5 s. GM1 molecules were subsequently discriminated according to the localization of their trajectories with respect to the aggregates (Fig.4B). The linear average mean square displacement (MSD) plot of GM1 molecules moving in regions far from D76N aggregates reflected a typical Brownian motion behaviour (Fig.4C). By contrast, GM1 molecules co-localizing with β2m aggregates displaied a curved average MSD plot that can be ascribed to a confined type of motion (Fig.4C). Furthermore, the cumulative distributions of the diffusion coefficients (D) of single GM1 molecules moving over and separately from D76N aggregates differed substantially (Fig.4D). The median D value of GM1 molecules overlapping with D76N aggregates is one order of magnitude lower (Table 4). The median D value of freely diffusing GM1 appears to be higher than that found previously (1.2×10^{-1} μm^2 s^{-1} with respect to 2.9×10^{-2} μm^2 s^{-}1 and 2.7×10^{-2} μm^2 s^{-1}) (Bucciantini *et al*. 2012; Calamai *et al.* 2013). This discrepancy is possibly due to the higher acquisition frame rate (100 Hz compared to 3 Hz) used here. Nevertheless, the change in D of GM1 due to the presence of D76N aggregates is comparable in absolute value to that observed in the case of amyloid aggregates of Aβ1-42, amylin and Sup35pNM (Bucciantini *et al.* 2012; Calamai *et al.* 2013). Overall, these data show that D76N aggregates interfere with the mobility of GM1 in living neuroblastoma cells.

D76N-β2m amyloid aggregates alter the lateral diffusion of GM1-CTXB on the plasma membrane of SH-SY5Y neuroblastoma cells

Condition	*n*	D_{median} ($\mu m^2 s^{-1}$)	λ_{max} [†]	p[‡]
GM1-CTXB out β2m	33	1.2×10^{-1}		
GM1-CTXB over β2m	25	2.1×10^{-2}	6.8×10^{-1}	$\leq 10^{-4}$

[†]Maximum difference in cumulative fraction between GM1-CTXB diffusion over and nearby D76N aggregates.

[‡]Kolmogorov-Smirnov test p-value calculated using λ_{max} as statistic.

Table 4. Analysis of GM1 in presence and in absence of D76N aggregates.

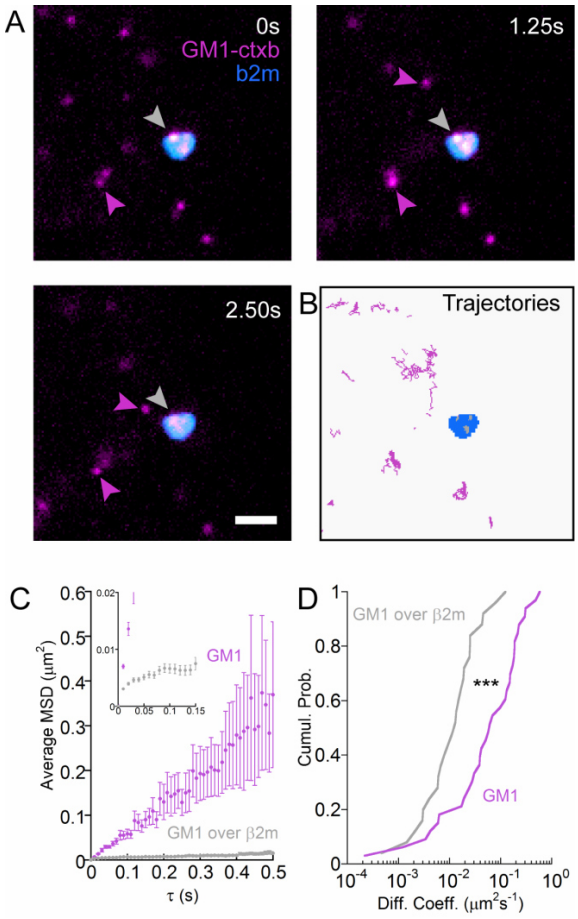

Figure 4. D76N aggregates affect the mobility of GM1 molecules in living neuroblastoma cells. A) Imaging of single GM1 molecules and β2m aggregate labeled with biotin-ctxb coupled to streptavidin-QD 655 (magenta) and anti-β2m and secondary Alexa 488 conjugated antibodies (cyan), respectively. Scale bar, 2μm. B) Trajectories of the GM1 molecules in the proximity of (magenta) or overlapping to (grey) the binary image of the β2m aggregate (cyan). (C and D) Average mean square displacement and cumulative probability distributions of diffusion coefficients of GM1molecules classified as over (grey) and apart (magenta) from β2m aggregates. The inset in C highlights the confined motion of GM1 induced by β2m aggregates.

Lipid raft disruption following GM1 depletion decreases the toxicity of D76N aggregates. Increasing evidence suggests that the interaction of misfolded protein oligomers with cell membranes is a primary event resulting in the cytotoxicity associated with many protein-misfolding diseases, including neurodegenerative disorders. The GM1 content was modulated by cell pre-treatment with PDMP (D-threo-1-phenyl-2-decanoylamino-3-morpholino-1-propanol(PDMP), a glucosylceramide synthase inhibitor that blocks the natural synthesis of GM1 (Tamboli *et al.* 2005) thus reducing about 2-fold the GM1 content (Fig.4F). SH-SY5Y cells depleted of GM1 were exposed for 24 h to D76N aggregates grown for 144 h and then stained with CTX-B. It was decided to test only the 144 h-D76N because it was the most toxic species. The treatment with PDMP affected the D76N fibrils/cells binding (Fig.4C) and reduced the FRET efficiency, confirming the importance of GM1 as binding site for aggregate/cell membrane interaction. Moreover, GM1 depletion suppressed cell vulnerability to D76N aggregates as showed by MTT assay (Fig.4A), confirming that GM1 is really important for the toxicity induced by 144h-D76N aggregates.

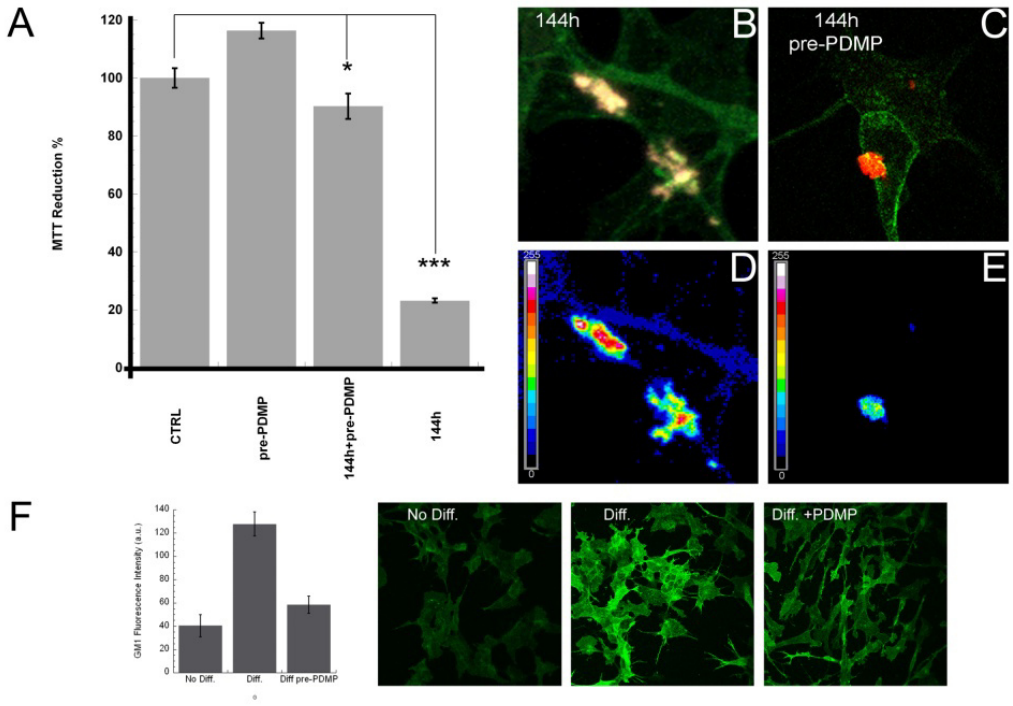

Figure 4. **GM1 as binding site for amyloid species.** (A) MTT assay on SH-SY5Y cells pre-treated for 72h with PDMP and exposed for 24h to 5μM 144h- D76N assemblies. Error bars indicate the standard deviation of triplicate independent experiments. T-student analysis: * p<0.005; ** p<0.001;***p<0.0001. (B and C) Immunolocalization and (D and E) FRET efficiency on SH-SY5Y pre-treated for 72h with PDMP and treated for 24h with5μM 144h- D76N aggregates. (F) GM1 quantification on SH-SY5Y cells undifferentiated, RA differentiated and PDMP treated.

Discussion

1. Oleuropein Aglycone: a natural polyphenol which protects against the cytotoxicity associated with Transthyretin fibrillogenesis

Recent studies indicate that several small polyphenol molecules have been demonstrated to remarkably inhibit the formation of fibrillar assemblies in vitro and their associated cytotoxicity (Wu *et al*. 2006; Bastianetto *et al*. 2004). Studies with model organisms have confirmed such beneficial affects against a number of amyloid diseases, such that some of these compounds have been, and presently are being, assayed in several clinical trials. In particular, previous studies on the interaction of polyphenols with TTR demonstrated that curcumin and NDGA bind to TTR at the T4 binding sites and stabilize the tetrameric form of TTR hindering its aggregation into toxic amyloid assemblies (Ferreira *et al*. 2012). Ole*A* is a phenol enriched in the extra virgin olive oil, and several studies have convincingly supported its beneficial effects against age-associated neurodegeneration and other pathologies including type 2 diabetes. However, no evidence on possible effects of Ole*A* against TTR aggregation and aggregate cytotoxicity has been reported so far. The data in this paper suggest that Ole*A* inhibits toxicity associated with TTR aggregation and modulates the appearance of soluble non-toxic TTR aggregates. Apparently, Ole*A* inhibition of TTR amyloid polymerization proceeds through a decrease of the exposure to the solvent of aromatic residues uncovered following tetramer disassembly and misfolding of the resulting monomers/dimers. The poor interaction between the resulting TTR/Ole*A* complex and membrane gangliosides in the lipid rafts of the exposed cells is probably related with the loss of amyloid TTR cytotoxicity. Our findings confirmed the higher toxicity of the mutant L55P-TTR with respect to the wt-TTR (Yang *et al*. 2003); in fact, the viability of HL-1 cells exposed to L55P-TTR aggregates obtained in the presence of Ole*A* was not restored completely as determined by the MTT assay. However, this residual toxicity of L55P did not match with CR data. In fact, the typical shift of the absorbance peak of Congo red bound to any amyloid assembly was absent both in aggregated L55P-TTR and wt-TTR incubated with Ole*A*, suggesting the absence of toxic amyloid species also in L55P mutant. On the other hand, this result can be explained by either any displacement of CR or by some conformational alteration induced by Ole*A* differently on the two proteins. In fact, the FTIR analysis of both L55P- and wt- TTR indicated that, for both proteins, misfolding is an irreversible process that is not affected

by Ole*A*. From these observations we suggest that Ole*A* interaction with aggregates could slightly alter the environment surrounding the CR binding-sites thus inhibiting the interaction of the latter with the amyloid structure. The occurrence of chemical interaction between Ole*A* and TTR is supported also by the emission spectra analysis of its aromatic residues, showing that during the protein aggregation, the decrease of the 320 nm component observed in the secondary derivative plots is reduced in presence of Ole*A*. Of note, the secondary derivative plots of both wt- and L55P- TTR most toxic species showed a peculiar minimum at about 335nm. Interestingly, the less toxic Ole*A*/fibrils complex did not show this spectral component. Therefore, we suggest that incubation of TTR with the phenolic compound affects the potential amyloid TTR toxicity by hampering TTR interaction with other molecules. Accordingly, acrylamide quenching analysis revealed that in the presence of Ole*A* some alteration of solvent-exposure of peptide aromatic residues did occur. Moreover, following Ole*A* treatment both wt- and L55P-TTR fibrils increased their resistance to Proteinase-K digestion. Recent papers suggested that aromatic interactions favour molecular recognition of amyloidogenic sequences by enhancing the directionality and orientation needed for the ordered self-assembly process and hence fibril assembly kinetics (Pawar *et al*. 2005).On the other hand, it has been reported that several polyphenolic compounds are able to interact with amyloidogenic aromatic residues hindering π-system stacking (Porat *et al*. 2004; Gazit E 2002) and inhibiting the elongation phase of fibril growth or the assembly of large oligomers without interfering with early nucleation events (Sekijima *et al*. 2008). Modeling studies have shown that several polyphenols share the ability to adopt a specific three-dimensional conformation that might be essential for early amyloid binding preventing the growth of typical amyloid fibrils (Porat *et al* 2006).Emerging evidences account for fibrils/membrane interaction as key factor of the cytotoxic potential of amyloid aggregates (Shnyrov *et al*. 2000; Porat *et al* 2006). Our confocal analysis supported the latter hypothesis revealing that exposed cells displayed a lower affinity to Ole*A* treated than to Ole*A*-untreated TTR samples. Moreover, TEM results were confirmed by a diffused FRET signal in Ole*A* treated sample indicating the presence of oligomer-like structures on plasma membrane of exposed cells. In addition, the low level efficiency of FRET signal between TTR and GM1 recorded in exposed cells linked the cytoprotective effects of Ole*A* with a decreased interaction between Ole*A*/TTR complex and plasmamembrane ganglioside with respect to Ole*A*-untreated samples. In conclusion, our results suggest that Ole*A* reduced amyloid TTR toxicity. Its

interaction with the TTR does not hinder its transition to an amyloid structure nor the interaction of the latter with the cell membrane. However, Ole*A* interferes with TTR fibrillation by stabilizing an oligomer like intermediate that interacts with the plasma membrane without altering its integrity. These data suggest that Ole*A*, or its molecular scaffold can be a good starting point to design novel therapeutic strategies for prevention and therapy of TTR-associated sporadic or familial amyloidoses.

2. Wild-type and Leu55Pro Transthyretin Homocysteynilation, worsening of cardiomiopathy onset

In intricate diseases such as amyloidosis, both genetic and environmental factors are involved in the disease process. The TTR amyloidosis include familial amyloid cardiomyopathy (FAC) and familial amyloid polyneuropathy (FAP). FAP is characterized by amyloid deposition in various organs; in particular the L55P mutation induces a cardiac involvement. Recently data showed how the cysteine 10 (Cys10) of monomeric TTR is reactive, it is likely that the thiolic residue of Cys10 through its oxidation is involved in the TTR teramer destabilization. Indeed, severe oxidative stress were observed in FAP patients (Ando *et al*. 1997). Hyperhomocysteinemia is an independent risk factor for cardiovascular disease and an emerging risk factor for cognitive dysfunction and Alzheimer's disease. Greater than 70% of the homocysteine in plasma is disulfide-bonded to protein cysteine residues. Considering that: high level of homocysteine can initiate and potentiate atherosclerosi, the cardiac involvement on TTR amyloidosis and that TTR undergoes homocysteinylation at its single Cys10 residue *in vitro* and *in vivo* (Lim *et al*. 2003), we decided to study the homocysteinylated TTR in terms of amyloid aggregation and toxicity. The data presented in this study establish that: 1) TTR can be homocysteynilated under physiological conditions; 2) wt-TTR is stabilized by Hcy in its tetrameric structure; 3) Hcy destabilizes L55P-TTR tetramer, inducing the formation of monomeric species. Experiments *in vitro* showed that the modification at pH 7.0 of wt-TTR on Cys10 by homocysteine stabilizes the tetrameric form. This data results be very important considering that during the process of aggregation the destabilization of tetrameric form it is a crux of the aggregation way (Cardoso *et al*. 2007). Instead on the mutant form L55P-TTR the modification on Cys10 promotes a further destabilization of TTR

tetramer with the subsequent appearance of monomeric toxic species. The presence of these monomeric species has been tested, in this study, by analysing the chaperonic ability of the homocysteinylated samples. In fact, recently, TTR was shown to inhibit aggregation and amyloid plaque formation of Aβ both in vitro and in vivo (Schwarzman, *et al.* 1994; Buxbaum *et al.* 2008). Analyses carried out in vitro have shown that monomeric TTR exhibits stronger binding to preformed oligomers formed by two different peptides/proteins, namely $A\beta_{42}$ and HypF-N, and reduces their toxicity. Taken together, our findings suggest that N-homocysteinylation destabilizes L55P-TTR structure and favors the appearance of partially unfolded intermediate species with a higher tendency to aggregates in well-organized fibrillar structures. Although different hypotheses have been proposed to describe the pathological consequences of hyperhomocysteinemia in humans, so far the cause of homocysteine toxicity has not been understood. It has been suggested that N-Hcy-protein accumulation is an important risk factor for cardiovascular and neurodegenerative diseases In this thesis we have shown that N-homocysteinylation could promote the further accumulation of L55P-TTR that by itself is considered the causative agent in early-onset familial amyloid polyneuropathy. The results reported in this article could have pathophysiological relevance and could contribute to clarify the mechanisms underlying some pathological consequences described in patients affected by hyperhomocysteinemia.

.

3. Molecular insights into membrane interaction of a new amyloidogenic variant of β2-microglobulin

β2-m is among the most extensively studied globular protein precursors of human amyloid fibrils. The D76N residue substitution allows a fully folded three-dimensional structure almost identical to that of the wild type protein that forms amyloid fibrils in dialysis-related amyloidosis. However, dissection of the mechanism of D76N fibrillogenesis established paradigm that the amyloidogenicity of monomeric globular proteins is intimately connected to destabilization of the native fold (Booth *et al*. 1997). Our data offer an elucidation about the mechanism of the highly amyloidogenic D76N variant cytotoxicity. The D76N resulted be most aggressive than wt β2-m, because this protein is able to aggregate under physiological conditions.

The mechanism of the toxicity has been studied extensively from both the experimental and theoretical perspectives: activation of inflammatory effects by interacting directly with the membrane (Verdier *et al*. 2004; Kourie and Henry, 2002 ; Kourie, 2001)) induction of oxidative stress and alteration of ionic homeostasis (Milhavet and Lehmann 2002; Wyttenbach *et al.* 2002), disruption of membrane receptors' function by intimate binding (Wang *et al*. 2004), lipid composition, especially the presence of negatively charged lipids in the membrane, appears as one of the primary factors that determine the extent of membrane-mediated aggregation (Sparr *et al.* 2004; Zhao *et al.* 2004).

Differently from the wild-type β2-m amyloid systems, but in line with other reported data on amyloid fibrils, aged D76N aggregates displayed higher cytotoxicity than their earlier precursor assemblies. We therefore investigated in detail the molecular and mechanistic ways of fibril cytotoxicity using differentiated SH-SY5Y cell line. We found that the fibrils bound to the cell membrane without penetrating inside the cells and that their cytotoxicity was associated to some modification of membrane permeability, suggesting that our fibrillar aggregates did heavily dismantle the phospholipid bilayer of the exposed cells. Yet, the apoptotic cascade was not triggered in the exposed cells, but only in presence of 144h-D76N aggregates was observed the presence of nectrotic cells. Membrane rafts are increasingly recognized to play pivotal roles in favouring protein/peptide aggregation as well as aggregate interaction with the cell membrane (Rushwort *et al*. 2010), even though these data refer mainly to oligomeric amyloid assemblies rather than to mature fibrils. Actually, our colocalization and FRET experiments showed that the interaction with the cell membrane of aged D76N aggregates occurred at the raft level and involved the GM1 ganglioside, a key raft component, particularly its sialic acid moiety. We here report that a clear interaction of amyloid fibrils with membrane rafts did occur and that GM1 was primarily involved in such interaction, favouring membrane permeabilization and impairment of cell viability. This finding can be related to previous data showing that Sup35p fibrils induced a GM1 clustering (Bucciantini *et al*. 2012). In conclusion, our data support the idea that GM1 is a key site of interaction of most preformed amyloid species with the cell membrane, further stressing the role of lipid rafts as fundamental mediators of amyloid toxicity and also give an explanation about the way of cytotoxicity induction by D76N aggregates.

References

Afolabi I, Hamidi Asl K, Nakamura M, Jacobs P, Hendrie H, Benson MD (2000); Transthyretin isoleucine-122 mutation in African and American blacks, Amyloid. 7(2):121-5.

Aggeli A, Bell M, Boden N, Keen JN, Knowles PF, McLeish TC, Pitkeathly M, Radford SE (1997); Responsive gels formed by the spontaneous self-assembly of peptides into polymeric beta-sheet tapes, Nature 386:259–262.

Alarcón JM, Brito JA, Hermosilla T, Atwater I, Mears D, Rojas E (2006); Ion channel formation by Alzheimer's disease amyloid beta-peptide (Abeta40) in unilamellar liposomes is determined by anionic phospholipids, Peptides. 27(1):95-104.

Almeida MR, Alves IL, Terazaki H, Ando Y, Saraiva MJ (2000); Comparative studies of two transthyretin variants with protective effects on familial amyloidotic polyneuropathy: TTR R104H and TTR T119M, Biochem. Biophys. Res Commun. 270(3):1024-8.

Ambrose JA, Barua RS (2004); The pathophysiology of cigarette smoking and cardiovascular disease: An update, J. Am. Coll. Cardiol. 43:1731-1737.

Ami D, Ricagno S, Bolognesi M, Bellotti V, Doglia SM, Natalello A (2012); Structure, stability, and aggregation of β-2microglobulin mutants: insights from a Fourier transform infrared study in solution and in the crystalline state, Biophys J.102(7):1676-84.

Amiot MJ, Fleuriet A, Macheix JJ (1989); Accumulation of oleuropein derivatives during olive maturation, Phytochemistry. 28: 67–70.
Anderson RG (1998); The caveolae membrane system, Annu. Rev. Biochem. 67:199–225.

Ando Y, Nyhlin N, Suhr O, Holmgren G, Uchida K, Sahly M, Yamashita T, Terasaki H, Nakamura M, Uchino M, Ando M (1997); Oxidative stress isfound in amyloid deposits in systemic amyloidosis, Biochem Biophys Res Commun 232:497–50.

Ando Y, Suhr OB (1998); Autonomic dysfunction in familial amyloidotic polyneuropathy (FAP), Amyloid 5 (4): 288–300.

Ando Y, Ueda M (2008); Review: Novel methods for detecting amyloidogenic proteins in transthyretin related amyloidosis, Front Biosci13:5548-58.

Andrade C (1952); A peculiar form of peripheral neuropathy; familiar atypical generalized amyloidosis with special involvement of the peripheral nerves, Brain. 75(3):408-27.

Andreadou I, Iliodromitis EK, Mikros E, Constantinou M, Agalias A, Magiatis P, Skaltsounis AL, Kamber E, Tsantili-Kakoulidou A, Kremastinos DT (2006); The olive

constituent oleuropein exhibits anti-ischemic, antioxidative, and hypolipidemic effects in anesthetized rabbits, J Nutr. 136: 2213–2219.

Andreadou I, Sigala F, Iliodromitis EK, Papaefthimiou M, Sigalas C, Aligiannis N, Savvari P, Gorgoulis V, Papalabros E, Kremastinos DT (2007); Acute doxorubicin cardiotoxicity is successfully treated with the phytochemical oleuropein through suppression of oxidative and nitrosative stress, J Mol Cell Cardiol. 42: 549–558.

Arispe N, Pollard HB, Rojas E (1993);Giant multilevel cation channels formed by Alzheimer disease amyloid beta-protein [A beta P-(1-40)] in bilayer membranes, Proc Natl Acad Sci U S A. 90(22):10573-7.

Arsequell G, Planas A (2012); Methods to evaluate the inhibition of TTR fibrillogenesis induced by small ligands, Curr Med Chem.19(15):2343-55.

Arts IC, Hollman PC (2005); Polyphenols and disease risk in epidemiologic studies, Am. J. Clin. Nutr. 81, 317S-325S.

Azevedo E, Silva FP, Palhano F, Braga CA, Foguel D (2013); Transthyretin-Related Amyloidoses: A Structural and Thermodynamic Approach "Amyloidosis", book edited by Dali Feng , ISBN 978-953-51-1100-9.

Ballardie FW, Kerr DNS, Tennent G, Pepys MB (1986); Haemodialysis versus CAPD: equal predisposition to amyloidosis?, Lancet I: 795-796.

Baron-Menguy C, Bocquet A, Guihot AL, Chappard D, Amiot MJ, Andriantsitohaina R, Loufrani L, Henrion D (2007);Effects of red wine polyphenols on postischemic neovascularization model in rats: low doses are proangiogenic, high doses anti-angiogenic. FASEB J. 21 (13):3511–21

Bartoli R, Fernandez-Banares F, Navarro E, Castella E, Mane J, Alvarez M, Pastor C, Cabre E, Gassull MA (2000); Effect of olive oil on early and late events of colon carcinogenesis in rats: Modulation of arachidonic acid metabolism and local prostaglandin E(2) synthesis, Gut 46:191-199.

Bateman DA, Tycko R, Wickner RB (2010); Experimentally derived structural constraints for amyloid fibrils of wild-type Transthyretin, Biophys J.101(10):2485-92.

Baures PW, Oza VB, Peterson SA, Kelly JW (1999); Synthesis and evaluation of inhibitors of transthyretin amyloid formation based on the nonsteroidal anti-inflammatory drug flufenamic acid, Bioorg Med Chem 7:1339–1347.

Baures PW, Peterson SA, Kelly JW (1998); Discovering transthyretin amyloid fibril inhibitors by limited screening, Bioorg Med Chem 6:1389–1401.

Bazoti FN, Bergquist J, Markides K, Tsarbopoulos A (2008); Localization of the non covalent binding site between amyloid-beta-peptide and oleuropein using electrospray ionization FT-ICR mass spectrometry, J Am Soc Mass Spectrom 19, 1078–1085.

Becket JW, Reeke GN Jr (1985); Three-dimensional structure of/beta2-microglobulin, Proc Natl Acad Sci USA 82:4225-4229.

Benson MD, Cohen AS (1977); Generalized amyloid in a family of Swedish origin. A study of 426 family members in seven generations of a new kinship with neuropathy, nephropathy, and central nervous system involvement, Ann Intern Med. 86(4):419-24.

Berlett BS, Stadtman ER (1997); Protein oxidation in aging, disease, and oxidative stress, J Biol Chem.272(33):20313-6.

Bhullar KS, Rupasinghe HP (2013); Polyphenols: multipotent therapeutic agents in neurodegenerative diseases. Oxid Med Cell Longev. 2013:891748.

Bjerrum OW, Plesner T (1985); Beta-2-microglobulin: a valuable parameter of stage, prognosis and response to treatment in myelomatosis, Scand J Haematol 35(1):22-5.

Bjorkman PJ, Saper MA, Samraoui B, Bennett WS, Strominger JL, Wiley DC (1987); Structure of the human class-I histocompatibility antigen,Hla-A2, Nature 329 506–512.

Blake CC, Swan ID, Rerat C, Berthou J, Laurent A, Rerat B (1971); An x-ray study of the subunit structure of prealbumin, Journal of Molecular Biology. 61(1):217-24.

Blevins G, Macaulay R, Harder S, Fladeland D, Yamashita T, Yazaki M, Hamidi Asl K, Benson MD, Donat JR (2003); Oculoleptomeningeal amyloidosis in a large kindred with a new transthyretin variant Tyr69His,Neurology. 60(10):1625-30.

Bokvist M, Lindström F, Watts A, Gröbner G (2004); Two types of Alzheimer's beta-amyloid (1-40) peptide membrane interactions: aggregation preventing transmembrane anchoring versus accelerated surface fibril formation, J Mol Biol. 335(4):1039-49.

Bonifacio MJ, Sakaki Y, Saraiva MJ (1996); In vitro amyloid fibril formation from transthyretin: The influence of ions and the amyloidogenicity of TTR variants, Biochim Bio- phys Acta 1316: 35– 42.

Booth DR, Sunde M, Bellotti V, Robinson CV, Hutchinson WL, Fraser PE, Hawkins PN, Dobson CM, Radford SE, Blake CC, Pepys MB (1997); Instability, unfolding and aggregation of human lysozyme variants underlying amyloid fibrillogenesis, Nature 385: 787–793.

Bourgault S, Solomon JP, Reixach N, Kelly JW (2011); Sulfated glycosaminoglycans accelerate transthyretin amyloidogenesis by quaternary structural conversion, Biochemistry 15;50(6):1001-15.

Brown EA, Arnold IR, Gower PE (1986); Dialysis arthropathy: complication of long term treatment with haemodialysis, Br Med J 292:163-166.

Brown EA, Gower PE (1982); Joint problems in maintenance haemodialysis, Clin Nephrol 18:247-250.

Bucciantini M, Giannoni E, Chiti F, Baroni F, Formigli L, Zurdo J, Taddei N, Ramponi G, Dobson CM, Stefani M (2002); Inherent toxicity of aggregates implies a common mechanism for protein misfolding diseases, Nature 416, 507-11.

Bucciantini M, Nosi D, Forzan M, Russo E, Calamai M, Pieri L, Formigli L, Quercioli F, Soria S, Pavone F, Savistchenko J, Melki R, Stefani M (2012); Toxic effects of amyloid fibrils on cell membranes: the importance of ganglioside GM1, FASEB J. 26 (2): 818–831.

Buxbaum JN1, Ye Z, Reixach N, Friske L, Levy C, Das P, Golde T, Masliah E, Roberts AR, Bartfai T (2008); Transthyretin protects Alzheimer's mice from the behavioral and biochemical effects of Abeta toxicity Proc. Natl. Acad. Sci. U. S. A., 105: 2681–2686.

Bychkova VE, Pam RH, Ptitsyh OB (1988); The molten globule state is involved in the traslocation of protein across membranes, FEBS Lett. 238, 231-234.

Calamai M, Pavone FS(2013);Partitioning and confinement of GM1 ganglioside induced by amyloid aggregates, FEBS Lett. 587(9):1385-91.

Campioni S, Mannini B, Zampagni M, Pensalfini A, Parrini C, Evangelisti E, Relini A, Stefani M, Dobson CM, Cecchi C, Chiti F (2010); A causative link between the structure of aberrant protein oligomers and their ability to cause cellular dysfunction, Nat. Chem. Biol. 6:140–147.

Cardoso I, Almeida MR, Ferreira N, Arsequell G, Valencia G, Saraiva MJ (2007); Comparative in vitro and ex vivo activities of selected inhibitors of transthyretin aggregation: relevance in drug design, Biochem J. 408(1):131-8.

Cardoso I, Brito M, Saraiva MJ (2008); Extracellular matrix markers for disease progressionand follow-up of therapies in familial amyloid polyneuropathy V30M TTR-related, Disease Markers. 25(1):37.

Cardoso J, Ferreira JR, Almeida J, Santos JM, Rodrigues F, Matos MJ, Gaspar M (2002); Chronic obstructive pulmonary disease in Portugal: Pneumobil (1995) and 2002 prevalence studies revisited, Rev Port Pneumol.19(3):88-95.

Carluccio MA, Siculella L, Ancora MA, Massaro M, Scoditti E, Storelli C, Visioli F, Distante A, De Caterina R (2003); Olive oil and red wine antioxidant polyphenols inhibit endothelial activation: antiatherogenic properties of mediterranean diet phytochemicals, Arterioscler Thromb Vasc Biol. 23: 622–629.

Carulla N, Caddy GL, Hall DR, Zurdo J, Gairí M, Feliz M, Giralt E, Robinson CV, Dobson CM (2005); Molecular recycling within amyloid fibrils, Nature 436(7050):554-8.

Cascella R, Conti S, Mannini B, Li X, Buxbaum JN, Tiribilli B, Chiti F, Cecchi C (2013); Transthyretin suppresses the toxicity of oligomers formed by misfolded proteins in vitro, Biochim Biophys Acta.1832(12):2302-14.

Cassuto JP, Krebs BP, Viot G, Dujardin P, Masseyeff R (1978) ; β2-microglobulin, a tumour marker of lymphoproliferative disorders. Lancet II: 108-109.

Cecil R, Wake RG (1962); The reactions of inter- and intra-chain disulphide bonds in proteins with sulphite, Biochem J. 82:401-6.

Chamberlain AK, MacPhee CE, Zurdo J, Morozova-Roche LA, Hill HA, Dobson CM, Davis JJ (2000); Ultrastructural organization of amyloid fibrils by atomic force microscopy, Biophys J. 79(6):3282-93.

Champe PC and Harvey RA (2008); Biochemistry. Lippincott's Illustrated Reviews" 4th ed. Lippincott Williams and Wilkins

Chanard J, Lavaud S, Toupance O, Mehi JP, Gillery P, Revillard JP (I986); β2-microglobulin-associated amyloidosis in chronic haemodialysis patients, Lancet I: 1212 .

Chapman, MR, Robinson LS, Pinkner JS, Roth R, Heuser J, Hammar M, Normark S, Hultgren SJ (2002); Role of Escherichia coli curli operons in directing amyloid fiber formation. Science 295, 851–855.

Checkoway H, Powers K, Smith-Weller T, Franklin GM, Longstreth WT, Jr Swanson PD (2002); Parkinson's disease risks associated with cigarette smoking, alcohol consumption, and caffeine intake, Am. J. Epidemiol. 155, 732-738.

Cheng B, Gong H, Xiao H, Petersen RB, Zheng L, Huang K (2013), Inhibiting toxic aggregation of amyloidogenic proteins:a therapeutic strategy for protein misfolding diseases, Biochimica et biophysica acta 1830, 4860-4871.

Chernoff, YO (2004); Amyloidogenic domains, prions and structural inheritance: rudiments ofearly life or recent acquisition?, Curr. Opin. Chem. Biol. 8, 665–671.

Cheung YT1, Lau WK, Yu MS, Lai CS, Yeung SC, So KF, Chang RC (2009); Effects of all-trans-retinoic acid on human SH-SY5Y neuroblastoma as in vitro model in neurotoxicity research. Neurotoxicology.30(1):127-35.

Chiti F, Bucciantini M, Capanni C, Taddei N, Dobson CM, Stefani M (2001); Solution conditions can promote formation of either amyloid protofilaments or mature fibrils from the Hypf N-temrinal domani, Protein Sci. 10 2541-2547.

Chiti F, De Lorenzi E, Grossi S, Mangione P, Giorgetti S, Caccialanza G, Dobson CM, Merlini G, Ramponi G, Bellotti V (2001);A partially structured species of β2-microglobulin is significantly populated under physiological conditions and involved in fibrillogenesis, J. Biol.Chem. 276, 46714–46721.

Chiti F, Dobson CM (2006); Protein misfolding, functional amyloid, and human disease, Annu Rev Biochem. 75:333-66.

Choi S, Reixach N, Connelly S, Johnson SM, Wilson IA, Kelly JW (2010); A substructure combination strategy to create potent and selective transthyretin kinetic

stabilizers that prevent amyloidogenesis and cytotoxicity, J Am Chem Soc 132:1359–1370.

Choi S, Reixach N, Connelly S, Johnson SM, Wilson IA, Kelly JW (2010); A substructure combination strategy to create potent and selective Transthyretin kinetic stabilizers that prevent amyloidogenesis and cytotoxicity, J Am Chem Soc.132:1359–1370.

Cicerale S, Conlan XA, Barnett NW, Sinclair AJ, Keast RS (2009); Influence of heat on biological activity and concentration of oleocanthal a natural anti-inflammatory agent in virgin olive oil, J Agric Food Chem.57(4):1326-30.

Claessen, D, Rink R, de Jong W, Siebring J, de Vreugd P, Boersma FG, Dijkhuizen L, Wosten HA (2003); A novel class of secreted hydrophobic proteins is involved in aerial hyphae formation in Streptomyces coelicolor by forming amyloid-like fibrils. Genes Dev. 17, 1714–1726.

Colon W, Kelly JW (1992); Partial denaturation of transthyretin is sufficient for amyloid fibril formation in vitro, Biochemistry. 31(36):8654-60.

Commenges D, Scotet V, Renaud S, Jacqmin-Gadda H, Barberger-Gateau P, Dartigues JF (2000); Intake of flavonoids and risk of dementia, Eur. J. Epidemiol. 16, 357-363.

Connors LH, Lim A, Prokaeva T, Roskens VA, Costello CE (2003); Tabulation of human transthyretin (TTR) variants, 2003, Amyloid.10(3):160-84.

Connors LH, Shirahama T, Skinner M, Fenves A, Cohen AS (1985); In vitro formation of amyloid fibrils from intact β2 microglobulin, Biochem Biophys Res Commun 131:1063-1068.

Conway KA, Rochet JC, Bieganski RM, Lansbury PT Jr (2001); Kinetic stabilization of the alpha-synuclein protofibril by a dopamine-alpha-synuclein adduct, Science 294:1346–1349.

Corazza A, Pettirossi F, Viglino P, Verdone G, Garcia J, Dumy P, Giorgetti S, Mangione P, Raimondi S, Stoppini M, Bellotti V, Esposito G (2004); Properties of some variants of human beta2-microglobulin and amyloidogenesis, J Biol Chem. 279(10):9176-89.

Cordeiro Y, Kraineva J, Suarez MC, Tempesta AG, Kelly JW, Silva JL, Winter R, Foguel D (2006); Fourier transform infrared spectroscopy provides a fingerprint for the tetramer and for the aggregates of Transthyretin, Biophys J. 91(3):957-67.

Costa R, Gonçalves A, Saraiva MJ, Cardoso I (2008); Transthyretin binding to A-Beta peptide--impact on A-Beta fibrillogenesis and toxicity. FEBS Lett. 582(6):936-42.

Crozier A (2009);Dietary phenolics, absorption, mammalian and microbial metabolism and colonic health, Mol Nutr Food Res. 53 Suppl 1:S5-6.

Crozier A, Borges G, and Ryan D (2010); The glass that cheers: phenolic and polyphenolic constituents and the beneficial effects of moderate red wine consumption, Biochemist 32: 4–9.

Dai Q, Borenstein AR, Wu Y, Jackson JC, Larson EB (2006); Fruit and vegetable juices and Alzheimer's disease: The Kame Project, Am. J. Med. 119, 751-759.

Datla KP, Christidou M, Widmer WW, Rooprai HK, Dexter DT (2001); Tissue distribution and neuroprotective effects of citrus flavonoid tangeretin in a rat model of Parkinson's disease, Neuroreport 12, 3871-3875.

Dedmon MM, Patel CN, Young GB, Pielak GJ (2002); F1gM gains structure in living cells, Proc. Natl. Acad. Sci. USA 99, 12681-12684.

Diociaiuti M, Polzi LZ, Valvo L, Malchiodi-Albedi F, Bombelli C, Gaudiano MC (2006); Calcitonin forms oligomeric pore-like structures in lipid membranes, Biophys J. 91(6):2275-81.

Dobson CM (2001); The structural basis of protein folding and links with human disease, Phil. trans. R. soc Lond. B. 356, 133-145.

Dobson CM (2003); Protein folding and misfolding, Nature 426, 884-891.

Dobson CM, Sali A and Karplus M (1998); Protein folding: a perspective from theory and experiment Angew. Chem. Int. Ed. Eng. 37, 868–893.

Duthie GG, Gardner PT, Kyle JA (2003); Review: Plant polyphenols: are they the new magic bullet?, Proc Nutr Soc. 62(3):599-603.

Ellis RJ (2001); Macromolecular crowding: an important but neglected aspect of the intracellular enviroment, Cun. Opin. Struct. Biol. 11, 114-119.

Engel, MF (2009); Membrane permeabilization by Islet amyloid polypeptide, Chem. Phys. Lipids 160 (1), 1–10.

Erlund I, Koli R, Alfthan G, Marniemi J, Puukka P, Mustonen P, Mattila P, Jula A (2008); Favorable effects of berry consumption on platelet function, blood pressure, and HDL cholesterol, Am. J. Clin. Nutr. 87, 323-331.

Esposito G, Michelutti R, Verdone G, Viglino P, Hernández H, Robinson CV, Amoresano A, Dal Piaz F, Monti M, Pucci P, Mangione P, Stoppini M, Merlini G, Ferri G, Bellotti V (2000); Removal of the N-terminal hexapeptide from human beta2-microglobulin facilitates protein aggregation and fibril formation, Protein Sci. 9: 831-45.

Esposito G, Ricagno S, Corazza A, Rennella E, Gümral D, Mimmi MC, Betto E, Pucillo CE, Fogolari F, Viglino P, Raimondi S, Giorgetti S, Bolognesi B, Merlini G, Stoppini M, Bolognesi M, Bellotti V (2008); The controlling roles of Trp60 and Trp95 in beta2-microglobulin function, folding and amyloid aggregation properties, J Mol Biol 378:887-97.

Estruch R, Ros E, Martínez-González MA (2013); Primary Prevention of Cardiovascular Disease with a Mediterranean Diet, N Engl J Med. 369(7):676-7.

Ferguson E, Parthasarathy S, Joseph J, and Kalyanaraman B(1998); Generation and initial characterization of a novel polyclonal antibody directed against homocysteine thiolactone-modified low density lipoprotein, J. Lipid Res. 39, 925–933.

Ferreira N, Saraiva MJ, Almeida MR (2011); Natural polyphenols inhibit different steps of the process of transthyretin (TTR) amyloid fibril formation, FEBS Lett. 585(15):2424-30.

Ferreira N, Saraiva MJ, Almeida MR (2012); Epigallocatechin-3-gallate as a potential therapeutic drug for TTR-related amyloidosis: "in vivo" evidence from FAP mice models, PLoS One.7(1):e29933.

Figueiras TS, Neves-Petersen MT, Petersen SB (2011); Activation energy of light induced isomerization of Resveratrol, J Fluoresc. 21(5):1897-906.

Foss TR, Wiseman RL, Kelly JW (2005); The pathway by which the tetrameric protein transthyretin dissociates, Biochemistry 44(47):15525-33.

Fowler DM, Koulov AV, Alory-Jost C, Marks MS, Balch WE, Kelly J (2006); Functional amyloid formation within mammalian tissue, PLoS Biol. 4(1):e6.

Fredrickson WR, F and S Group, Inc.(2000); Method and Composition for Antiviral Therapy with Olive Leaves, U.S. Patent. 6: 117,884.

Frid P, Anisimov SV, Popovic N (2007); Congo red and protein aggregation in neurodegenerative diseases, Brain Res Rev.53(1):135-60.

Furukawa K, Ohmi Y, Ohkawa Y, Tokuda N, Kondo Y, Tajima O, Furukawa K (2011); Regulatory mechanisms of nervous systems with glycosphingolipids, Neurochem. Res. 36 (9), 1578–1586.

Gales L, Almeida MR, Arsequell G, Valencia G, Saraiva MJ, Damas AM (2008); Iodination of salicylic acid improves its binding to Transthyretin, Biochim Biophys Acta, Proteins Proteomics 1784:512–517.

Gallai V, Caso V, Paciaroni M, Cardaioli G, Arning E, Bottiglieri T, Parnetti L (2001); Mild hyperhomocyst(e)inemia: a possible risk factor for cervical artery dissection, Stroke. 32(3):714-8.

Ganji V, Zhang X, Tangpricha V (2012); Serum 25-hydroxyvitamin D concentrations and prevalence estimates of hypovitaminosis D in the U.S. population based on assay-adjusted data, J Nutr. 142(3):498-507.

Gasperini RJ1, Hou X, Parkington H, Coleman H, Klaver DW, Vincent AJ, Foa LC, Small DH (2011); TRPM8 and Nav1.8 sodium channels are required for transthyretin-induced calcium influx in growth cones of small-diameter TrkA-positive sensory neurons, Mol Neurodegener. 6(1):19.

Gasset M, Mancheño JM, Laynez J, Lacadena J, Fernández-Ballester G, Martinez del Pozo A (1995); Thermal unfolding of the cytotoxin alpha-sarcin: phospholipid binding induces destabilization of the protein structure, Biochim Biophys Acta.1252(1):126-34.

Gazit E (2002) Mechanistic studies of the process of amyloid fibrils formation by the use of peptide fragments and analogues: implications for the design of fibrillization inhibitors, Curr Med Chem 9:1725–1735.

Gejyo F, Homma N, Suzuki Y, Arakawa M(1986); Serum levels of β2-microglobulin as a new form of amyloid protein in patients undergoing long-term hemodialysis, N Engl J Med 314:585-586.

Gellermann GP, Appel TR, Tannert A, Radestock A, Hortschansky P, Schroeckh V, Leisner C, Lütkepohl T, Shtrasburg S, Röcken C, Pras M, Linke RP, Diekmann S, Fändrich M (2005); Raft lipids as common components of human extracellular amyloid fibrils, Proc. Natl. Acad. Sci. USA 102 (18), 6297–6302.

Gharibyan AL, Zamotin V, Yanamandra K, Moskaleva OS, Margulis BA, Kostanyan IA, Morozova-Roche LA (2007); Lysozyme amyloid oligomers and fibrils induce cellular death via different apoptotic/necrotic pathways J Mol Biol 365(5):1337-49.

Giorgetti S, Raimondi S, Cassinelli S, Bucciantini M, Stefani M, Gregorini G, Albonico G, Moratti R, Montagna G, Stoppini M, Bellotti V (2009); β2-microglobulin is potentially neurotoxic, but the blood brain barrier is likely to protect the brain from its toxicity, Nephrol Dial Transplant. 24(4):1176-81.

Glenner GG (1980); Amyloid deposits and amyloidosis, The fl-fibrilloses. N Engl J Med 302: 1183-1232, 1333-1342

Gonzalez A, Quirante J, Nieto J, Almeida MR, Saraiva MJ, Planas A, Arsequell G, Valencia G (2009); Isatin derivatives, a novel class of transthyretin fibrillogenesis inhibitors, Bioorg Med Chem Lett 19:5270–5273.

Gorevic PD, Munoz PC, Casey TT et al (1986); Polymerization of intact beta-2 microglobulin in tissue causes amyloidosis in patients on chronic hemodialysis, Proc Natl Acad Sci USA 83:7908-7912.

Goyarzu P, Malin DH,, Lau FC, Taglialatela G, Moon WD, Jennings R, Moy E, Moy D, Lippold S, Shukitt-Hale B, Joseph JA (2004); Blueberry supplemented diet: Effects on object recognition memory and nuclear factor-kappa B levels in aged rats, Nutr. Neurosci. 7, 75-83.

Groenning M, Campos RI, Fagerberg C, Rasmussen AA, Eriksen UH, Powers ET, Hammarström P, (2011); Thermodynamic stability and denaturation kinetics of a benign natural transthyretin mutant identified in a Danish kindred, Amyloid.18(2):35-46.

Grossi C, Rigacci S, Ambrosini S, Ed Dami T, Luccarini I, Traini C, Failli P, Berti A, Casamenti F, Stefani M (2013); The polyphenol oleuropein aglycone protects TgCRND8 mice against Aβ plaque pathology. Submitted for publication.

Guijarro JI, Sunde M, Jones JA, Campbell ID, Dobson CM (1998) Amyloid fibril formation by an SH3 domain, Proc Natl Acad Sci U S A. 95(8): 4224-8.

Haass and Selkoe (2007); Soluble protein oligomers in neurodegeneration: lessons from the Alzheimer's amyloid beta-peptide, Nat Rev Mol Cell Biol. 8(2):101-12.

Hagen GA, Elliott WJ (1973); Transport of thyroid hormones in serum and cerebrospinal fluid, The Journal of Clinical Endocrinology and Metabolism 37(3):415-22.

Hakomori S, Handa K, Iwabuchi K, Yamamura S, Prinetti A (1998); New insights in glycosphingolipid function: "glycosignaling domain," a cell surface assembly of glycosphingolipids with signal transducer molecules, involved in cell adhesion coupled with signalling, Glycobiology. 8:xi–xix

Hamilton JA, Benson MD (2001); Transthyretin: a review from a structural perspective, Cellular and Molecular Life Sciences 58(10):1491-521.

Hammarström P, Wiseman RL, Powers ET, Kelly JW (2003); Prevention of transthyretin amyloid disease by changing protein misfolding energetics, Science 299 (5607):713–6.

Hardy J, Selkoe DJ (2002); Review: The amyloid hypothesis of Alzheimer's disease: progress and problems on the road to therapeutics. Science 297(5580):353-6.

Harper JD, Lieber CM, Lansbury PT Jr. (1997); Atomic force microscopic imaging of seeded fibril formation and fibril branching by the Alzheimer's disease amyloid-beta protein. Chem Biol. 4(12):951-9.

Hartl FU, Hayer-Hartl M (2002); Molecular chaperones in the cytosol: from nascent chain to folded protein, Science 295, 1852-1858.

Hashim YZ, Rowland IR, McGlynn H, Servili M, Selvaggini R, Taticchi A, Esposto S, Montedoro G, Kaisalo L, Wahala K, Gill CI (2008); Inhibitory effects of olive oil phenolics on invasion in human colon adenocarcinoma cells in vitro, Int. J. Cancer 122, 495-500.

Hirakura Y, Kagan BL (2001);Pore formation by beta-2-microglobulin: a mechanism for the pathogenesis of dialysis associated amyloidosis, Amyloid 8(2):94-100.

Hofmann MA, Lalla E, Lu Y, Gleason MR, Wolf BM, Tanji N, Ferran LJ Jr, Kohl B, Rao V, Kisiel W, Stern DM, Schmidt AM (2001); Hyperhomocysteinemia enhances vascular inflammation and accelerates atherosclerosis in a murine model, J Clin Invest. 107(6):675-83.

Holmgren G, Ericzon BG, Groth CG, Steen L, Suhr O, Andersen O, Wallin BG, Seymour A, Richardson S, Hawkins PN (1993); Clinical improvement and amyloid regression after liver transplantation in hereditary transthyretin amyloidosis, Lancet 341 8853: 1113–6.

Hou X, Mechler A, Martin LL, Aguilar MI, Small DH (2008); Cholesterol and anionic phospholipids increase the binding of amyloidogenic transthyretin to lipid membranes, Biochimica et Biophysica Acta 1778(1):198-205.

How PS, Cox R, Ellis JA, Spencer JPE (2007); The impact of plant-derived flavonoids on mood, memory and motor skills in UK adults, Proc. Nutr. Soc. 66, 87A.

Hurshman AR, White JT, Powers ET, Kelly JW (2004); Transthyretin aggregation under partially denaturing conditions is a downhill polymerization, Biochemistry 43(23):7365-81.

Hurst NP, Berg R van den, Disney A, Alcock M, Albertyn L, Green M, Pascoe V (1989); Dialysis related arthropathy: a survey of 95 patients receiving chronic haemodialysis with special reference to β2-microglobulin related amyloidosis, Ann Rheum Dis 48:409-420.

Iconomidou VA, Chryssikos GD, Gionis V, Galanis AS, Cordopatis P, Hoenger A, Hamodrakas SJ (2006); Amyloid fibril formation propensity is inherent into the hexapeptide tandemly repeating sequence of the central domain of silkmoth chorion proteins of the A-family, J Struct Biol. 156: 480-8.

Izumoto S, Younger D, Hays AP, Martone RL, Smith RT, Herbert J (1992); Familial amyloidotic polyneuropathy presenting with carpal tunnel syndrome and a new transthyretin mutation, asparagine 70, Neurology. 42(11):2094-102.

Jacobson DR, Khan NS, Collé R, Fitzgerald R, Laureano-Pérez L, Bai Y, Dmochowski IJ (2011); Measurement of radon and xenon binding to a cryptophane molecular host, Proc Natl Acad Sci U S A. 2011 Jul 5;108(27):10969-73.

Jacobson DR, McFarlin DE, Kane I, Buxbaum JN (1992); Transthyretin Pro55, a variant associated with early-onset, aggressive, diffuse amyloidosis with cardiac and neurologic involvement, Hum Genet. 89(3):353-6.

Jacobson DR, Pastore RD, Yaghoubian R, Kane I, Gallo G, Buck FS, Buxbaum JN (1997);Variant-sequence transthyretin (isoleucine 122) in late-onset cardiac amyloidosis in black Americans, N Engl J Med.336(7):466-73.

Jiang X, Smith CS, Petrassi HM, Hammarstrom P, White JT, Sacchettini, JC, Kelly JW (2001); An engineered transthyretin monomer that is nonamyloidogenic, unless it is partially denatured, Biochemistry 40:11442–11452.

Johnson SM, Connelly S, Fearns C, Powers ET, Kelly JW (2012); The transthyretin amyloidoses: from delineating the molecular mechanism of aggregation linked to pathology to a regulatory-agency-approved drug, Journal of Molecular Biology. 421(2-3):185-203.

Johnson SM, Connelly S, Wilson IA, Kelly JW (2008); Biochemical and structural evaluation of highly selective 2-arylbenzoxazole-based transthyretin amyloidogenesis inhibitors, J Med Chem 51:260–270.

Johnson SM, Connelly S, Wilson IA, Kelly JW (2008); Toward optimization of the linker substructure common to transthyretin amyloidogenesis inhibitors using biochemical and structural studies, J Med Chem 51:6348–6358.

Johnson SM, Connelly S, Wilson IA, Kelly JW (2009); Toward optimization of the secondary substructure common to transthyretin amyloidogenesis. Inhibitors using biochemical and structural studies, J Med Chem 52:1115–1125.

Johnson SM, Petrassi HM, Palaninathan SK, Mohamedmohaideen NN, Purkey HE, Nichols C, Chiang KP, Walkup T, Sacchettini JC, Sharpless KB, Kelly JW (2005); Bisaryloxime ethers as potent inhibitors of transthyretin amyloid fibril formation, J Med Chem 48:1576–1587.

Johnson SM, Wiseman RL, Sekijima Y, Green NS, Adamski-Werner SL, Kelly JW (2005); Native state kinetic stabilization as a strategy to ameliorate protein misfolding diseases: a focus on the transthyretin amyloidosis, Acc Chem Res 38:911–921.

Jones S, Smith DP, Radford SE (2003); Role of the N and C-terminal strands of beta 2-microglobulin in amyloid formation at neutral pH, J Mol Biol. 330(5):935-41.

Joseph JA, Shukitt-Hale B, Denisova NA, Prior RL, Cao G, Martin A, Taglialatela G, Bickford PC (1998); Long-term dietary strawberry, spinach, or vitamin E supplementation retards the onset of age-related neuronal signal-transduction and cognitive behavioral deficits, J. Neurosci. 18, 8047-8055.

Jukes TH (1989); The prevention and conquest of scurvy, beri-beri, and pellagra, Prev Med 18:877 – 83.

Kabat EA, Moore DH, Landow H (1942); An electrophoretic study of the protein components in cerebrospinal fluid and their relationship to the serum proteins, Journal of Clinical Investigation 21(5):571-7.

Kaida K, Ariga T, Yu RK (2009); Review: Antiganglioside antibodies and their pathophysiological effects on Guillain-Barre syndrome and related disorders, Glycobiology 19:676–692.

Kalanj-Bognar S (2006); Ganglioside catabolism is altered in fibroblasts and leukocytes from Alzheimer's disease patients, Neurobiol. Aging. 27: 1354–1356.

Kawahara M, Kuroda Y, Arispe N, Rojas E (2000); Alzheimer's beta-amyloid, human islet amylin, and prion protein fragment evoke intracellular free calcium elevations by a common mechanism in a hypothalamic GnRH neuronal cell line, J Biol Chem. 275(19):14077-83.

Kayed R, Head E, Sarsoza F, Saing T, Cotman CW, Necula M, Margol L, Wu J, Breydo L, Thompson JL, Rasool S, Gurlo T, Butler P, Glabe CG (2007); Fibril specific, conformation dependent antibodies recognize a generic epitope common to amyloid fibrils and fibrillar oligomers that is absent in prefibrillar oligomers, Mol Neurodegener. 2:18.

Kayed R, Head E, Thompson JL, McIntire TM, Milton SC, Cotman CW, Glabe CG (2003); Common structure of soluble amyloid oligomers implies common mechanism of pathogenesis, Science 300(5618):486-9.

Keetch CA, Bromley EH, McCammon MG, Wang N, Christodoulou J, Robinson CV (2005); L55P transthyretin accelerates subunit exchange and leads to rapid formation of hybrid tetramers, J Biol Chem. 280(50):41667-74.

Keys A. (1997); Coronary heart disease in seven countries, Nutrition 13(3):250-2.

Khan N, Afaq F, Saleem M, Ahmad N, Mukhtar H (2006); Targeting multiple signaling pathways by green tea polyphenol (−)-epigallocatechin-3-gallate, Cancer Res. 66,2500-2505.

Kingsbury JS, Laue TM, Klimtchuk ES, Théberge R, Costello CE, Connors LH (2008); The modulation of transthyretin tetramer stability by cysteine 10 adducts and the drug diflunisal. Direct analysis by fluorescence-detected analytical ultracentrifugation, J Biol Chem.283(18):11887-96.

Kishikawa M, Nakanishi T, Miyazaki A, Shimizu A (1999); Enhanced amyloidogenicity of sulfonated transthyretin in vitro, a hypothetical etiology of senile amyloidosis, Amyloid Int. J. Exp. Clin. Invest. 6, 183-186.

Kisilevsky R, Snow AD, Subrahmanyan L, Boudreau L, Tan R (1986); What factors are necessary for the induction of AA amyloidosis?, In: Marrink L Rijswijk MH van (eds) Amy-loidosis. Nijhoff, Dordrecht, pp 301-310.

Klabunde T, Petrassi HM, Oza VB, Raman P, Kelly JW, Sacchettini JC (2000); Rational design of potent human transthyretin amyloid disease inhibitors, Nat Struct Biol. 2000 Apr;7(4):312-21.

Kostomoiri M, Fragkouli A, Sagnou M, Skaltsounis LA, Pelecanou M, Tsilibary EC, Szinia AK (2013); Oleuropein, an anti-oxidant polyphenol constituent of olive promotes α-secretase cleavage of the amyloid precursor protein (AβPP), Cell. Mol. Neurobiol. 33, 147–154.

Kourie JI (2001); Mechanisms of amyloid beta protein-induced modification in ion transport systems: implications for neurodegenerative diseases, Cell. Mol. Neurobiol. 21, 173-213.

Kourie JI, Henry CL (2002), Review: Ion channel formation and membrane-linked pathologies of misfolded hydrophobic proteins: the role of dangerous unchaperoned molecules, Clin Exp Pharmacol Physiol. 29(9):741-53.

Kourie JI, Shorthouse AA (2000); Properties of cytotoxic peptide-formed ion channels, Am J Physiol Cell Physiol. 2000 Jun;278(6):C1063-87.

Krikorian R, Shidler MD, Nash TA, Kalt W, Vinqvist-Tymchuk MR, Shukitt-Hale B, Joseph, JA (2010); Blueberry supplementation improves memory in older adults, J. Agric. Food Chem. 58, 3996-4000.

Kuriyama S, Shimazu T, Ohmori K, Kikuchi N, Nakaya, N, Nishino Y, Tsubono Y, Tsuji I (2006); Green tea consumption and mortality due to cardiovascular disease, cancer, and all ca uses in Japan: The Ohsaki study, JAMA 296, 1255-1265.

Lai Z, Colón W, Kelly JW (1996); The Acid-Mediated Denaturation Pathway of Transthyretin Yields a conformational intermediate that can self-assemble into amyloid, Biochemistry 35: 6470-6482.

Lancet D, Parham P, Strominger JL (1979); Heavy chain of HLA-A and HLA-B antigens is conformationally labile: a possible role for β2-microglobulin, Proc Natl Acad Sci USA 76: 3844- 3848.

Landete JM. Ellagitannins, ellagic acid and their derived metabolites: a review about source, Larrosa M, Garcı´a-Conesa MT, Espin JC, and Toma´s-Barbera´n FA. Bioavailability and metabolism of ellagic acid and ellagitannins. In: Flavonoids and Related Compounds: Bioavailability and Function, edited by Spencer JPE and Crozier A. Oxidative Stress and Disease, Vol. 30, edited by Packer L and Cadenas H. Boca Raton, FL: CRC Press, 2012, pp. 183–199metabolism, functions and health. Food Res Int 44: 1150–1160, 2011

Langcake P and Pryce RJ (1977); A new class of phytoalexins from grapevines, Experientia 33: 151–152.

Lansbury PT, Lashuel HA (2006); Review: A century-old debate on protein aggregation and neurodegeneration enters the clinic, Nature 443, 774-9.

Lashuel HA, Hartley D, Petre BM, Walz T, Lansbury PT Jr.(2002); Neurodegenerative disease: amyloid pores from pathogenic mutations, Nature 418(6895):291.

Lashuel HA, Lai Z, Kelly JW (1998); Characterization of the transthyretin acid denaturation pathways by analytical ultracentrifugation: implications for wild-type, V30M, and L55P amyloid fibril formation, Biochemistry.37(51):17851-64.

Lashuel HA, Wurth C, Woo L, Kelly JW (1999); The most pathogenic transthyretin variant, L55P, forms amyloid fibrils under acidic conditions and protofilaments under physiological conditions, Biochemistry. 38(41):13560-73.

Laurine E, Grégoire C, Fändrich M, Engemann S, Marchal S, Thion L, Mohr M, Monsarrat B, Michel B, Dobson CM, Wanker E, Erard M, Verdier JM (2003); Lithostathine quadruple-helical filaments form proteinase K-resistant deposits in Creutzfeldt-Jakob disease, J Biol Chem. 278(51):51770-8.

Layfield R, Alban A, Mayer RJ, Lowe J (2001); The ubiquitin protein catabolic disorders, Neurophatal Appl. NeuroBiol. 27, 171-179.

Leclercq C and Ferro-Luzzi A (1991); Total and domestic consumption of salt and their determinants in three regions of Italy, European Journal of Clinical Nutrition 45 (3): 151–9.

Ledeen RW, Wu G (2008); Nuclear sphingolipids: metabolism and signalling, J. Lipid Res. 2008; 49:1176-1186.

Lei M, Yang M, Huo S (2004); Intrinsic versus mutation dependent instability/flexibility: a comparative analysis of the structure and dynamics of wild-type transthyretin and its pathogenic variants, J Struct Biol.148(2):153-68.

Leikert JF, Rathel TR, Wohlfart P, Cheynier V, Vollmar AM, Dirsch VM (2002); Red wine polyphenols enhance endothelial nitric oxide synthase expression and subsequent nitric oxide release from endothelial cells, Circulation 106, 1614-1617.

Letenneur L, Proust-Lima C, Le GA, Dartigues JF, Barberger-Gateau P (2007); Flavonoid intake and cognitive decline over a 10-year period, Am. J. Epidemiol. 165, 1364-1371.

LeVine H III (1993); Thioflavine T interaction with syntetic Alzheimer's disease beta-amyloid peptides: detection of amyloid aggregation in solution, Protein Sci. 2: 404-410.

Levinthal C (1968); Are there pathways for protein folding?, J. Chem. Phys.85, 44-45.

Li X, Masliah E, Reixach N, Buxbaum JN (2011); Neuronal production of transthyretin in human and murine Alzheimer's disease: is it protective?, J Neurosci. 2011 Aug 31;31(35):12483-90.

Lillycrop KA, Burdge GC (2012); Epigenetic mechanisms linking early nutrition to long term health, Best Pract Res Clin Endocrinol Metab 26:667 – 76.

Lim A, Prokaeva T, McComb ME, Connors LH, Skinner M, Costello CE (2003); Identification of S-sulfonation and S-thiolation of a novel transthyretin Phe33Cys variant from a patient diagnosed with familial transthyretin amyloidosis, Protein Science. 12(8):1775-85.

Lin YM, Raffen R, Zhou Y, Cassidy CS, Flavin MT, Stevens FJ (2001); Amyloid fibril formation in microwell plates for screening of inhibitors, Amyloid 8(3):182-93.

Link CD (1995); Expression of human beta-amyloid peptide in transgenic Caenorhabditis elegans, Proc Natl Acad Sci USA 92: 9368–9372.

Linke RP, Bommer J, Ritz E, Waldherr R, Eulitz M (1986); Amyloid kidney stones of uremic patients consist of beta2-microglobulin fragments. Biochem Biophys Res Commun 136:665-671.

Litvinovich SV, Brew SA, Aota S, Akiyama SK, Haudenschild C, Ingham KC (1998); Formation of amyloid-like fibrils by self-association of a partially unfolded fibronectin type III module, J Mol Biol. 280(2): 245-58.

Liu G, Nellaiappan K, and Kagan HM (1997); Irreversibleinhibition of lysyl oxidase by homocysteine thiolactone and itsselenium and oxygen analogues, J. Biol. Chem. 272, 32370–32377.

Llor X, Pons E, Roca A, Alvarez M, Mane J, Fernandez-Banares F, Gassull MA (2003); The effects of fish oil, olive oil, oleic acid and linoleic acid on colorectal neoplastic processes. Clin. Nutr. 2, 71-7.

Lue LF, Kuo YM, Roher AE, Brachova L, Shen Y, Sue L, Beach T, Kurth JH, Rydel RE, Rogers J (1999); Soluble amyloid beta peptide concentration as a predictor of synaptic change in Alzheimer's disease, Am. J. Pathol. 155, 853-62.

Lührs T, Ritter C, Adrian M, Riek-Loher D, Bohrmann B, Döbeli H, Schubert D, Riek R (2005); 3D structure of Alzheimer's amyloid-β (1–42) fibrils, Proc. Natl. Acad. Sci.U.S.A. 102, 17342–17347.

Macario AJL, De Macario EC (2001); Sick chaperones and agenig: a perspective agening, Res. Rev. 1, 295-311.

Mackay JP, Matthews JM, Winefield RD, Mackay LG, Haverkamp RG, Templeton MD (2001); The hydrophobin EAS is largely unstructured in solution and functionsby forming amyloid-like structures, Structure 9, 83–91.

Maia F, Almeida Mdo R, Gales L, Kijjoa A, Pinto MM, Saraiva MJ, Damas AM (2005); The binding of xanthone derivatives to Transthyretin, Biochem Pharmacol 70:1861–186.

Majors AK, Sengupta S, Willard B, Kinter MT, Pyeritz RE, Jacobsen DW (2002); Homocysteine binds to human plasma fibronectin and inhibits its interaction with fibrin, Makarov DE and Plaxco KW (2003); The topomer search model: a simple, quantitative theory of two state protein folding kinetics. Protein Sci. 12, 17–26.

Makin OS, Serpell LC (2005) Structures for amyloid fibrils, FEBS J. 272(23): 5950-61.

Mandel SA, Avramovich-Tirosh Y, Reznichenko L, Zheng H, Weinreb O, Amit T, Youdim MB (2005); Multifunctional activities of green tea catechins in neuroprotection. Modulation of cell survival genes, iron-dependent oxidative stress and PKC signaling pathway, Neurosignals.14(1-2):46-60.

Mangione P, Sunde M, Giorgetti S, Stoppini M, Esposito G, Gianelli L, Obici L, Asti L, Andreola A, Viglino P, Merlini G, Bellotti V (2001); Amyloid fibrils derived from the apolipoprotein A1 Leu174Ser variant contain elements of ordered helical structure, Protein Sci 10:187-99.

Mattson MP, Begley JG, Mark RJ, Furukawa K (1997); Abeta25-35 induces rapid lysis of red blood cells: contrast with Abeta1-42 and examination of underlying mechanisms, Brain Res. 77, 147-53.

Maury CPJ (1988); Amyloidosis Scand J Rheum [suppl 74]: 33 -39.

Maury CPJ, Helve T, Sj6blom C (1982) ; Serum β2-microglobulin, sialic acid, and C-reactive protein in systemic lupus erythematosus, Rheumatol Int 2:145-149.

Mercer LD1, Kelly BL, Horne MK, Beart PM (2005); Dietary polyphenols protect dopamine neurons from oxidative insults and apoptosis: investigations in primary rat mesencephalic cultures, Biochem Pharmacol. 69(2):339-45.

Milhavet O, Lehmann S (2002); Review: Oxidative stress and the prion protein intransmissible spongiform encephalopathy, Brain Res. 38,328-339.

Miller SR, Sekijima Y, Kelly JW (2004); Native state stabilization by NSAIDs inhibits transthyretin amyloidogenesis from the most common familial disease variants, Lab Invest 84:545–552.

Mink PJ, Scrafford CG, Barraj LM, Harnack L, Hong CP, Nettleton JA, Jacobs, DR Jr (2007); Flavonoid intake and cardiovascular disease mortality: A prospective study in postmenopausal women, Am. J. Clin. Nutr. 85, 895-909.

Mita S, Maeda S, Shimada K, Araki S (1984); Cloning and sequence analysis of cDNA for human prealbumin, Biochemica et Biophysica Research Communications 124(2):558-64.

Monaco HL, Rizzi M, Coda A (1995); Structure of a complex of two plasma proteins: transthyretin and retinol-binding protein, Science 268(5213):1039-41.

Mori T, Rezai-Zadeh K, Koyama N, Arendash GW, Yamaguchi H, Kakuda N, Horikoshi-Sakuraba Y, Tan J, Town T (2012); Tannic acid is a natural beta-secretase inhibitor that prevents cognitive impairment and mitigates Alzheimer-like pathology in transgenic mice, J BiolChem 287: 6912–6927.

Morris MC, Evans DA, Tangney CC, Bienias JL, Wilson RS (2006); Associations of vegetable and fruit consumption with age-related cognitive change, Neurology 67, 1370-1376.

Mosmann T (1983); Rapid colorimetric assay for cellular growth and survival: application to proliferation and cytotoxicity assays, J Immunol Methods. 65(1-2):55-63.

Munishkina LA and Fink AL (2007); Fluorescence as a method to reveal structures and membrane-interactions of amyloidogenic proteins, Biochim. Biophys. Acta. 1768:1862-1885.

Murakami T, Yi S, Maeda S, Tashiro F, Yamamura K, Takahashi K, Shimada K, Araki S (1992); Effect of serum amyloid P component level on transthyretin-derived amyloid deposition in a transgenic mouse model of familial amyloidotic polyneuropathy, American Journal of Pathology141(2):451-6.

Mutoh T, Hirabayashi Y, Mihara T, Ueda M, Koga H, Ueda A, Kokura T, Yamamoto H (2006); Role of glycosphingolipids and therapeutic perspectives on Alzheimer's disease, CNS Neurol. Disord. Drug Targets. 5: 375–380.

Nakanishi T, Yoshioka M, Moriuchi K, Yamamoto D, Tsuji M, Takubo T. S-sulfonation of transthyretin is an important trigger step in the formation of transthyretin-related amyloid fibril. Biochimica et Biophysica Acta. 2010 ;1804(7):1449-56.

Natalello A, Ami D, Doglia SM (2012); Fourier transform infrared spectroscopy of intrinsically disordered proteins: measurement procedures and data analyses, Methods Mol Biol.895:229-44.

Ngoungoure VL, Schluesener J, Moundipa PF, Schluesener H (2014); Natural polyphenols binding to amyloid: A broad class of compounds to treat different human amyloid diseases, Mol Nutr Food Res. doi: 10.1002/mnfr.201400290.

NIH Office of Dietary Supplements (2012) Dietary supplements: what you need to know NIH Office of Dietary Supplements Web site; Gold LS.

Nilson MR (2004); Techniques to study amyloid fibril formaions in vitro, Methods 34, 151-160.

Novitskaya V, Makarava N, Bellon A, Bocharova OV, Bronstein IB, Williamson RA, Baskakov IV (2006); Probing the conformation of the prion protein within a single amyloid fibril using a novel immunoconformational assay, J Biol Chem 281(22):15536-45.

Owen RW, Giacosa, A, Hull WE, Haubner R, Spiegelhalder B, Bartsch H (2000); The antioxidant/anticancer potential of phenolic compounds isolated from olive oil, Eur. J. Cancer 36, 1235-1247.

Owen RW, Giacosa A, Hull WE, Haubner R, Würtele G, Spiegelhalder B, Bartsch H (2000); Olive oil consumption and health: the possible role of antioxidants, Lancet Oncol. 1: 107–112.

Ozawa D, Hasegawa K, Lee YH, Sakurai K, Yanagi K, Ookoshi T, Goto Y, Naiki H (2011); Inhibition of β2 -microglobulin amyloid fibril formation by β2-macroglobulin, J. Biol. Chem. 286, 9668–9676.

Palaninathan SK, Mohamedmohaideen NN, Orlandini E, Ortore G, Nencetti S, Lapucci A, Rossello A, Freundlich JS, Sacchettini JC (2009); Novel transthyretin amyloid fibril formation inhibitors: synthesis, biological evaluation, and X-ray structural analysis, PLoS One 4:e6290.

Papamichael C, Karatzis E, Karatzi K, Aznaouridis K, Papaioannou T, Protogerou A, Stamatelopoulos K, Zampelas A, Lekakis J, Mavrikakis M (2004); Red wine's antioxidants counteract acute endothelial dysfunction caused by cigarette smoking in healthy nonsmokers, Am. Heart J. 147, E5.

Papatheodorou L, Weiss N (2007); Vascular oxidant stress and inflammation in hyperhomocysteinemia, Antioxid Redox Signal. 9(11):1941-58.

Pedersen LO, Hansen AS, Olsen AC, Gerwien J, Nissen MH, Buus S (1994); The interaction between β2-microglobulin (β2m) and purified class-I major histocompatibility (MHC) antigen, Scand J Immunol 39:64–72.

Pernber Z, Blennow K, Bogdanovic N, Månsson JE, Blomqvist M (2012); Altered distribution of the Gangliosides GM1 and GM2 in Alzheimer's disease, Dement. Geriatr. Cogn. Disord. 33 (2–3), 174–188.

Peterson PA, Cunningham BA, Berggård I, Edelman GM (1972); β2-microglobulin-a free immunoglobulin domain, Proc Natl Acad Sci U S A.69, 1697-1972.

Petkova AT, Leapman RD, Guo Z, Yau WM, Mattson MP, Tycko R (2005); Self-propagating, molecular-level polymorphism in Alzheimer's beta-amyloid fibrils. Science 307(5707):262-5.

Petrassi HM, Johnson SM, Purkey HE, Chiang KP, Walkup T, Jiang X, Powers ET, Kelly JW (2005); Potent and selective structure-based dibenzofuran inhibitors of transthyretin amyloidogenesis: kinetic stabilization of the native state, J Am Chem Soc 127:6662–6671.

Petrassi HM, Klabunde T, Sacchettini J, Kelly JW (2000); Structure-based design of N-phenyl phenoxazine transthyretin amyloid fibril inhibitors, J Am Chem Soc 122:2178-2192.

Piazza R, Pierno M, Iacopini S, Mangione P, Esposito G, Bellotti V (2006); Micro-heterogeneity and aggregation in Beta2-microglobulin solutions: affects of temperature, pH, and conformational variant addition, Eur Biophys J 35: 439-445.

Pitt J, Roth W, Lacor P, Smith AB III, Blankenship M, Velasco P, De Felice F, Breslin P, Klein WL (2009); Alzheimer's-associated Aβ oligomers show altered structure, immunoreactivity and synaptotoxicity with low doses of oleocanthal, Toxicol. Appl. Pharmacol. 240, 189–197.

Platt GW, McParland VJ, Kalverda AP, Homans SW, Radford SE (2005); Dynamics in the unfolded state of beta2-microglobulin studied by NMR, J Mol Biol 346:279–294.

Poirier MA, Li H, Macosko J, Cai S, Amzel M, Ross CA (2002);Huntingtin spheroids and protofibrils as precursors in polyglutamine fibrilization J Biol Chem 277(43):41032-7.

Pokrzywa M, Dacklin I, Hultmark D, Lundgren E (2007); Misfolded transthyretin causes behavioral changes in a Drosophila model for transthyretin-associated amyloidosis, Eur J Neurosci.26(4):913-24.

Porat Y, Abramowitz A, Gazit E (2006); Inhibition of amyloid fibril formation by polyphenols:structural similarity and aromatic interactions as a common inhibition mechanism, Chem Biol Drug Des 67, 27-37.

Quintas A, Vaz DC, Cardoso I, Saraiva MJ, Brito RM (2001); Tetramer dissociation and monomer partial unfolding precedes protofibril formation in amyloidogenic transthyretin variants, J Biol Chem. 276(29):27207-13.

Ramirez MR, Izquierdo I, do Carmo Bassols Raseira M, Zuanazzi JA, Barros D, Henriques AT (2005); Effect of lyophilised Vaccinium berries on memory, anxiety and locomotion in adult rats, Pharmacol. Res. 52, 457-4.

Rashid SA, Axon ATR, Bullen AW, Cooper EH (1981) ; Serum-β2-microglobulin in hepato-biliary diseases, Clin Chim Acta 114:83-91.

Razavi H, Palaninathan SK, Powers ET, Wiseman RL, Purkey HE, Mohamedmohaideen NN, Deechongkit S, Chiang KP, Dendle MT, Sacchettini JC, Kelly JW (2003); Benzoxazoles as transthyretin amyloid fibril inhibitors: synthesis, evaluation, and mechanism of action, Angew. Chem. Int. Ed. Engl. 42 (24): 2758–61.

Refsum H, Helland S, Ueland PM (1985) Radioenzymic determination of homocysteine in plasma and urine, Clin. Chem. 31, 624-628.

Renner M, Lacor PN, Velasco PT, Xu J, Contractor A, Klein WL, Triller A (2010); Deleterious effects of amyloid beta oligomers acting as an extracellular scaffold for mGluR5, Neuron 66 (5), 739–754.

Rigacci S, Guidotti V, Bucciantini M, Parri M, Nediani C, Cerbai E, Stefani M, Berti A (2010); Oleuropein aglycon prevents cytotoxic amyloid aggregation of human amylin, J Nutr Biochem 21: 726–735.

Rigacci, S, Guidotti V, Bucciantini M, Nichino D, Relini A, Berti A, Stefani M (2011); Aβ(1–42) aggregates into non-toxic amyloid assemblies in the presence of the natural polyphenol oleuropein aglycon. Curr. Alzheimer Res. 8, 841–852.

Rigacci, S, Guidotti V, Bucciantini M, Parri M, Nediani C, Cerbai E, Stefani M, Berti A (2010); Oleuropein aglycon prevents cytotoxic amyloid aggregation of human amylin, J. Nutr. Biochem. 21, 726–735.

Roberts RA, Laskin DL, Smith CV, Robertson FM, Allen EM, Doorn JA, Slikker W (2009); Nitrative and oxidative stress in toxicology and disease, Toxicol Sci 112:4 – 16.

Ruscin JM, Page RL 2nd, Valuck RJ (2002); Vitamin B(12) deficiency associated with histamine(2)-receptor antagonists and a proton-pump inhibitor. Ann Pharmacother. 36(5):812-6.

Rushwort JV and Hopoper NM (2010) Lipid rafts: linking Alzheimer's amyloid-β production, aggregation and toxicity at neuronal membranes. Int. J. Alzheimers Dis. 2011, 6030-52.

Sakuta H, Suzuki T (2005); Alcohol consumption and plasma homocysteine. Alcohol. 37(2):73-7.

Salmona M, Forloni G, Diomede L, Algeri M, De Gioia L, Angeretti N, Giaccone G, Tagliavini F, Bugiani O (1997); A neurotoxic and gliotrophic fragment of the prion protein increases plasma membrane microviscosity, Neurobiol Dis.4(1):47-57.

Samieri C, Sun Q, Townsend MK, Chiuve SE, Okereke OI, Willett WC, Stampfer M, Grodstein F (2013); The association between dietary patterns at midlife and health in aging: an observational study, Ann Intern Med 159 (9): 584–91.

Saper MA, Bjorkman PJ, Wiley DC (1991);Refined structure of the human histocompatibility antigen HLA-A2 at 2.6 A resolution. J Mol Biol. 1991 May 20;219(2):277-319.

Saraiva MJ, Birken S, Costa PP, Goodman DS (1984); Amyloid fibril protein in familial amyloidotic polyneuropathy, Portuguese type. Definition of molecular abnormality in transthyretin (prealbumin), J Clin Invest.74(1):104-19.

Sartiani L, Bochet P, Cerbai E, Mugelli A, Fischmeister R (2002); Functional expression of the hyperpolarization-activated, non-selective cation current I(f) in immortalized HL-1 cardiomyocytes, J Physiol. 545(Pt 1):81-92.

Scarmeas N, Luchsinger JA, Mayeux R, Stern Y (2006); Mediterranean diet and Alzheimer disease mortality, Neurology. 2006-11-21.

Schormann N, Murrell JR, Benson MD (1998); Tertiary structures of amyloidogenic and non-amyloidogenic transthyretin variants: new model for amyloid fibril formation, Amyloid. 5(3):175-87.

Schramm DD, Karim M, Schrader HR, Holt RR, Kirkpatrick NJ, Polagruto JA, Ensunsa, JL, Schmitz HH, Keen CL (2003); Food effects on the absorption and pharmacokinetics of cocoa flavanols, Life Sci. 73, 857-869.

Schwarz A, Keller F, Seyfert S, Poll W, Molzahn M, Distler A (1984); Carpal tunnel syndrome: a major complication in longterm haemodialysis patients, Clin Nephrol 22:133-137.

Schwarzman AL, Gregori L, Vitek MP, Lyubski S, Strittmatter WJ, Enghilde JJ, Bhasin R, Silverman J, Weisgraber KH, Coyle PK, et al. (1994); Transthyretin sequesters amyloid beta protein and prevents amyloid formation Proc. Natl. Acad. Sci. U. S. A., 91:8368–8372.

Sebastião MP, Saraiva MJ, Damas AM (1998); The crystal structure of amyloidogenic Leu55 --> Pro transthyretin variant reveals a possible pathway for transthyretin polymerization into amyloid fibrils, J Biol Chem.273(38):24715-22.

Selhub J, Jacques PF, Rosenberg IH, Rogers G, Bowman BA, Gunter EW, Wright JD, Johnson CL (1999); Serum total homocysteine concentrations in the third National Health and Nutrition Examination Survey (1991-1994): population reference ranges and contribution of vitamin status to high serum concentrations. Ann Intern Med. 131(5):331-9.

Sengupta S, Chen H, Togawa T, DiBello PM, Majors AK, Büdy B, Ketterer ME, Jacobsen DW (2001); Relative roles of albumin and ceruloplasmin in the formation of homocystine, homocysteine-cysteine-mixed disulfide, and cystine in circulation, J. Biol. Chem. 276, 30111-30117.

Serpell LC, Sunde M, Benson MD, Tennet GA, Pepys MB and Fraser PE (2000), The protofilament substructure of amyloid fibrils, J. Mol. Biol. 300:1033-1039.

Serpell LC, Sunde M, Fraser PE, Luther PK, Morris EP, Sangren O, Lundgren E, Blake CC (1995); Examination of the structure of the transthyretin amyloid fibril by image reconstruction from electron micrographs, J Mol Biol.254(2):113-8.

Sgarbossa A (2012); Natural Biomolecules and Protein Aggregation: Emerging Strategies against Amyloidogenesis, Int J Mol Sci 13, 17121-17137.

Silva JL, Cordeiro Y, Foguel D (2006); Protein folding and aggregation: two sides of the, same coin in the condensation of proteins revealed by pressure studies, Biochimica et Biophysica Acta. 1764(3):443-51.

Simons K, Toomre D (2000); Lipid rafts and signal transduction, Nat. Rev. Mol. Cell Biol. 1:31–39.

Slone TH, Ranking MS (1999) Possible toxic hazards of dietary supplements compared to other natural and synthetic substances. Testimony to the FDA, Docket No. 99N-1174.

Smith DP1, Jones S, Serpell LC, Sunde M, Radford SE (2003); A systematic investigation into the effect of protein destabilisation on beta 2-microglobulin amyloid formation, J Mol Biol. 330(5):943-54.

Sofi F, Cesari F, Abbate R, Gensini GF, Casini A (2008); Adherence to Mediterranean diet and health status: meta-analysis, BMJ (Clinical research ed.) 337: a1344.

Soler-Rivas C, Espin JC, Wichers HJ (2000); Oleuropein and related compounds, J Sci Food Agric 80: 1013–1023.

Souillac PO, Uversky VN, Fink AL (2003); Structural transformations of oligomeric intermediates in the fibrillation of the immunoglobulin light chain LEN, Biochemistry. 42(26):8094-104.

Sousa MM, Saraiva MJ (2001); Internalization of transthyretin. Evidence of a novel yet unidentified receptor-associated protein (RAP)-sensitive receptor, J Biol Chem. 276(17):14420-5.
Spencer JP (2008); Food for thought: The role of dietary flavonoids in enhancing human memory, learning and neuro-cognitive performance. Proc. Nutr. Soc. 67, 238-252.

Stefani M, Dobson CM (2003); Protein aggregation and aggregate toxicity: new insights into protein folding, misfolding diseases and biological evolution, J. Mol. Med. 81, 678-699.

Stefani M (2004); Protein misfolding and aggregation: new examples in medicine and biology of the dark side of the protein world, Biochim Biophys Acta. 1739: 5-25.

Stefani M. (2008); Protein folding and misfolding on surfaces, Int. J. Mol. Sci. 9,2515-2542.

Suhr, OB, Svendsen IH, Ohlsson P, Lendoire J, Trigo P, Tashima K, Ranlov PJ, Ando Y (1999); Impact of age and amyloidosis on thiol conjugation of transthyretin in hereditary transthyretin amyloidosis, Int. J. Exp. Clin. Invest. 6, 187-191.

Sunde M, Serpell LC, Bartlam M, Fraser PE, Pepys MB, Blake CC (1997); Common core structure of amyloid fibrils by synchrotron X-ray diffraction, J Mol Biol. 273(3): 729-39.

Suzuki Y (2005); Sialobiology of influenza: molecular mechanism of host range variation of influenza viruses, Biol. Pharm. Bull. 28:399–408.

Tagliavini F, Forloni G, D'Ursi P, Bugiani O, Salmona M (2001); Studies on peptide fragments of prion proteins, Adv Protein Chem.57:171-201.

Tallmadge DH, Huebner JS, Borkman RF (1989); Acrylamide quenching of tryptophan photochemistry and photophysics, Photochem Photobiol. 49(4):381-6.

Tamboli IY, Prager K, Barth E, Heneka M, Sandhoff K, Walter J (2005); Inhibition of glycosphingolipid biosynthesis reduces secretion of the beta-amyloid precursor protein and amyloid beta-peptide, J Biol Chem.280(30):28110-7.

Temple ME, Luzier AB, Kazierad DJ (2000); Homocysteine as a risk factor for atherosclerosis, Ann Pharmacother. 34(1):57-65.

Terry CJ, Damas AM, Oliveira P, Saraiva MJ, Alves IL, Costa PP, Matias PM, Sakaki Y, Blake CC (1993); Structure of Met30 variant of transthyretin and its amyloidogenic implications, EMBO J.12(2):735-41.

Thielemans C, Dratwa M, Bergmann P, Goldman M, Flamion B, Collart F, Wens R (1988); Continuous ambulatory peritoneal dialysis vs haemodialysis: a lesser risk of amyloidosis, Nephrol Dial Transplant 3:291-294.

Thomas PJ, Qu BH, Pedersen PL (1995); Defective protein folding as a basis of human disease, Trends Biochem. Sci 20, 456-459.

Tripoli E, Giammanco M, Tabacchi G, Di Majo D, Giammanco S, La Guardia M (2005); The phenolic composition of olive oil: structure, biological activity, and beneficial effects on human health, Nutr Res Rev.18: 98–112.

Ueda M, Ageyama N, Nakamura S, Nakamura M, Chambers JK, Misumi Y, Mizuguchi M, Shinriki S, Kawahara S, Tasaki M, Jono H, Obayashi K, Sasaki E, Une Y, Ando Y (2011);Aged vervet monkeys developing transthyretin amyloidosis with the human disease-causing Ile122 allele: a valid pathological model of the human disease, Lab Invest. 92(3):474-84.

Ueland PM, Mansoor MA, Guttormsen AB, Müller F, Aukrust P, Refsum H, Svardal AM (1996);Reduced, oxidized and protein-bound forms of homocysteine and other aminothiols in plasma comprise the redox thiol status--a possible element of the extracellular antioxidant defense system, J Nutr.126(4 Suppl):1281S-4S.

Uemichi T, Uitti RJ, Koeppen AH, Donat JR, Benson MD (1999);Oculoleptomeningeal amyloidosis associated with a new transthyretin variant Ser64, Arch Neurol. 56(9):1152-5.

Uversky VN (2002); Natively unfolded proteins: a point where biology waits for physics, Protein Sci. 11,739-756.

Uversky VN, Fink AL (2004); Review. Conformational constraints for amyloid fibrillation: the importance of being unfolded, Biochim Biophys Acta.1698(2):131-53.

Valleix S, Gillmore JD, Bridoux F, Mangione PP, Dogan A, Nedelec B, Boimard M, Touchard G, Goujon JM, Lacombe C, Lozeron P, Adams D, Lacroix C, Maisonobe T, Planté-Bordeneuve V, Vrana JA, Theis JD, Giorgetti S, Porcari R, Ricagno S, Bolognesi M, Stoppini M, Delpech M, Pepys MB, Hawkins PN, Bellotti V (2012); Hereditary systemic amyloidosis due to Asp76Asn variant β2-microglobulin, N Engl J Med. 366(24):2276-83.

Varadarajan S, Yatin S, Aksenova M, Butterfield DA (2000); Review: Alzheimer's amyloid beta-peptide-associated free radical oxidative stress and neurotoxicity, J Struct Biol.130(2-3):184-208.

Vastrano BC, Chen Y, Zhu N, Ho CT, Zhou Z, and Rosen RT (2000); Isolation and identification of stilbenes in two varieties of Polygonum cuspidatum. J Agric Food Chem 48: 253–256.

Vauzour D, Corona G, Spencer JP (2010); Caffeic acid, tyrosol and p-coumaric acid are potent inhibitors of 5-S-cysteinyl-dopamine induced neurotoxicity, Arch. Biochem. Biophys. 501,106-111.

Vauzour D, Rodriguez-Mateos A, Corona G, Oruna-Concha MJ, Spencer JP (2010); Polyphenols and human health: prevention of disease and mechanisms of action, Nutrients 2(11):1106-31.

Vauzour D, Vafeiadou K, Corona G, Pollard SE, Tzounis X, Spencer JP (2007); Champagne wine polyphenols protect primary cortical neurons against peroxynitrite-induced injury, J. Agric. Food Chem. 55, 2854-2860.

Verdier Y, Penke B (2004); Binding sites of amyloid beta-peptide in cell plasma membrane and implications for Alzheimer's disease. Curr. Protein Pept. Sci 5:19–31.

Vincent C, Pozet N, Revillard JP(1980); Plasma β2-m turnover in renal insufficiency, Acta Clin Belg 35: 2- 13.

Virmani A, Binienda Z, Ali S, Gaetani F (2006); Links between nutrition, drug abuse, and the metabolic syndrome, Ann N Y Acad Sci 1074:303 – 14.

Virmani A, Pinto L, Binienda Z, Ali S (2013); Food, nutrigenomics, and neurodegeneration--neuroprotection by what you eat!, Mol Neurobiol. 48(2):353-62.

Visioli F, Bellosta S, Galli C (1998); Oleuropein, the bitter principles of olives, enhances nitric oxide production by mouse macrophages, Life Sci. 62: 541–546.

Visioli F, Poli A, Galli C (2002); Antioxidant and other biological activities of phenols from olives and olive oil, Med Res Rev. 22: 65–75.

Volles MJ, Lee SJ, Rochet JC, Shtilerman MD, Ding TT, Kessler JC, Lansbury PT Jr. (2001); Vesicle permeabilization by protofibrillar alpha-synuclein: implications for the pathogenesis and treatment of Parkinson's disease. Biochemistry. 40(26):7812-9.

Wakabayashi M and Matsuzaki K (2009); Ganglioside-induced amyloid formation by human islet amyloid polypeptide in lipid rafts, FEBS Lett. 583 (17), 2854–2858.

Wan Y, Vinson JA, Etherton TD, Proch J, Lazarus SA, Kris-Etherton PM (2001); Effects of cocoa powder and dark chocolate on LDL oxidative susceptibility and prostaglandin concentrations in humans. Am. J. Clin. Nutr. 74, 596-602.

Wang Q, Walsh DM, Rowan MJ, Selkoe DJ, Anwyl R (2004); Block of long-term potentiationby naturally secreted and synthetic amyloid beta-peptide in hippocampal slices is mediated via activation of the kinases c-Jun N-terminal kinase, cyclin-dependent kinase 5, and p38 mitogen-activated protein kinase as well as metabotropic glutamate receptor type 5. J. Neurosci. 24: 3370–3378

Warren DJ, Otieno LS (1975); Carpal tunnel syndrome in patients on intermittent hemodialysis, Postgrad Med J 51:450- 454.

Wetzel R. (2002); Review. Ideas of order for amyloid fibril structure, Structure. 10(8):1031-6.

Wibell L, Evrin PE, Berggfird I (1973); Serum/32-microglobulin in renal disease, Nephron 10:320-331.

Wisniewski T, Castano E, Ghiso J, Frangione B (1993); Cerebrospinal fluid inhibits Alzheimer beta-amyloid fibril formation in vitro, Ann. Neurol. 34:631–633.

Wojtczak A, Cody V, Luft JR, Pangborn W (1996); Structures of human transthyretin complexed with thyroxine at 2.0 A resolution and 3',5'-dinitro-N-acetyl-L-thyronine at 2.2 A resolution, Acta Crystallogr D Biol Crystallogr. 52(Pt 4):758-65.

Wojtczak A, Luft J, Cody V (1992); Mechanism of molecular recognition. Structural aspects of 3,3′-diiodo-l-thyroxine binding to human serum transthyretin. J Biol Chem 267:353–357.

Woo P, O'Brien J, Robson M, Ansell BM (1987); A genetic marker for systemic amyloidosis in juvenile arthritis, Lancet II: 767-769.

Wright PE, Dyson HJ (1999); Intrinsically unstructured proteins: reassessing the protein structure-function paradigm, J. Mol.Biol. 293, 321-331.

Wu C, Lei H, Wang Z, Zhang W, Duan Y (2006); Phenol Red Interacts with the Protofibril-Like Oligomers of an Amyloidogenic Hexapeptide NFGAIL through Both Hydrophobic and Aromatic Contacts, Biophys J 91, 3664-3672.

Wu Y, Wu Z, Butko P, Christen Y, Lambert MP, Klein WL, Link CD, Luo Y (2006); Amyloid-beta-induced pathological behaviors are suppressed by Ginkgo biloba extract EGb761 and ginkgolides in transgenic Caenorhabditis elegans. J Neurosci 26: 13102–13113.

Wulffelé MG, Kooy A, Lehert P, Bets D, Ogterop JC, Borger van der Burg B, Donker AJ, Stehouwer CD (2003); Effects of short-term treatment with metformin on serum concentrations of homocysteine, folate and vitamin B12 in type 2 diabetes mellitus: a randomized, placebo-controlled trial, J Intern Med. 254(5): 455-63.

Wyttenbach A, Sauvageot O, Carmichael J, Diaz-Latoud C, Arrigo AP, Rubinsztein DC (2002); Heat shock protein 27 prevents cellular polyglutamine toxicity and suppresses the increase of reactive oxygen species caused by Huntingtin, Hum Mol Genet. 11(9):1137-51.

Yu RK, Nakatani Y, Yanagisawa M (2009); The role of glycosphingolipid metabolism in the developing brain, J. Lipid Res. 50(Suppl):S440–S445.

Yu RK, Tsai YT and Ariga T (2012); Functional roles of gangliosides in neurodevelopment: an overview of recent advances, Neurochem. Res. 37 (6), 1230–1244.

Yu RK, Tsai YT, Ariga T, Yanagisawa M (2011); Structures, biosynthesis, and functions of gangliosides--an overview, J Oleo Sci. 60(10):537-44.

Zandomeneghi G, Krebs MR, McCammon MG, Fändrich M (2004); FTIR reveals structural differences between native beta-sheet proteins and amyloid fibrils, Protein Sci.13(12):3314-21.

Zeng X, Dai J, Remick DG, Wang X (2003); Homocysteine mediated expression and secretion of monocyte chemoattractant protein-1 and interleukin-8 in human monocytes. Circ Res. 93(4):311-20.

Zhang Q, Kelly JW (2003); Cys10 mixed disulfides make transthyretin more amyloidogenic under mildly acidic conditions. Biochemistry. 2003 Jul 29;42(29):8756-61.

Zhu M, Souillac PO, Ionescu-Zanetti C, Carter SA, Fink AL (2002); Surface-catalyzed amyloid fibril formation, J Biol Chem. 277(52):50914-22.

Zhu YJ, Lin H, Lal R (2000); Fresh and nonfibrillar amyloid beta protein(1-40) induces rapid cellular degeneration in aged human fibroblasts: evidence for AbetaP-channel-mediated cellular toxicity, FASEB J.14(9):1244-54.

Zykova TA, Zhu F, Zhai X, Ma WY, Ermakova SP, Lee KW, Bode AM, Dong Z (2008); Resveratrol Directly Targets COX-2 to Inhibit Carcinogenesis, Mol Carcinog. 47(10): 797–805.

Ringraziamenti

Eccomi di nuovo qui dopo 3 anni a scrivere nuovamente i ringraziamenti. La sensazione che si prova è sempre piacevole, perché questo momento segna la fine di un percorso e forse l'inizio di qualcosa di nuovo e stimolante. In queste pagine colgo l'occasione di ringraziare tutte le persone che mi sono state vicine nel raggiungimento di questo traguardo e spero vivamente di non dimenticare nessuno. Prima di tutto un grazie speciale và a mia nonna, Gilda, lei che ogni sera si preoccupava per i miei viaggi in treno e stava ad ascoltare tutto ciò che le dicevo. Lei che quando mi vedeva entrare mi salutava con un sorriso e bastava quel sorriso per far passare la stanchezza della giornata. Insieme a lei, al mio fianco, c'è sempre tutta la mia famiglia, zii e cugini inclusi che mi hanno seguita in ogni mia tappa. La mamma che mi ha permesso di studiare e ha sempre appoggiato ogni mia scelta e poi beh "la mamma è sempre la mamma". Mia sorella, che ho stressato con i miei discorsi sul lavoro, penso che a questo punto anche lei sappia cosa sia l'amiloide e il folding delle proteine e che mi prende in giro chiedendomi: "a quando il Nobel?". Gildo che ha fatto le corse con me per farmi prendere il treno la mattina o la sera per riprendermi, e si sorbiva i ritardi e le mie paranoie. Marco, non basterebbe una tesi per scrivere tutto ciò che abbiamo condiviso, sicuramente questi ultimi anni ci hanno portati ad affrontare un nuovo importante traguardo, un piccolo pezzetto per il nostro futuro insieme. Vanna e Valerio, grazie per farmi sempre sentire come a casa ed avermi incoraggiata. Oltre alla mia famiglia, in Dipartimento ho trovato una nuova "famiglia", prima di tutti la Dott.ssa Monica Bucciantini che è dalla triennale che mi sopporta ed insegna, spesso in questi anni mi ha vista comparire alla sua porta e mi chiedeva sorridendo: "che è successo? Tutto apposto?", io o avevo combinato qualcosa o c'era qualche interpretazione dei dati che non mi tornava e lei non si è mai arrabbiata, anzi mi ha sempre dato consigli su come migliorare e mi ha permesso di appassionarmi sempre di più a questo lavoro che non potrei mai smettere di fare. Il Prof. Massimo Stefani che mi ha dato la possibilità di iniziare a capire cosa vuol dire fare Ricerca.

Oltre al lavoro in questi anni ho conosciuto voi "*I ragazzi del Dipartimento*", un gruppo incredibile che ha riempito questi 3 anni di risate, ci siamo supportati e sopportati per ogni nostra disavventura in laboratorio e ci siamo fatti compagnia nelle pause caffè.

Cate e Cami diventate care amiche sempre disposte ad ascoltare le mie vicissitudini, soprattutto durante la stesura della tesi, mi avete vista avere attimi di sconforto e siete

sempre state lì pronte ad accogliere ogni mia lamentela e a farmi ridere. Pippo grazie per avermi aspettata ogni mattina per prendere il caffè insieme anche quando i treni erano in ritardo. Senza togliere niente agli altri, un grazie particolare và al Rama, mio vicino di banco che si è letteralmente sorbito ogni mio vagheggiamento sull'aggregazione amiloide e su come potessi interpretare i miei dati e mi stava ad ascoltare interessato anche quando aveva da fare mille cose già per conto suo. Un grazie anche ai dottorandi conosciuti a Brallo di Pregola che hanno reso la settimana del congresso indimenticabile, come ogni nostro ritrovo successivo.

Ovviamente tra gli amici nuovi non posso dimenticarmi delle mie amiche di una vita Ele e Lau, con le piccole Rachele e Vittoria, che ogni volta che mi sentono parlare pensano che un giorno scoprirò qualcosa di incredibile, grazie ragazze per la fiducia!! Lucia che ha la mia stessa passione e anche se ci vediamo poco è sempre rimasta la mia compagna di banco delle superiori e abbiamo condiviso l'ansia degli esami universitari e adesso lo stress da Dottorato. In fine ci sono gli amici di Firenze che mi sopportano ogni week-end da ben 9 anni e solo per questo GRAZIE!

Spero di aver ringraziato tutti e nel modo migliore, comunque questi tre anni oltre che belli in ambito lavorativo sono stati intensi anche a livello personale, scoprire nuovi amici e a volte perderne altri è comunque un percorso importante che mi ha portata ad affrontare e migliorare molti lati di me, perciò non posso far altre che ringraziarvi di cuore per avermi seguita in questo mio percorso formativo.

Grazie a tutti per essermi stati vicini.